HOPE CREEK GENERATING STATION
FACILITY OPERATING LICENSE NPF-57
DOCKET NO. 50-354

REQUEST FOR LICENSE AMENDMENT
EXTENDED POWER UPRATE

Stress Analysis of the Hope Creek Unit 1 Steam Dryer Using 1/8th scale Model Pressure Measurement Data

CDI Report No. 06-27
September 2006

C.D.I. Report No. 06-27

Stress Analysis of the Hope Creek Unit 1 Steam Dryer at CLTP and EPU Conditions Using 1/8th Scale Model Pressure Measurement Data

Revision 0

Prepared by

Continuum Dynamics, Inc.
34 Lexington Avenue
Ewing, NJ 08618

Prepared under Purchase Order No. 4500366543 for

Nuclear Business Unit, PSEG Nuclear LLC
Materials Center, Alloway Creek Neck Road
Hancocks Bridge, NJ 08038

Approved by

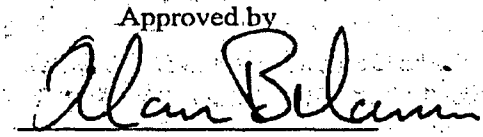

Alan J. Bilanin

Reviewed by

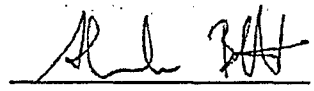

Alexander H. Boschitsch

September 2006

Executive Summary

In this analysis, stresses induced by the flow of steam through the steam dryer at Hope Creek Unit 1 are calculated and evaluated using 1/8th scale pressure measurement data at Current Licensed Thermal Power (CLTP), Extended Power Uprate (EPU) conditions and EPU conditions with frequencies scaled up and down by 10%. The fluctuating pressure loads induced by the flowing steam were predicted by a separate acoustic circuit analysis of the steam dome and main steam lines[1]. These loads were then applied to the steam dryer structure for 2 seconds at CLTP and EPU conditions and the resulting stresses are calculated by performing a time history structural dynamics analysis using the commercial finite element model, ANSYS 10.0.

Assessment of the stress results for compliance with the ASME B&PV Code, Section III, subsection NG, was carried out for the load combination corresponding to normal operation (the Level A Service Condition). This combination consists of the fluctuating pressure loads and weight. The evaluation is done for both maximum (peak) and cyclic (fatigue type) stresses. Level B service conditions, which include seismic loads, are not included in this evaluation.

The results show that on the basis of these 1/8th scale pressure measurements at CLTP condition the minimum stress ratio (allowable stress divided by the computed stress with appropriate adjustments made for stress type and weld factors) is 1.53, occurring at the welded junction of thin closure plate and inner hood, and does not exceed the allowable. At EPU operation the minimum stress ratio occurs on the welded junction between the drain channel and the skirt, and is 1.09 indicating that allowable values are also not exceeded. Finally, the EPU load conditions with frequencies shifted by 10% are also examined. For the case with a downward 10% shift in frequencies, the minimum stress ratio is 0.984 and occurs at the top of the thin closure plate where it joins to the middle hood. For the case with the frequencies shifted up by 10%, the minimum stress ratio is 0.832 and occurs on the junction between the middle hood and its end plate. This is the smallest stress ratio encountered in these calculations and indicates that allowable stress levels are exceeded in this case. Stress ratios for specific locations on the steam dryer are tabulated in the report in Table 7. It is emphasized that no additional adjustments associated with modeling uncertainty, correlations with plant data and uncertainty in measurements are reflected in these stress ratios. Accounting for these adjustments is expected to significantly increase (almost double) the stress ratios so that at both CLTP and EPU conditions operational stresses are expected to be well within allowable levels.

This analysis includes all Hope Creek Unit 1 dryer modifications and accounts for the current power generation rate. To evaluate additional dryer modifications and/or power uprates, the stresses should be recomputed using appropriately modified structural models to account for steam dryer modifications, and main steam line strain gage measurements taken during power uprate and processed by a separate acoustic circuit analysis.

Table of Contents

1. Introduction and Purpose

Recent inspections of the steam dryers in Mark I plants have shown cracks in the fillet welds and nearby structures. The industry has addressed this problem with physical modifications to the dryers, as well as a program to define steam dryer loads and their resulting stresses. Hope Creek Unit 1 (HC1) is part of this program and the purpose of the stress analysis discussed here is to calculate the peak and alternating stresses generated during both CLTP and EPU conditions and determine whether these stresses are within the acceptance criteria dictated by the ASME Code. This step establishes whether the modifications are adequate for sustaining structural integrity and preventing future weld cracking under both current (CLTP) and planned (EPU) operating conditions.

The damaging steam dryer loads are due to pressure fluctuations, induced by steam flow through the dryer. Over a long period of time, cyclic stresses from these loads can produce fatigue cracking if loads are sufficiently high. Since fillet welds are the structural features most susceptible to fatigue failure, most of the failures have been found in these areas.

The fluctuating pressure loads, induced by the flowing steam, were previously predicted by a separate acoustic circuit analysis of the steam dome and main steam lines [1]. In the present analysis, these loads are applied to the steam dryer structure and the resulting stresses are calculated using a finite element model (the ANSYS 10.0 computer code). The loads are applied to the structure at 1.422×10^{-3} sec intervals for 2.0 sec (1405 time steps), and the equations representing the structural dynamics solved using time history dynamic analysis.

One way to evaluate the sensitivity of the stress results to modeling approximations and perturbations in the applied loading is to perturb the frequencies in the applied load history and determine whether this produces significant changes in the structural response. In the context of the transient simulations performed here, this frequency scaling is easily effected and is tantamount to modifying the time step (a 10% reduction in the time step corresponds to a 10% increase of all frequencies). Thus, two additional cases are considered here where the dryer structural model is subjected to the same EPU load history, but with the time step reduced by 10% to 1.28×10^{-3} sec for scaling frequencies up (EPU+10%FS) and increased by 10% to 1.564×10^{-3} sec for scaling frequencies down (EPU-10%FS).

The load combination considered here corresponds to normal operation (the Level A Service Condition) and consists almost entirely of the fluctuating pressure loads and weight. The resulting stresses are examined for compliance with the ASME B&PV Code, Section III, subsection NG. Both maximum and cyclic (fatigue type) stresses are considered in this evaluation. Level B service conditions, which include seismic, are not addressed here.

2. Model Description

A description of the ANSYS model of the HC1 steam dryer follows.

2.1 Steam Dryer Geometry

A geometry model of the HC1 steam dryer was developed from available drawings, as well as from field measurements taken by C.D.I. on an identical spare dryer for the cancelled Hope Creek Unit 2. The completed model is shown in Figure 1.

This model includes modifications made to the HC1 steam dryer on-site, prior to commercial operation. These are:

- Tie bars, hoods, and end plates were replaced on the original dryer (FDI-041-79450).
- Reinforcement bars were added to the hoods (FDDR-KT1-415 and KT1-444)

The modified areas are shown in Figure 2.

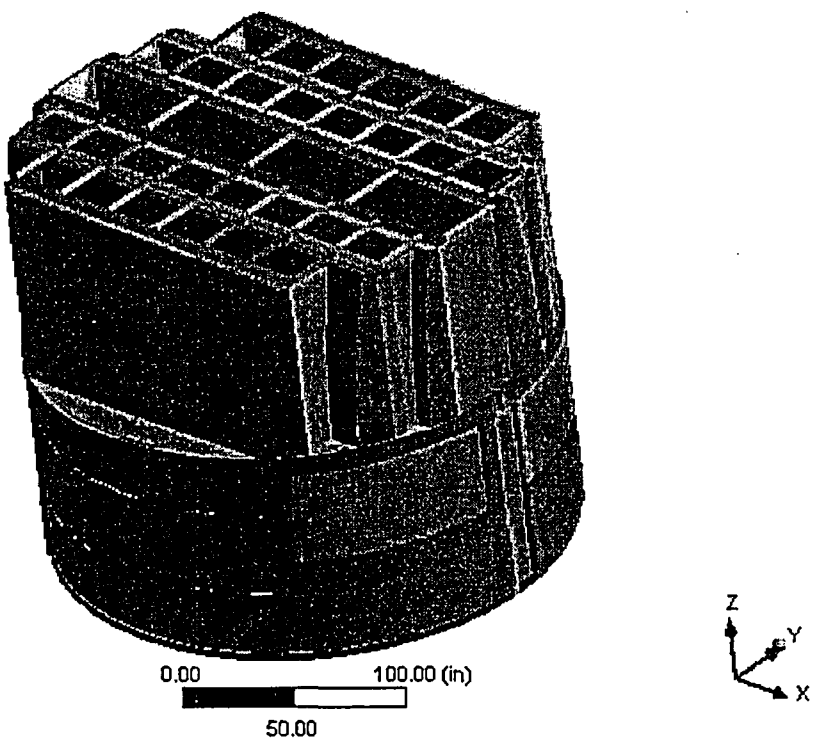

Figure 1. Overall geometry of the HC1 steam dryer model.

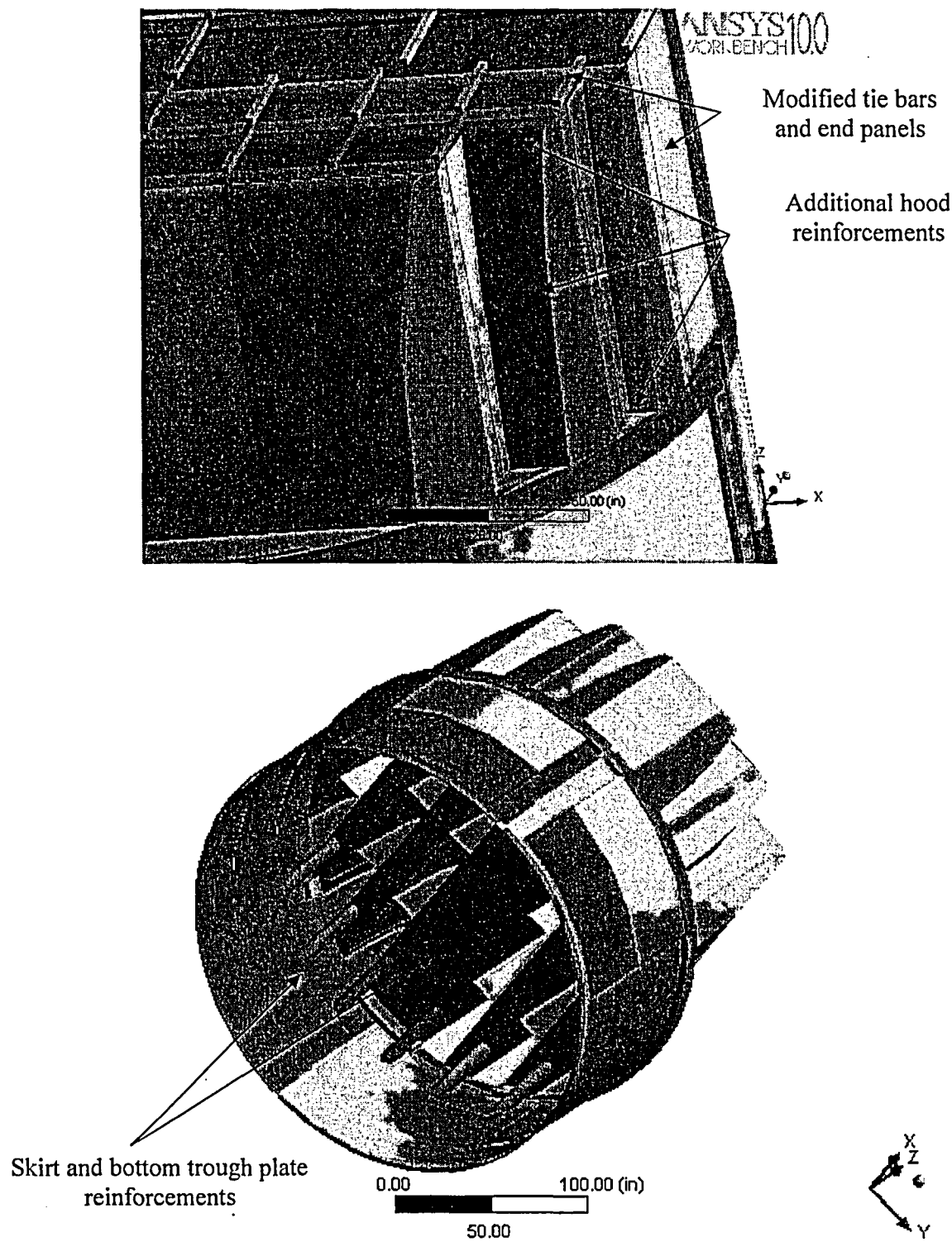

Figure 2. On-site modifications accounted for in the model and associated geometrical details.

2.2 Material Properties

The steam dryer is constructed from Type 304 stainless steel and has an operating temperature of 550°F. Properties used in the analysis are summarized below in Table 1.

Table 1. Material properties.

	Young's Modulus (10^6 psi)	Density (lbm/in^3)	Poisson Ratio
Structural Steel	25.55	0.284	0.3
Structural Steel for Perforated Plates	15.33	0.227	0.3
Structural Steel with Added Water Inertia Effect	25.55	1.183	0.3

The structural steel modulus is taken from Appendix A of the ASME Code for Type 304 Stainless Steel at an operating temperature 550°F. The effective properties of perforated plates and submerged parts are discussed in Section 3.

2.3 Pressure Loading

The transient loads are produced by the unsteady pressures acting on the exposed surfaces of steam dryer. The pressure time history loading was obtained from an acoustic circuit model of the HC1 steam dryer, performed by C.D.I. using data obtained from a 1/8th scale rig and detailed in [1]. This loading was provided over the steam dryer surface on a three-inch grid, at a total of 10,963 locations. The time interval spanned the 2.0 sec of data that contained the peak minimum and maximum pressures on a low-resolution grid of the dryer (including only corners and edges, a total of 104 locations). The pressure time history is shown in Figure 3, at a location on the outer bank hood opposite the A and B main steam lines.

These results were interpolated onto the detailed structural grid of the HC1 steam dryer, and the ANSYS calculation was then undertaken. The program was developed to properly convert the data into a format recognizable by the ANSYS software. Inspection of the resulting pressures at selected nodes shows that these pressures vary in a well-behaved manner between the nodes with prescribed pressures. Graphical depictions of the resulting pressures, comparisons between the peak pressures in the original nodal histories and those in the final surface load distributions produced in ANSYS, and comparison of the pressure histories at randomly selected nodes in the original pressure history data files and the ANSYS loading arrays, all confirm that the load data are interpolated accurately and transferred correctly to ANSYS.

The fluctuating pressure loads were applied to surfaces above the water level, as indicated in Figure 4. In addition to the fluctuating pressure load, the static loading by the weight of the steam dryer is analyzed separately. The resulting static and transient stresses are linearly combined to obtain total values which are then processed to calculate peak and alternating stress intensities for assessment in Section 5.

To evaluate the sensitivity of the stress results to approximations in the structural modeling and applied loads, the EPU loads were modified by rescaling the frequencies over the range

±10% and the stress response recomputed. In the context of the transient simulations performed here, this frequency scaling is easily effected and is tantamount to modifying the time step. The EPU load was modified by rescaling the frequencies ±2.5%, ±5%, ±7.5% and ±10%, and applied to the structure over 50 time steps. The peak and alternating stress intensities for each rescaled frequency were then calculated and compared to identify the case producing the highest increase in stresses. The objective in limiting the response to only 50 steps when performing this assessment, was to identify the condition most likely to produce the highest stresses at minimum computation time. On the basis of this 50-step simulation the ±10% frequency scaled loads produced the highest stresses and were selected to generate stresses over the full 2 sec run.

The unsteady pressure loads applied to the dryer contain a strong 80Hz component which has been shown to be fictitious [4]. Specifically, the signal arises from the interaction between sensors used to record the unsteady pressures. Therefore the stress ratios were calculated with the 80Hz signal removed. For frequencies scaled up by 10%, the 88 Hz component corresponds to the signal 80 Hz in original EPU loading and was therefore removed. Similarly, for the case with frequencies scaled down by 10% the 72 Hz component was filtered out. Due to linearity of the model, the relevant component can be removed during post-processing of the results. The power spectrum density (PSD) of the pressure loading at a location on the outer bank hood is shown on Figure 5 where the curves both with and without the 80 Hz signal are compared. The time pressure loading time histories with and without the 80 Hz component removed are compared in Figure 6. All stress results and stress ratios are obtained with the 80 Hz signal removed.

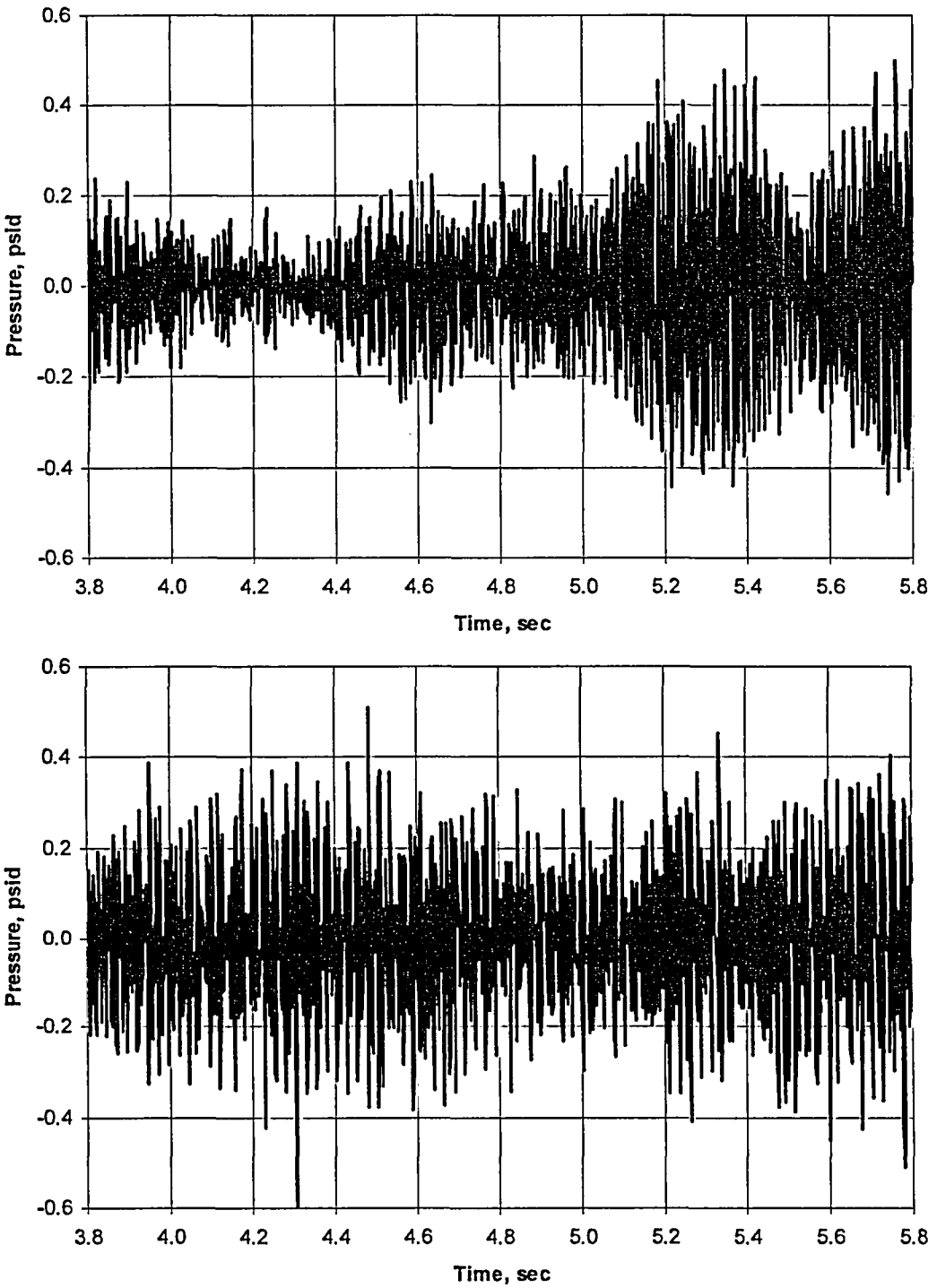

Figure 3. Pressure time history applied to the ANSYS model at the bottom of the outer hood (side MSL AB). CLTP loading (top), EPU loading (bottom).

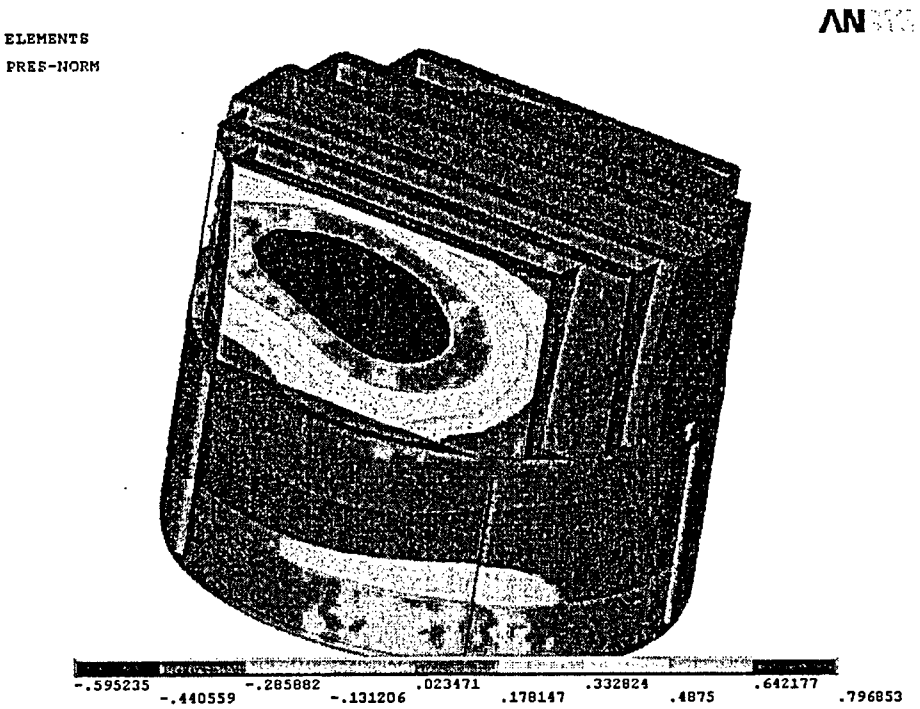

t=0.711s (500 time steps)

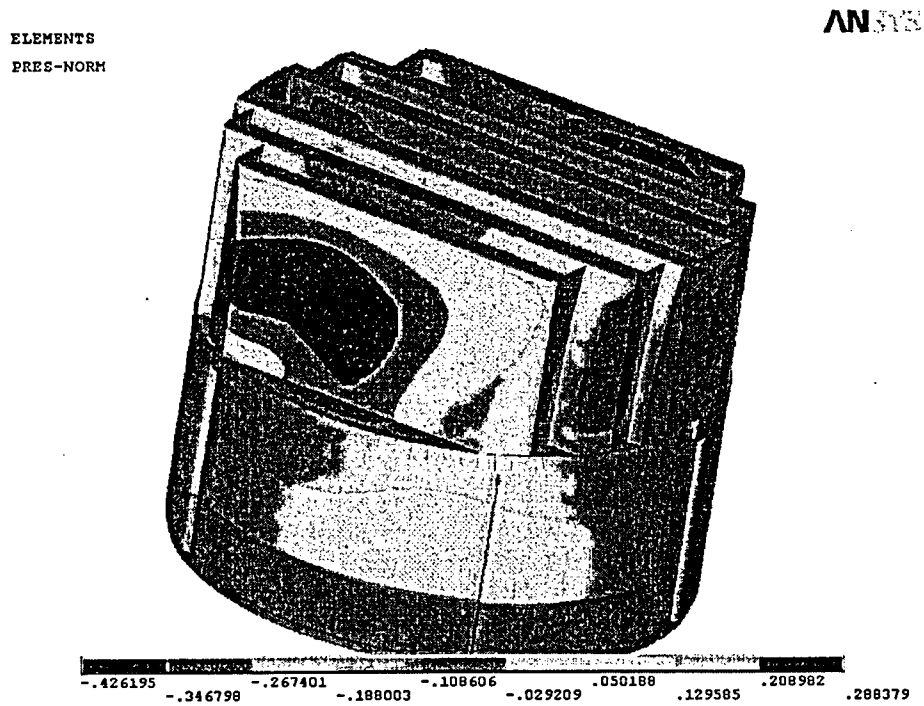

t=1.422s (1000 time steps)

Figure 4a. CLTP pressure loading (in psid) on the steam dryer at different time steps. No loading is applied to the submerged light blue surface.

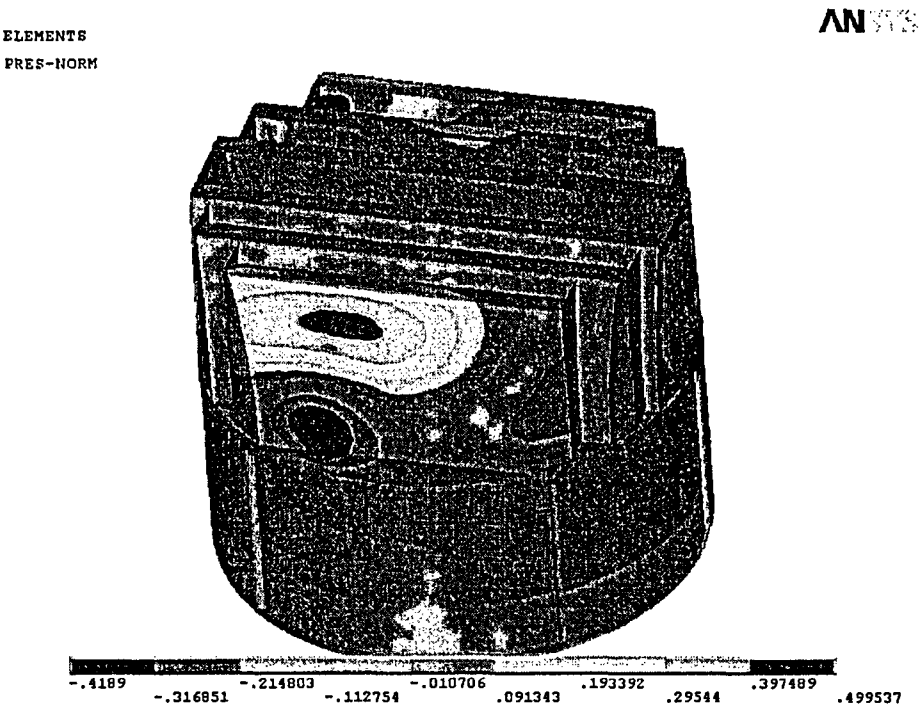

t=0.711s (500 time steps)

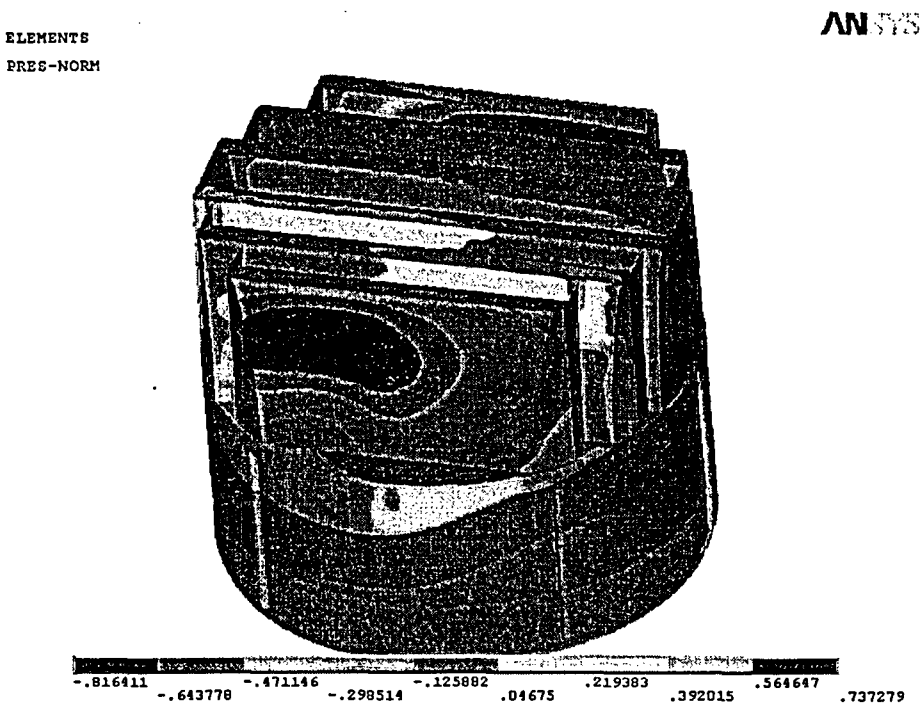

t=1.422s (1000 time steps)

Figure 4b. EPU pressure loading (in psid) on the steam dryer at different time steps. No loading is applied to the submerged light blue surface.

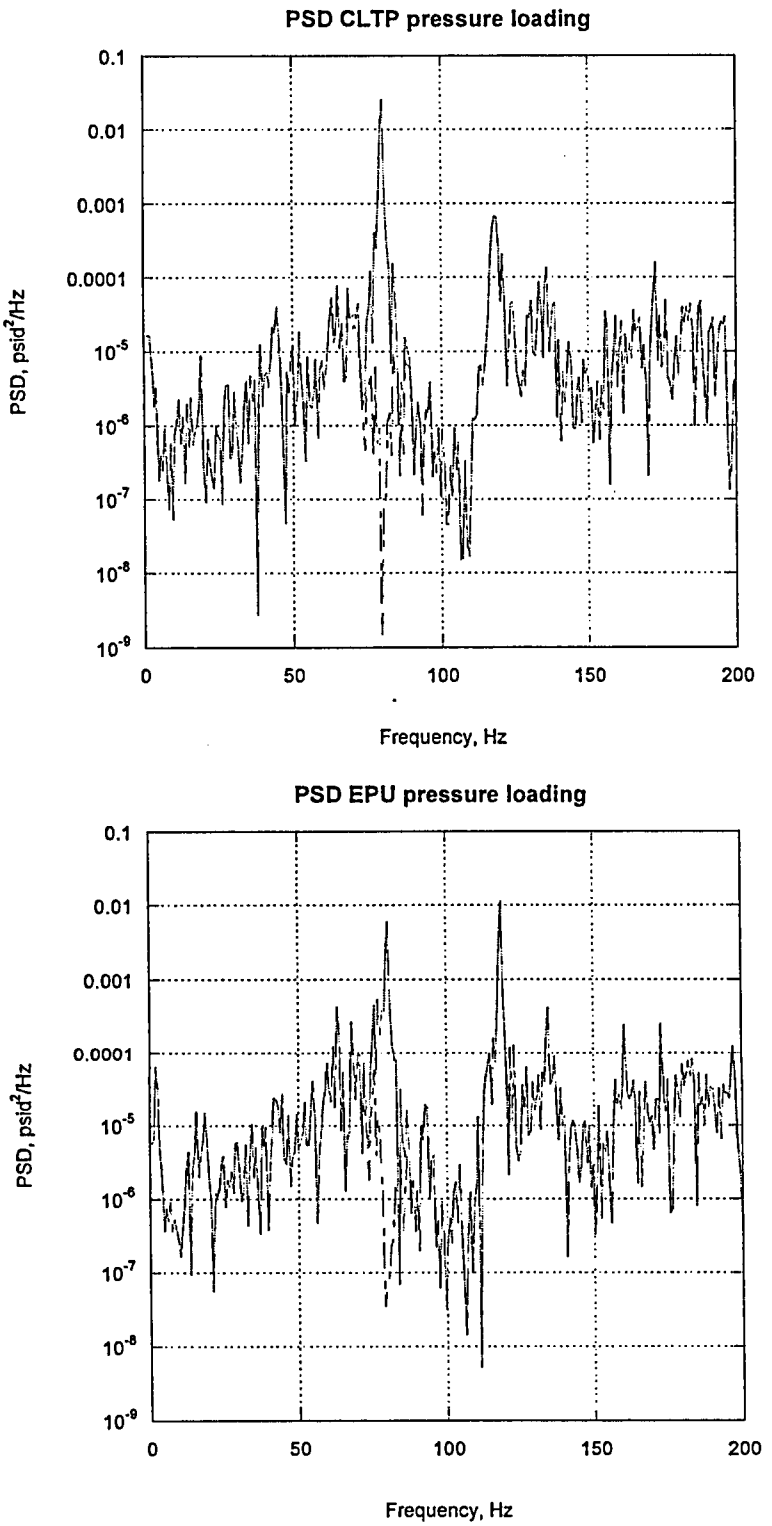

Figure 5. PSD of pressure loading on the outer hood. The red curve corresponds to the original pressure loading; the blue curve corresponds to the loading with the 80 Hz component removed.

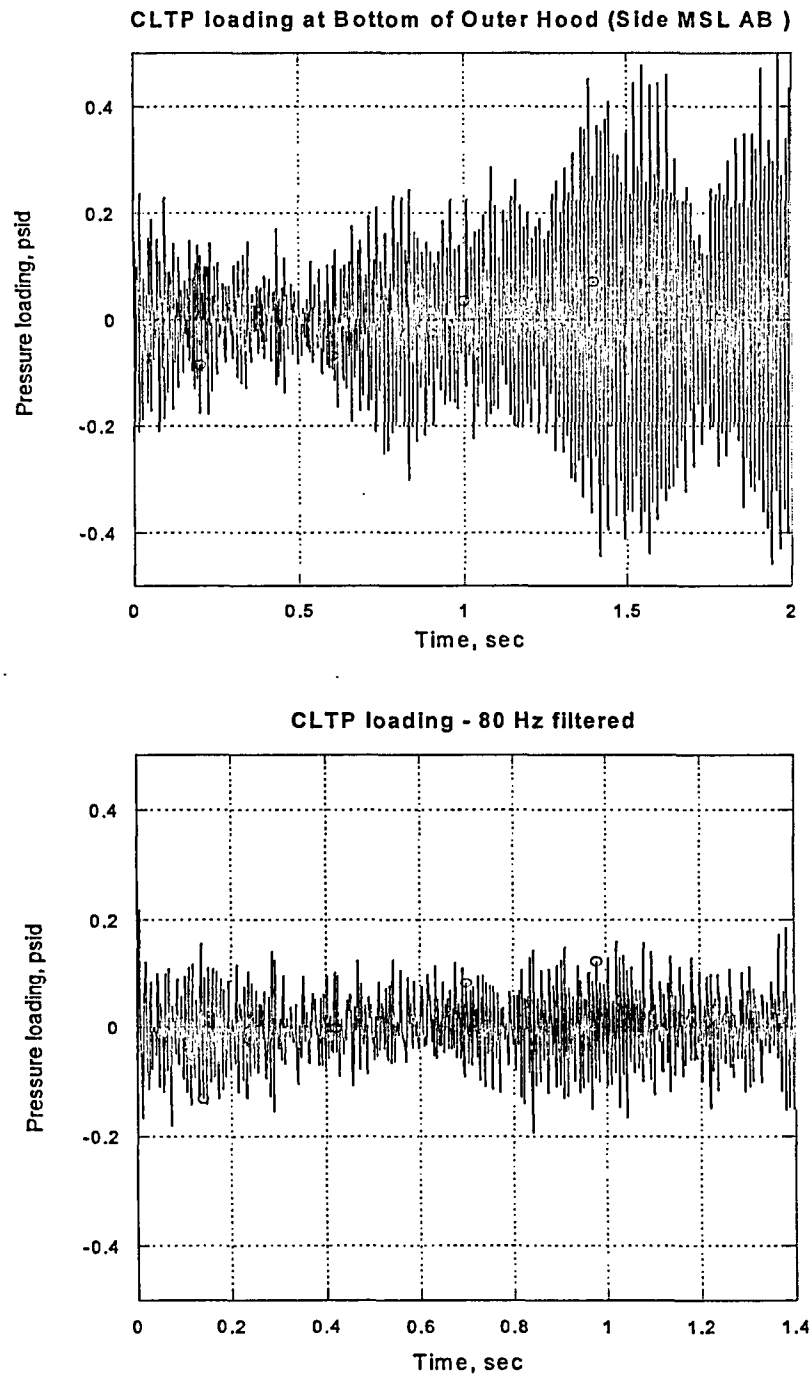

Figure 6a. Comparison of the time histories at the CLTP condition with and without the 80 Hz component.

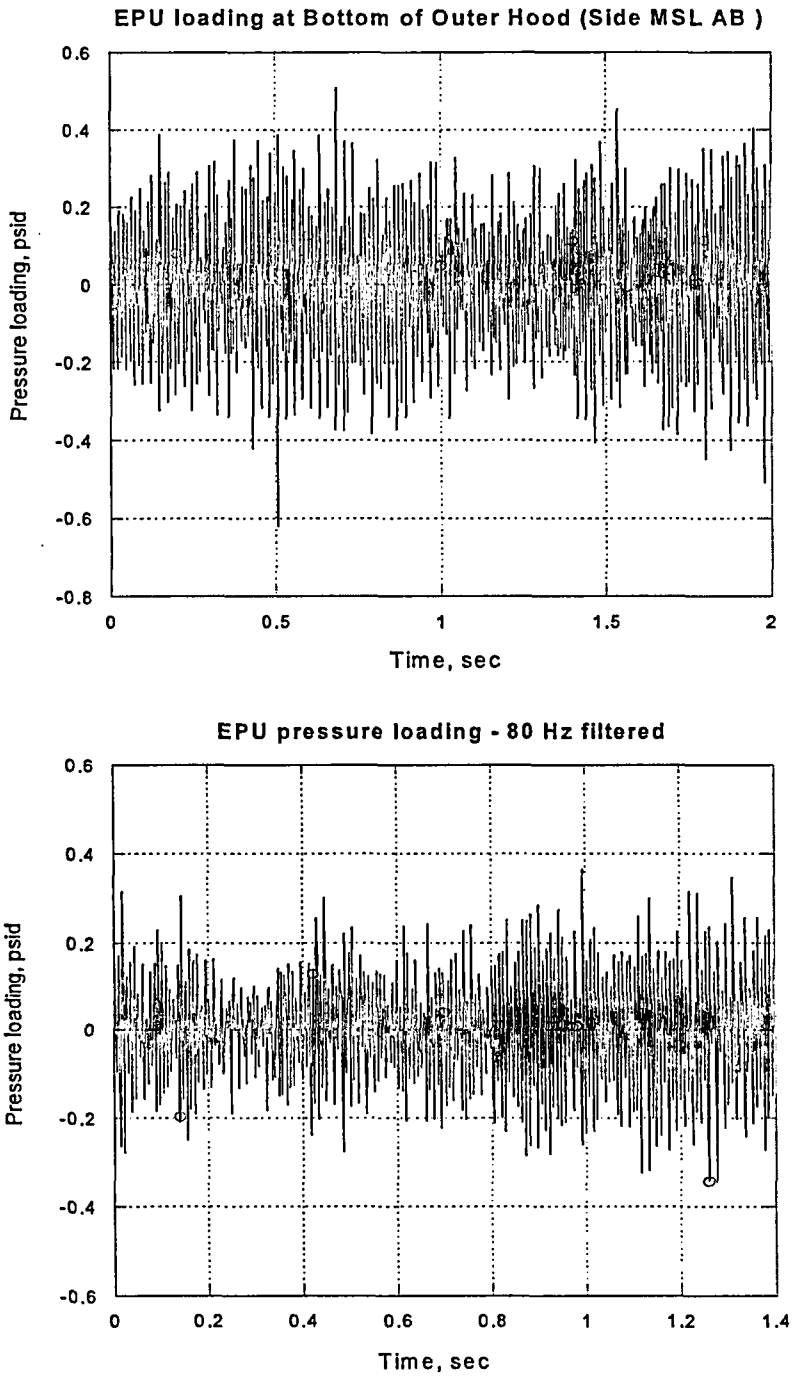

Figure 6b. Comparison of the time histories at the EPU condition with and without the 80 Hz component.

3. Finite Element Model

The dynamics of the steam dryer were modeled using the ANSYS computer code.

3.1 Model Simplifications

The following simplifications were made in order to reduce model size while retaining key structural properties:

- Most welds were replaced by node-to-node connections; interconnected parts share the common nodes along the welds. In other locations the constraint equations between nodal degrees of freedom were introduced.

- The drying vanes were replaced by point masses, attached to the corresponding trough bottom plates and vane bank top covers (Figure 7). The bounding perforated plates, vane bank end plates, and vane bank top covers were explicitly modeled.

- The lower part of the skirt and drain channels are below the reactor water level. An analysis was used to calculate the effective mass of this water and thus account for its interaction with the structure. This added water mass was included in the ANSYS model by appropriately modifying the density of the submerged structural elements when computing transient loads.

- Fixed constraints were imposed at the underside of the steam dryer upper support ring where it makes contact with the four steam dryer support brackets that are located on the reactor vessel and spaced at 90° intervals (Figure 8). No credit was taken for the constraints from the reactor vessel lift lugs.

3.2 Perforated Plate Model

The perforated plates were modeled as solid plates with adjusted elastic and dynamic properties. Properties of the perforated plates were assigned according to the type and size of perforation. Based on [2], for an equilateral triangular pattern with given hole size and spacing the effective modulus of elasticity was found to be a factor of 0.6 times the original modulus, while the effective density was a factor of 0.8 times the original steel density. These adjusted properties were shown in Table 1.

3.3 Vane Bank Model

The vanes were modeled as point masses, located at the center of mass for each vane bank. The following approximate masses were used for the vanes, based on data found on drawings supplied by PSE&G: inner banks, 6,545 lbm; middle banks, 5,970 lbm; and outer banks, 4,685 lbm. These weights were applied to the base plates and vane top covers using the standard ANSYS point mass modeling option, element MASS21. ANSYS automatically distributes the point mass inertial loads to the nodes of the selected structure. The distribution algorithm minimizes the sum of the squares of the nodal inertial forces, while ensuring that the net forces and moments are conserved. Vane banks are not exposed to main steam lines directly, but rather shielded by the hoods. Thus, compared to the hoods, less motion is anticipated on the vane banks

so that approximating their inertial properties with equivalent point masses is justified. Nevertheless, the bounding parts, such as perforated plates, side panels, and top covers, are retained in the model.

3.4 Water Inertia Effect on Submerged Panels

Water inertia was modeled by an increase in density of the submerged structure. The added mass was found by a separate analysis to be 0.225 lbm/in^2 of submerged skirt area.

3.5 Structural Damping

Time history analysis in the ANSYS program requires that the damping be specified in terms of mass and stiffness Raleigh damping (i.e., the damping parameters, α and β, defined in Section 5.9.3 of the ANSYS 10.0 documentation). These material constants can be defined from the damping ratio over the range of frequencies examined. For the calculation presented here, a damping ratio of 1% was assumed over the range of frequencies from 10 to 150 Hz. This assumption leads to the following values used in the analysis: $\alpha = 1.18$ and $\beta = 2 \times 10^{-5}$. This damping is consistent with guidance given in NUREG-1.61.

3.6 Mesh Details and Element Types

Shell elements were employed to model the skirt, hoods, perforated plates, side and end plates, trough bottom plates, reinforcements, and cover plates. Specifically, the four-node, Shell Element 63, was selected to model most of these structural components. This element models bending and membrane stresses, but omits transverse shear. Compared to the default shell element in ANSYS, Shell Element 181, the Shell Element 63 is more sensitive to warping and requires higher resolution of curved regions. Care was taken to ensure that adequate resolution was provided on the curved hoods (one element per 15° arc). Shell Element 181 was used only for modeling submerged parts of the drain channels. This is due to less number of elements needed to adequately resolve curved regions, also, more accurate stresses are computed as considerable shear components develop in these areas. All other parts, including tie bars and the upper and lower support rings, were modeled with solid brick elements. The elements SURF154 are used to assure proper application of pressure loading to the structure. Mesh details and element types are shown in Table 2 and Table 3. Details of the finite element mesh are shown in Figure 9.

3.7 Connections Between Structural Components

Most connections between parts were modeled as node-to-node connections. However, in several places, such as connections between shell and solid elements or dissimilarly meshed parts, constraint equations were used to connect adjacent structures. Basically, all such constraints express the deflection (and rotation for shell elements) of a node, R_1, on one structural component in terms of the deflections/rotations of the corresponding point, P_2, on the other connected component. Specifically, the element containing P_2 is identified and the deformations at P_2 determined by interpolation between the element nodes. Several types of connections arose in the steam dryer model including the following:

1. Shell edge to shell edge connections with dissimilar meshes.
2. Connections of shell faces to solid faces (Figure 10a). While only displacement degrees of freedom are explicitly constrained, this approach also implicitly constrains the rotational degrees of freedom when multiple shell nodes on a sufficiently dense grid are connected to the same solid face.
3. Connections of shell edges to solids (e.g., connection of the bottom of closure plates with the upper ring). Since solid elements do not have rotational degrees of freedom, the coupling approach consisted of having the shell penetrate into the solid by one shell thickness and then constraining both the embedded shell element nodes (inside the solid) and the ones located on the surface of the solid structure (see Figure 10b). Numerical tests involving simple structures showed that this approach reproduces both the deflections and stresses of the same structure modeled using only solid elements or ANSYS' bonded contact technology. Continuity of rotations and displacements is achieved as illustrated in Figure 11 in the vicinity of the junction between inlet end plate and upper support ring.
4. Connections of solid elements to shells, e.g., connections of the tie bars to the vane covers.

The use of constraint conditions rather than the bonded contacts advocated by ANSYS for connecting independently meshed structural components, confers two useful numerical advantages to the structural analysis of the steam dryer. First it results in better conditioned and smaller matrices. The smaller size results from the fact that equations and degrees of freedom are eliminated rather than augmented (in Lagrange multiplier-based methods) by additional degrees of freedom. Also, the implementation of contact elements relies on the use of very high stiffness elements (in penalty function-based implementations) or results in indefinite matrices (Lagrange multiplier implementations) with poorer convergence behavior compared to positive definite matrices. Secondly, elimination of contact elements allows ANSYS to reuse the decomposed solution matrix so that only a single (expensive) LU-decomposition is required at the start of the calculation. In subsequent steps only inexpensive back-substitutions are required to update the structural state. This results in faster simulation times than models employing contact elements which require a LU decomposition at every time step.

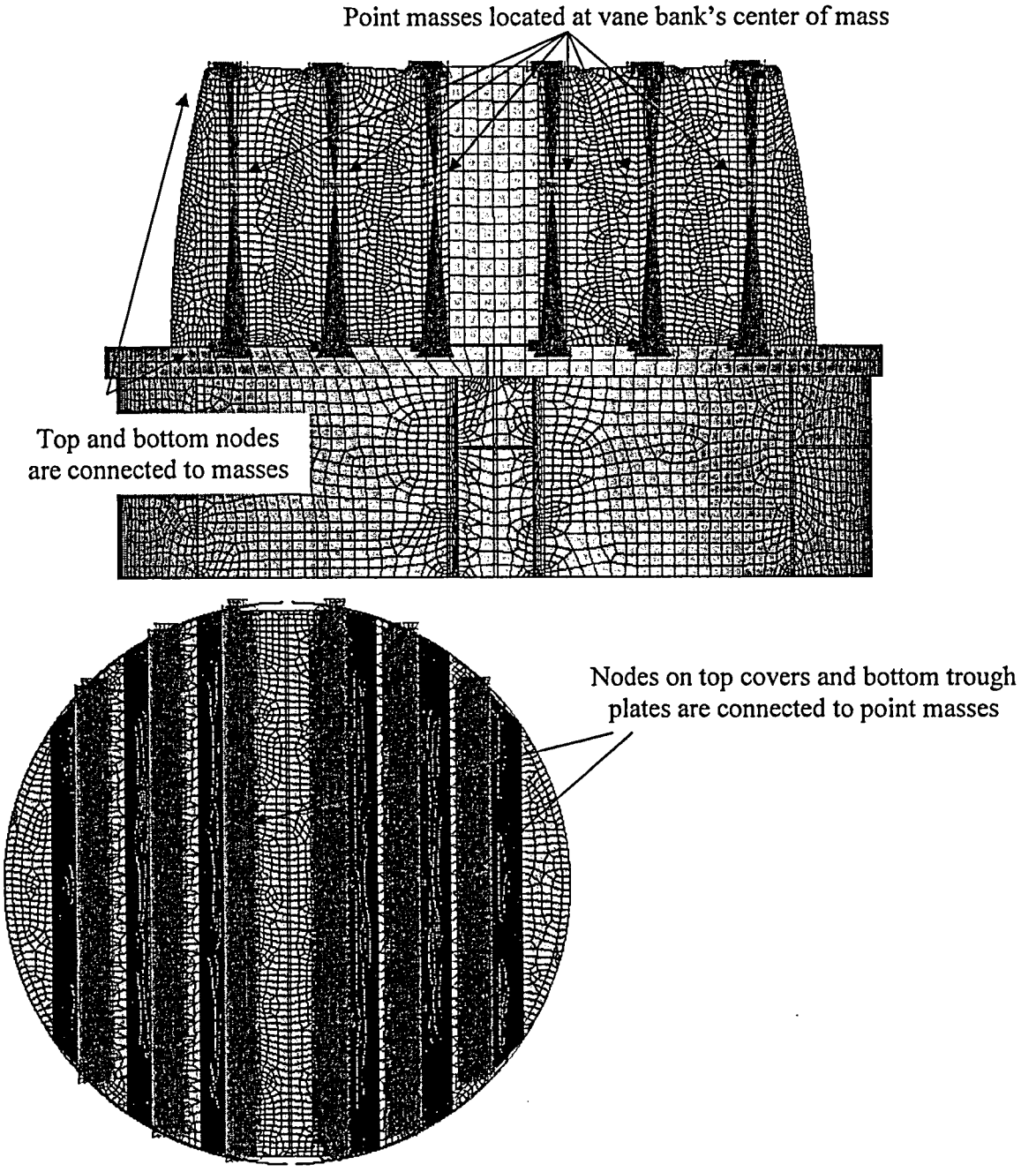

Figure 7. Point masses representing the vanes. The pink shading represents where constraint equations between nodes are applied in the point mass implementation.

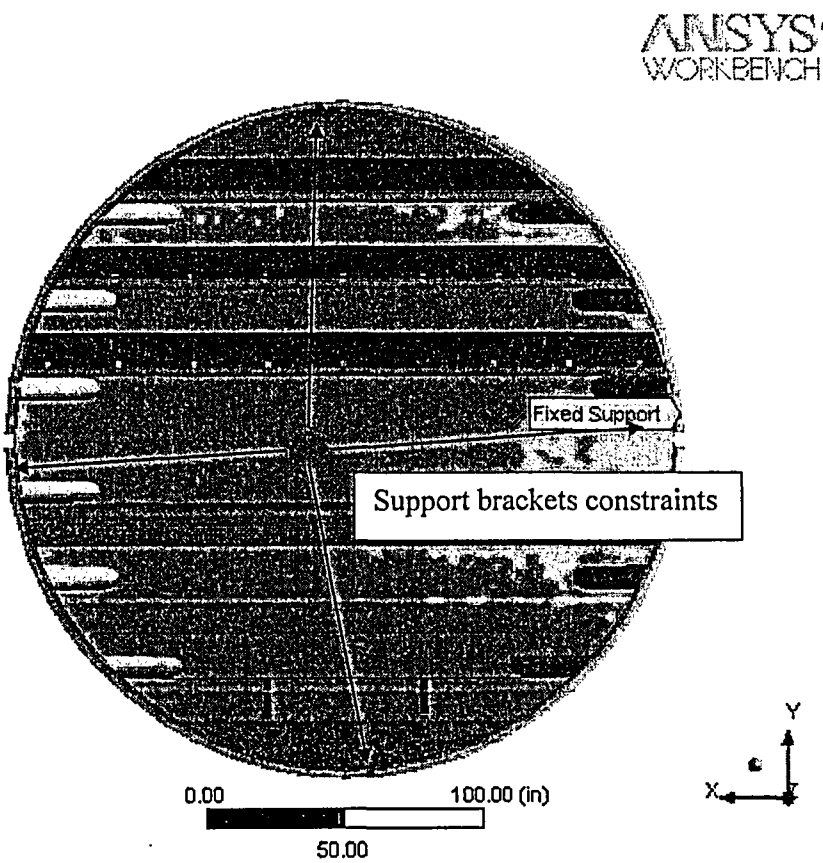

Figure 8. Fixed support constraints.

Table 2. FE Model Summary.

Description	Quantity
Total Nodes	93,951
Total Structural Elements	126,322
Element Types	5
Materials	3

Table 3. Listing of Element Types.

Generic Element Type Name	Element Name	ANSYS Name
20-Node Quadratic Hexahedron	SOLID186	20-Node Hexahedral Structural Solid
4-Node Elastic Shell	SHELL63	4-Node Elastic Shell
4-Node Linear Quadrilateral Shell	SHELL181	4-Node Finite Strain Shell
Mass Element	MASS21	Structural Mass
Pressure Surface Definition	SURF154	3D Structural Surface Effect

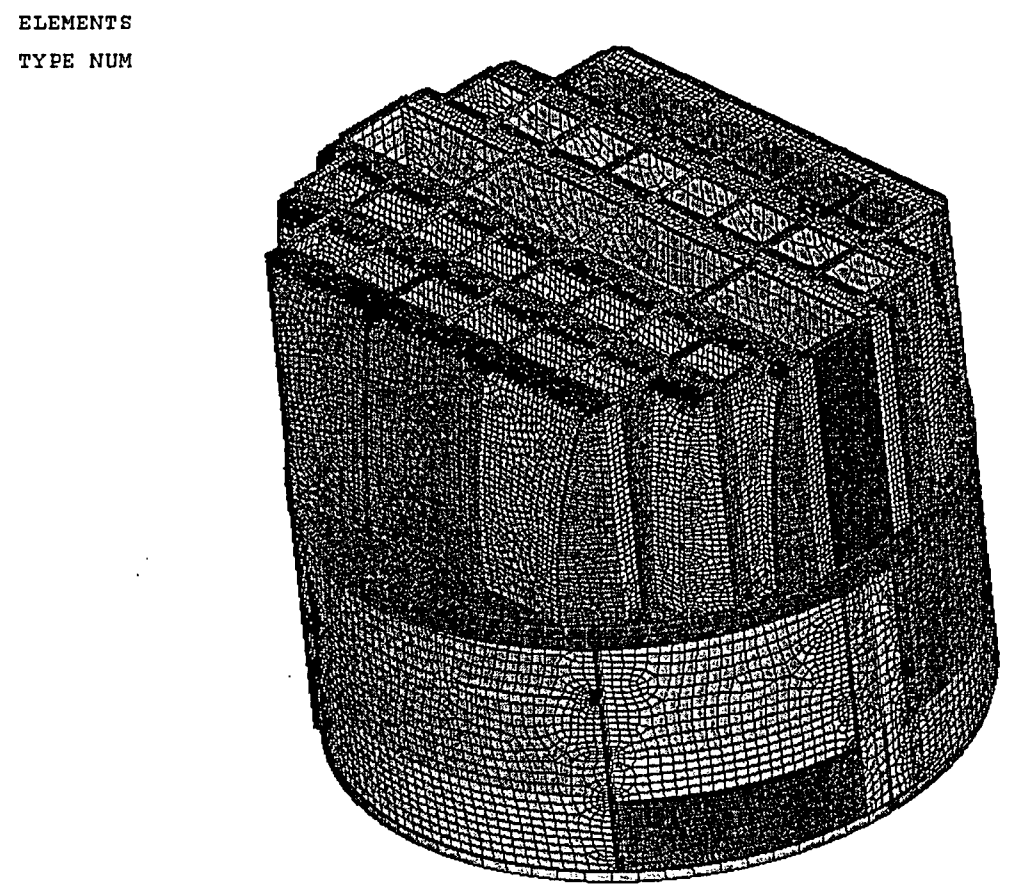

Figure 9a. Mesh overview. The colors emphasize element type.

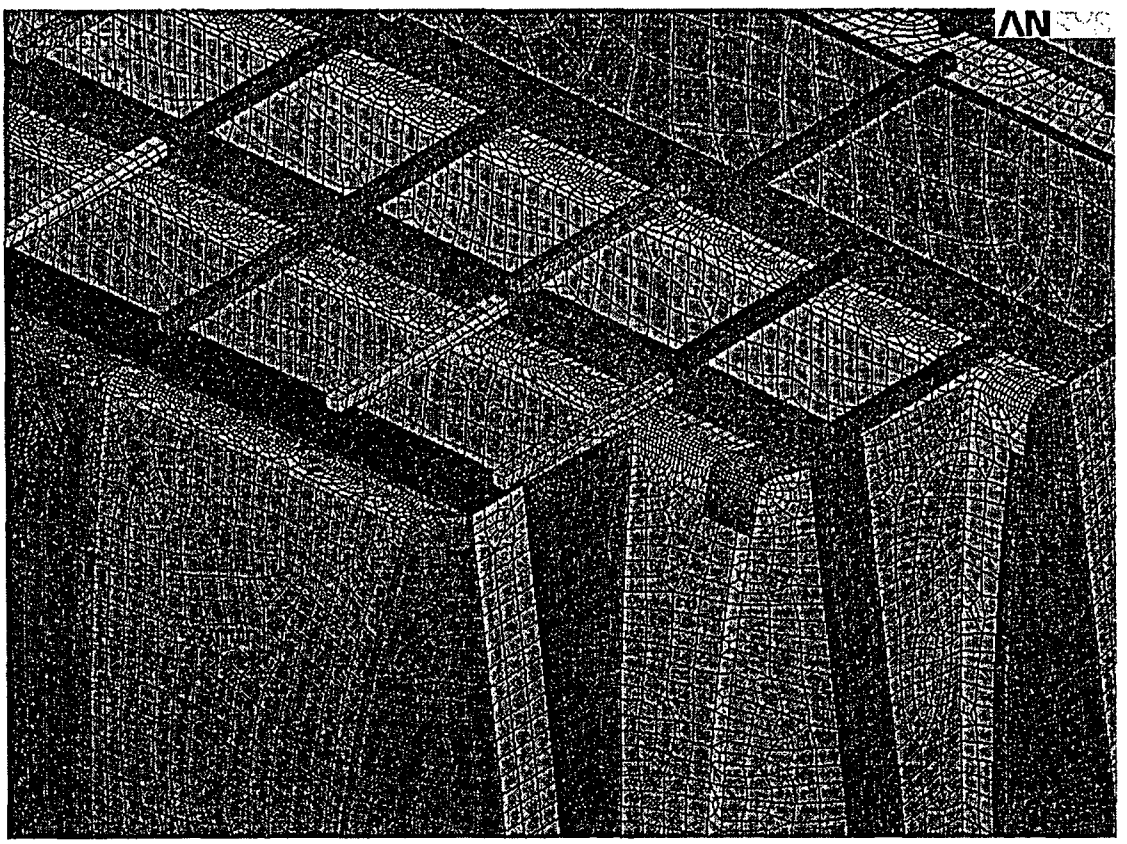

Figure 9b. Close up of mesh showing hoods, reinforcement panels, and tie bars. The colors emphasize element type.

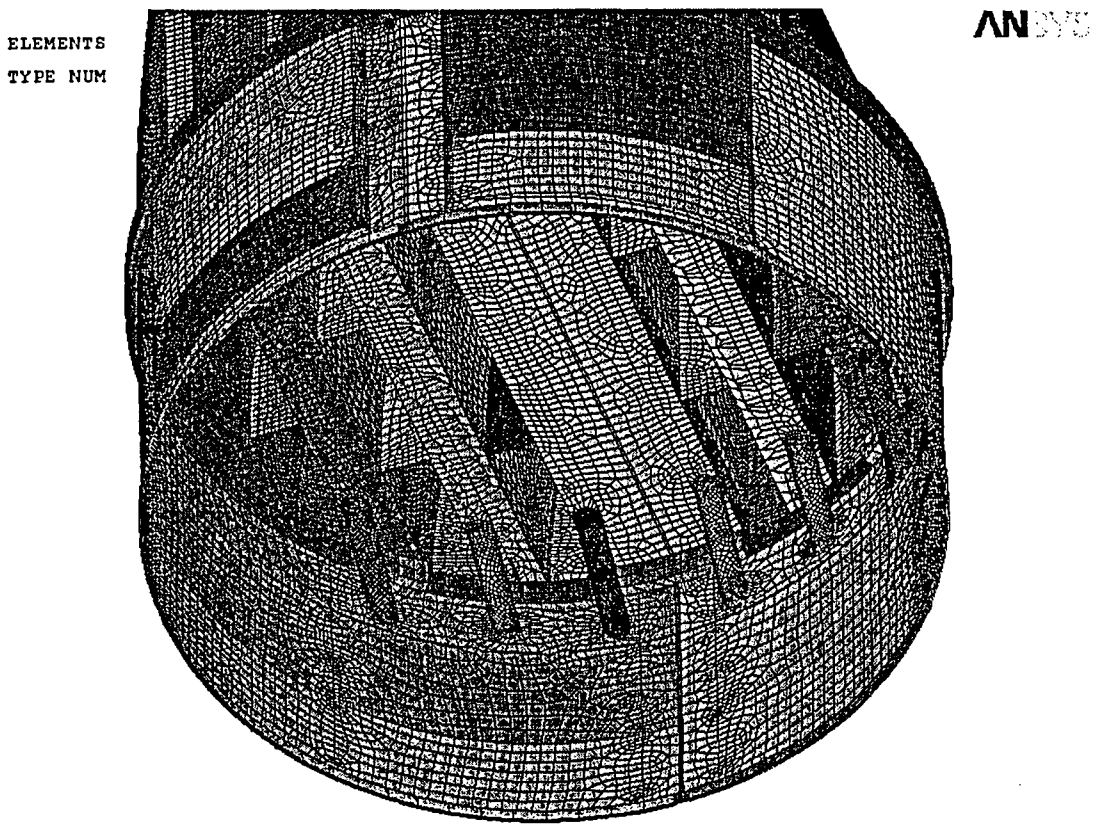

Figure 9c. Close up of mesh showing drain pipes and hood supports. The colors emphasize element type.

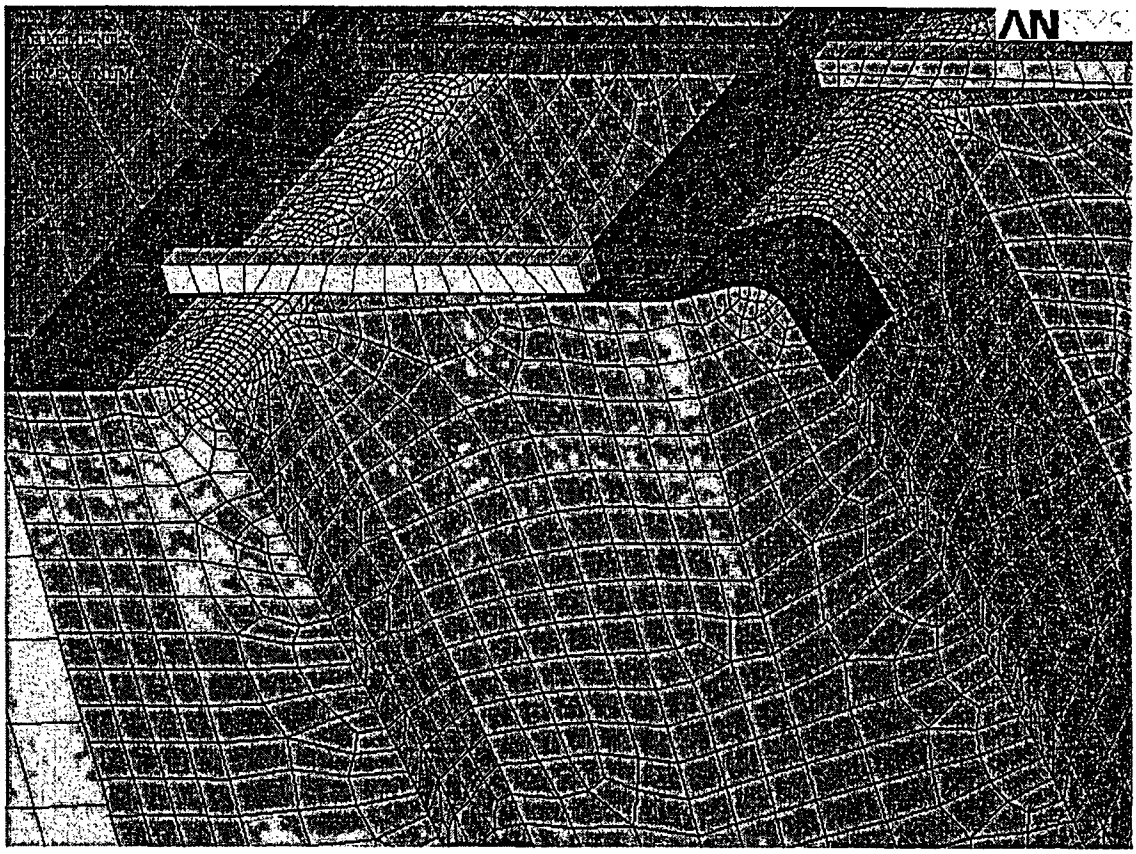

Figure 9d. Close up of mesh showing node-to-node connections between closure plates, end plates, and hoods. The colors emphasize element types.

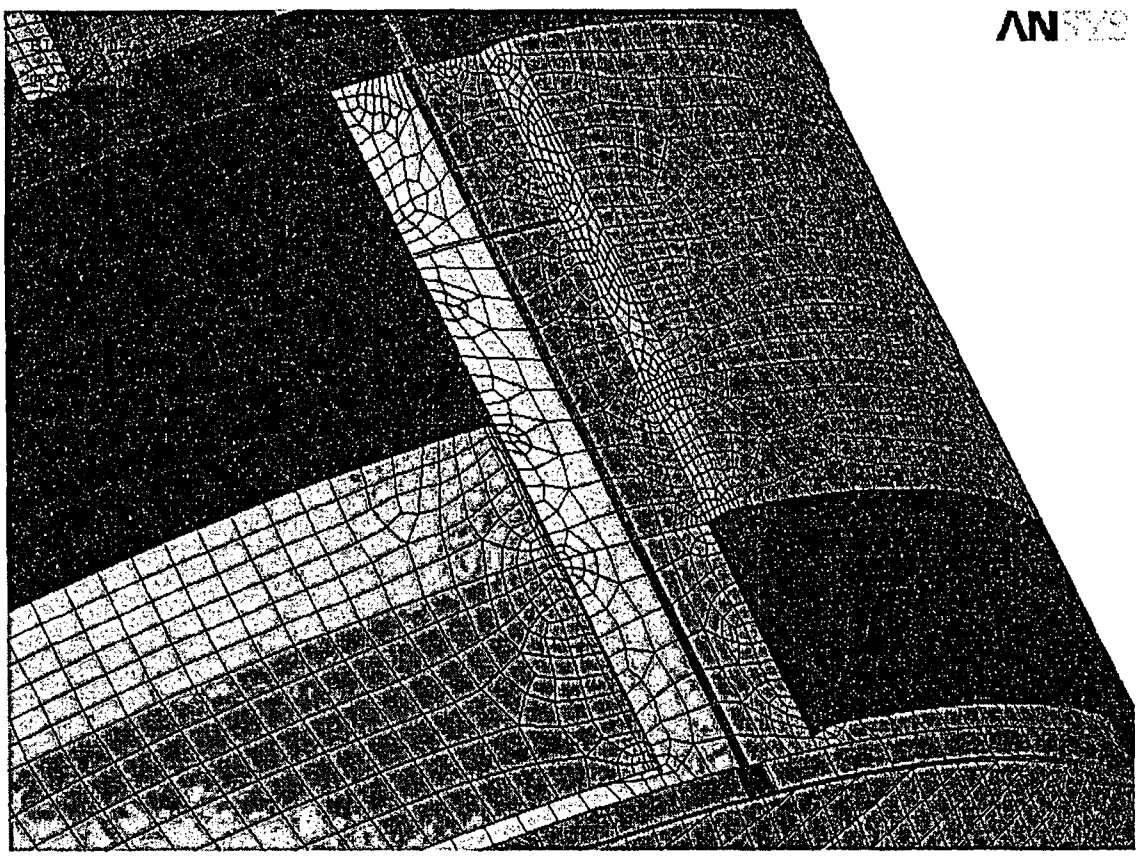

Figure 9e. Close up of mesh showing node-to-node connections between the skirt and drain channels. The colors emphasize element type.

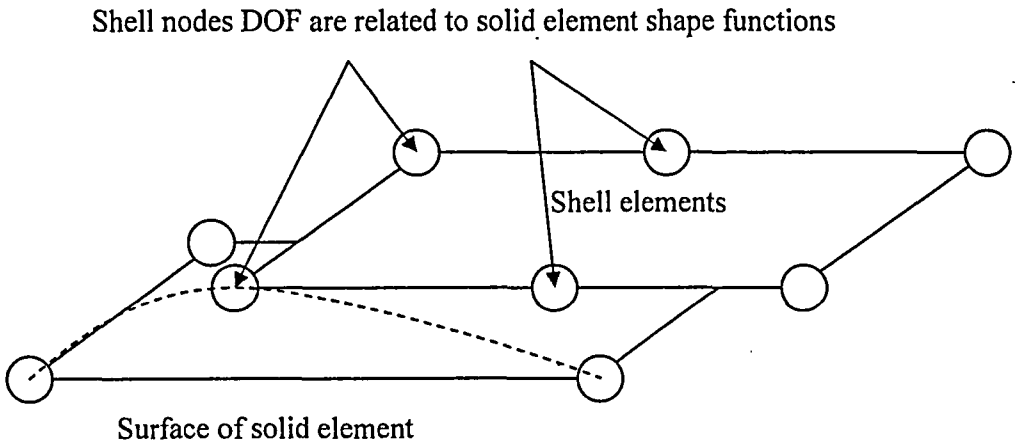

Figure 10a. Face-to-face shell to solid connection.

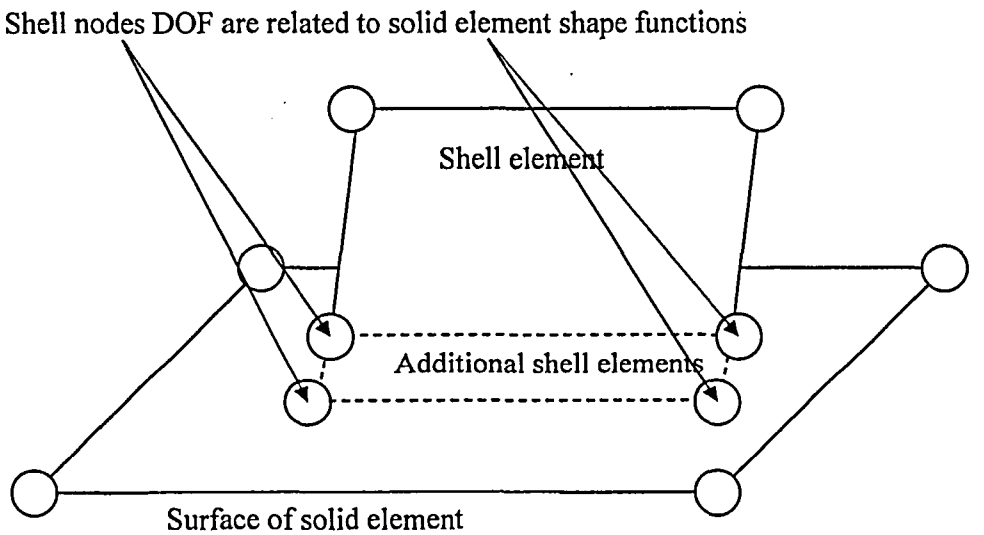

Figure 10b. Shell edge-to-solid face connection.

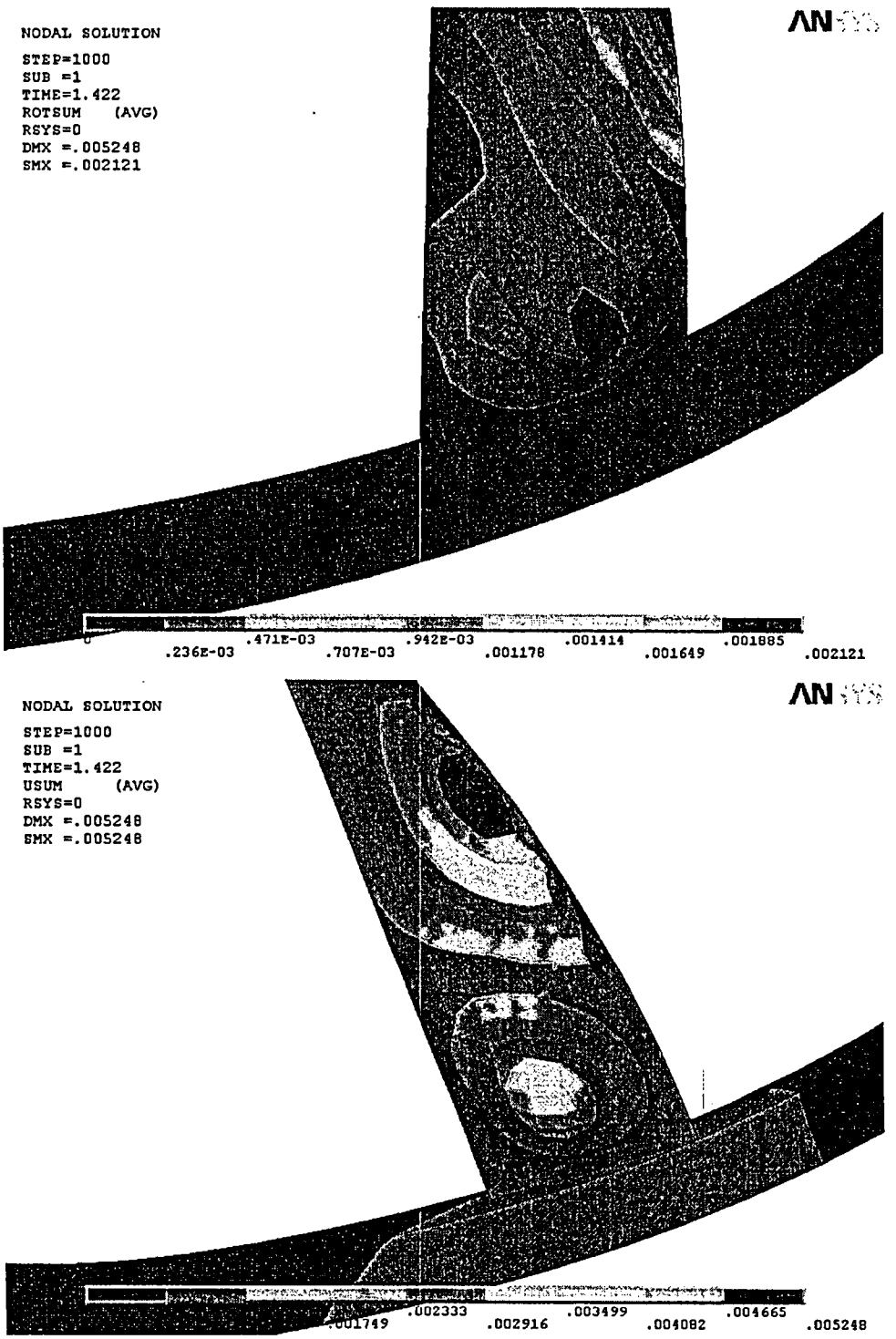

Figure 11. Shell edge-to-solid face connection between inlet end plate and upper support ring. Rotations (top) and displacements (bottom). Time t=1.422 sec.

4. Structural Analysis

The solution is decomposed into static and transient parts. The static solution produces the stress field induced by the supported structure subjected to its own weight, whereas the transient solution accounts for the unsteady stress field due to the acoustic loads acting on the dryer. The two solutions are linearly combined to obtain the final displacement and stress histories. This decomposition facilitates prescription of the added mass model accounting for hydrodynamic interaction and allows one to compare the stress contributions arising from static and unsteady loads separately. Alternating stresses are independent of static loads and thus can be obtained using only the transient response due to pressure loads. Proper evaluation of the peak membrane and membrane+bending stresses, however, requires that the static loads due to weight be accounted for. Hence both static and transient analyses must be carried out.

4.1 Static Analysis

The results of the static analysis are shown on Figure 12. Only a few locations exhibited high stress intensity levels. These locations include the skirt/upper support ring connection with stress intensity 8,775 psi, the trough thin section/vane bank end plate/thick closure plate junction with stress intensity 5,416 psi and the thin closure plate/inner hood junction with stress intensity 8,133 psi. All locations are near the steam dryer support brackets. The locations with high static stress intensity are shown in Figure 13. Note that these locations have high stress intensity also when static and transient runs are combined, primarily due to static loading.

4.2 Transient Analysis

The fluctuating pressure loads were applied to the structural model at all surface nodes described in Section 2.3. The pressures were varied at increments of 1.422×10^{-3} sec for 1405 time steps both for CLTP and EPU loadings – a total time of 2 sec. For the EPU cases with frequency shift the same 1405 steps of EPU loading were used, but with different time steps: 1.28×10^{-3} sec with total time 1.8 sec for scaling 10% up, and 1.564×10^{-3} sec with total time 2.2 sec for scaling 10% down. These stress results are discussed in Section 5. Typical stress intensity distributions over the structure are shown in Figure 14.

To evaluate peak stresses, the static and transient stresses were combined and peak stress intensities during the response, evaluated. According to ASME B&PV Code, Section III, Subsection NG-3216.2 the following procedure was established to calculate alternating stresses. For every node, the stress difference tensors, $\sigma'_{nm} = \sigma_n - \sigma_m$, were considered for all possible pairs of the stresses σ_n and σ_m at different time levels, t_n and t_m. Note that all possible pairs require consideration since there are no 'obvious' extrema in the stress responses. For each stress difference tensor, the principal stresses S_1, S_2, S_3 were computed and the maximum absolute value among principal stress differences, $S_{nm} = \max\{|S_1 - S_2|, |S_1 - S_3|, |S_2 - S_3|\}$, obtained. The alternating stress at the node was then one-half the maximum value of S_{nm} taken over all combinations (n,m), i.e., $S_{alt} = \frac{1}{2}\max_{n,m}\{S_{nm}\}$. This alternating stress was compared against allowable values, depending on the node location with respect to welds.

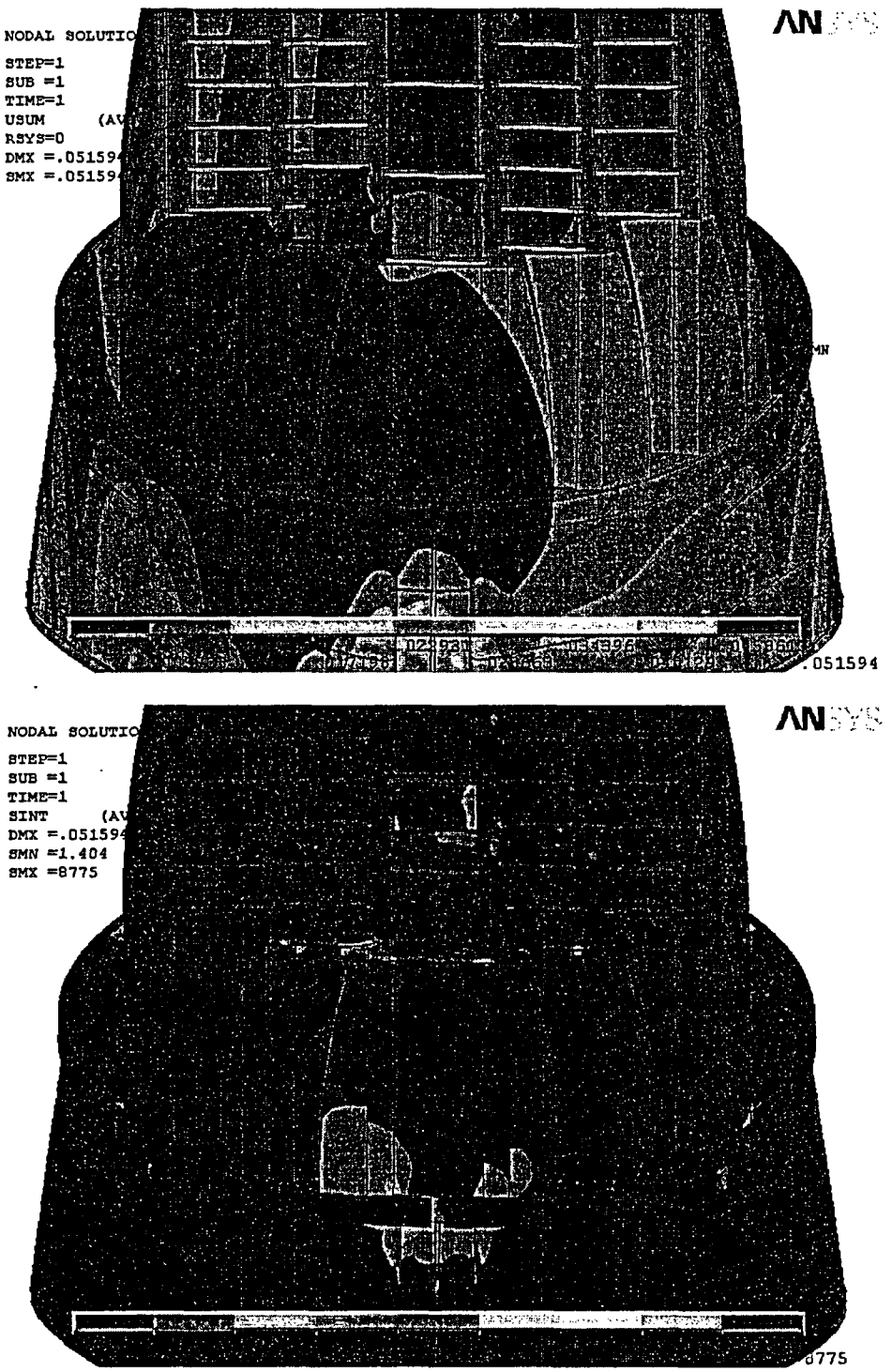

Figure 12. Overview of static calculations showing displacements (top, in inches) and stress intensities (bottom, in psi). Maximum displacement (DMX) is 0.052"; maximum stress intensity (SMX) is 8,775 psi.

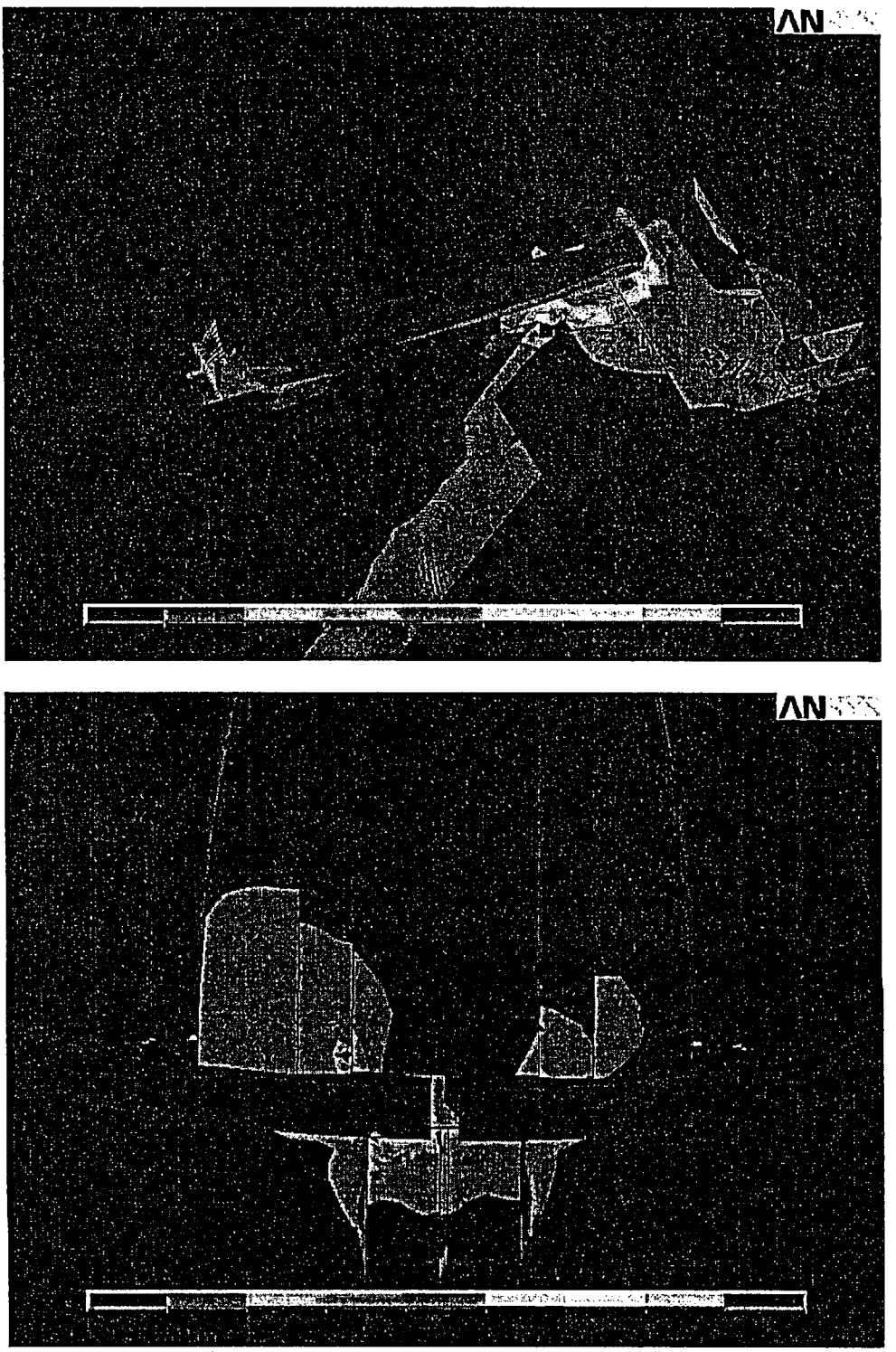

Figure 13. Close up of high static stress intensity (in psi) locations at closure plates and near support brackets.

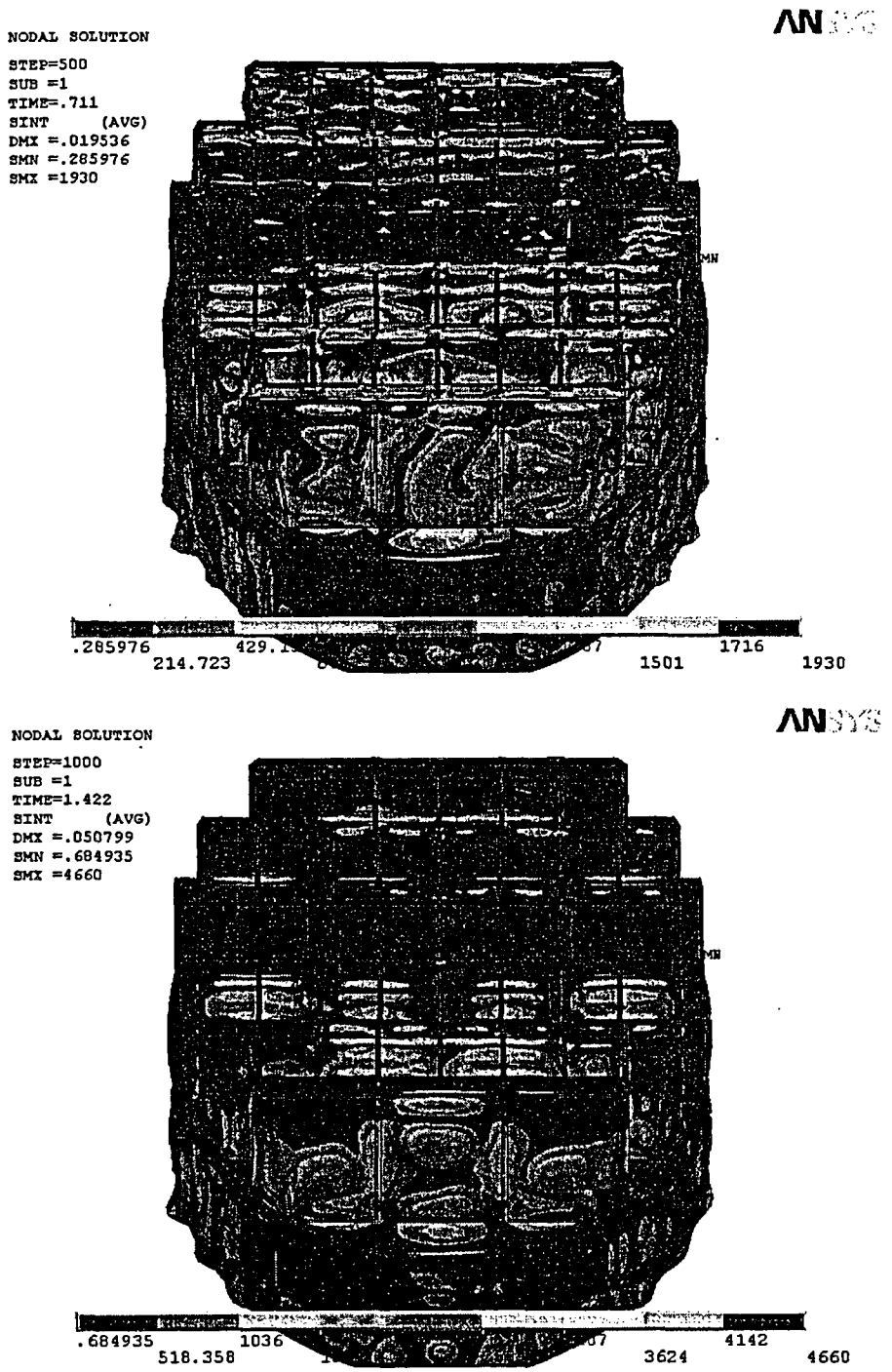

Figure 14a. Overview of transient calculations for CLTP loading showing stress intensities (in psi) along with displacements. Time step 500 (top) and 1000 (bottom).

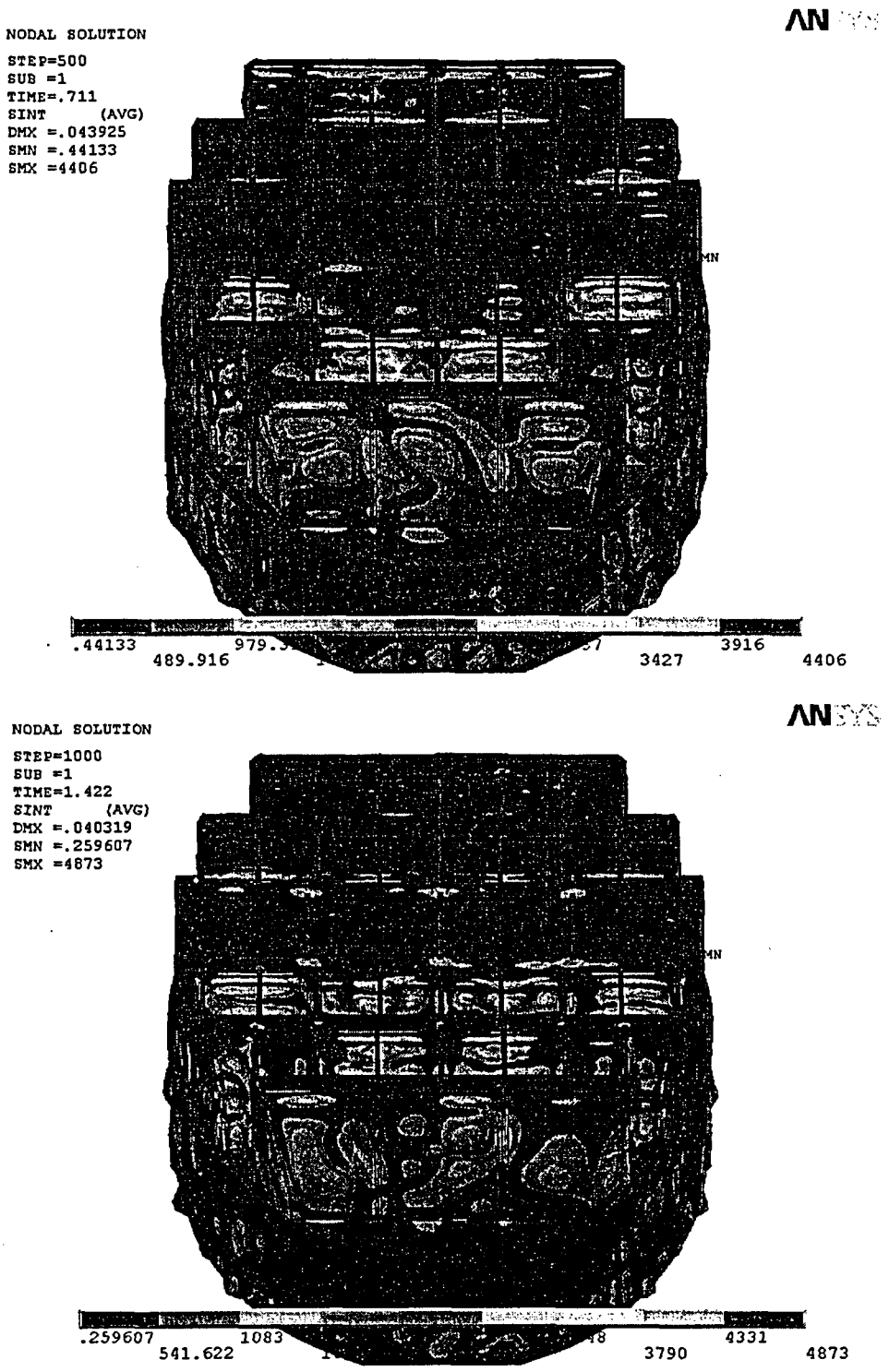

Figure 14b. Overview of transient calculations for EPU loading showing stress intensities (in psi) along with displacements. Time step 500 (top) and 1000 (bottom).

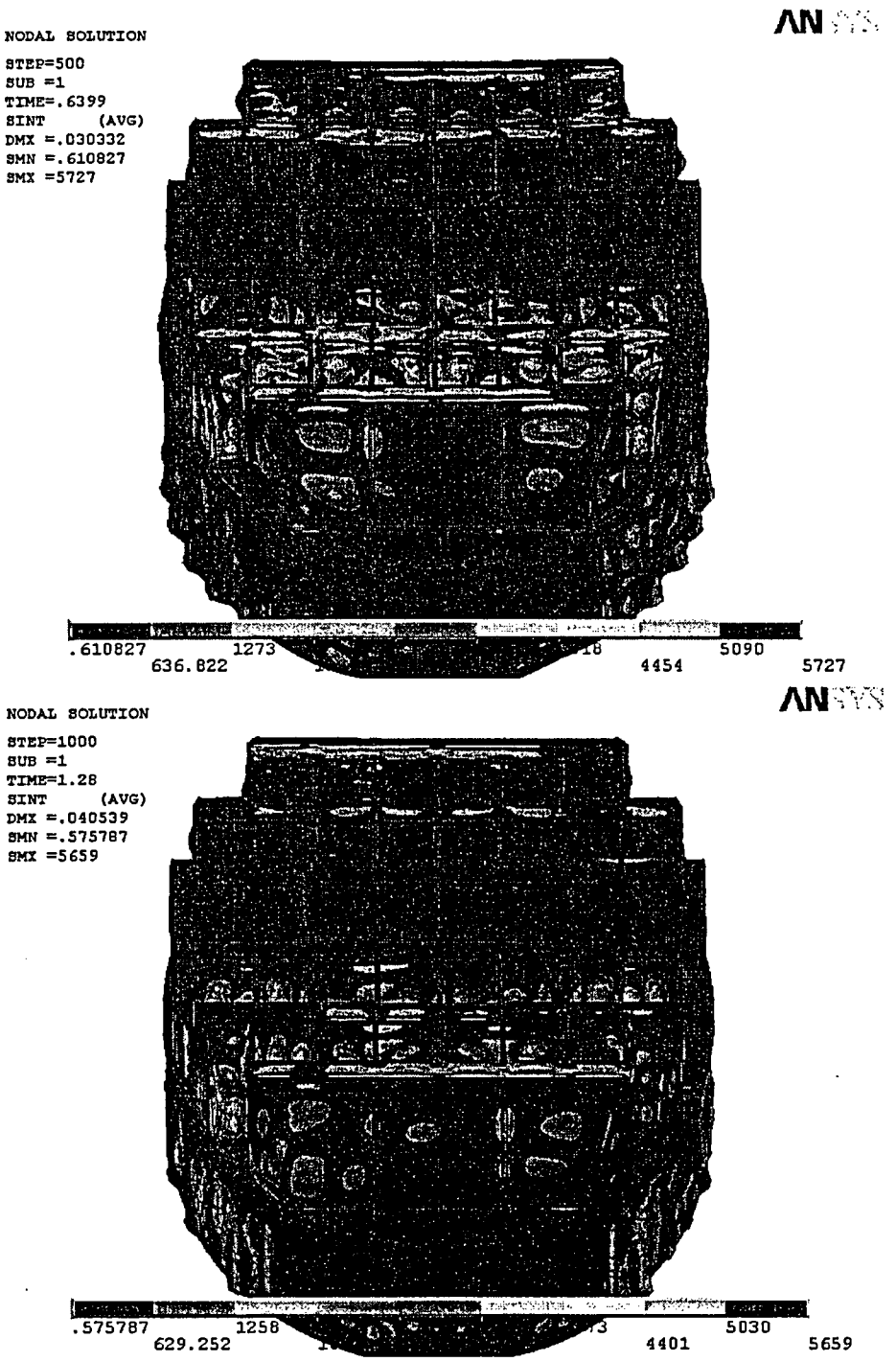

Figure 14c. Overview of transient calculations for EPU loading with +10% frequency shift showing stress intensities (in psi) along with displacements. Time step 500 (top) and 1000 (bottom).

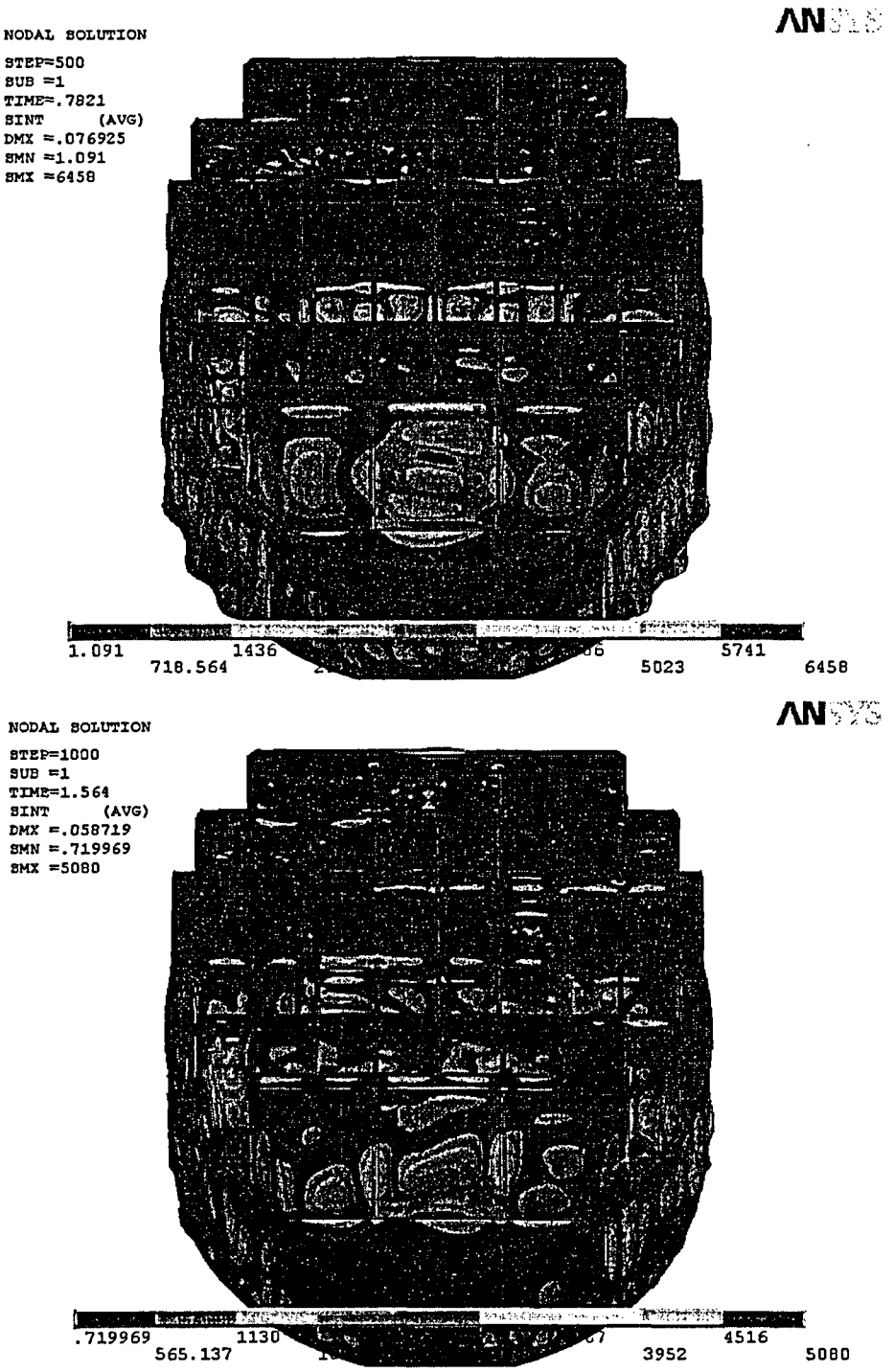

Figure 14d. Overview of transient calculations for EPU loading with -10% frequency shift showing stress intensities (in psi) along with displacements. Time step 500 (top) and 1000 (bottom).

4.3 Post-Processing

The static and transient stresses computed at every node with the ANSYS program were exported into files for subsequent post-processing. These files were then read in with separate customized software to compute the peak and alternating stresses at every node. The peak stress was defined for each node as the largest stress intensity occurring during the time history. Alternating stresses were calculated according to the ASME standard described above. For shell elements the peak stresses were calculated separately at the mid-plane, where only membrane stress is present, and at top/bottom of the shell, where bending stresses are also present.

For nodes that are shared between several structural components or lie on junctions, the peak and alternating stress intensities are calculated as follows. First the nodal stress tensor is computed separately for each individual component by averaging over all finite elements meeting at the node and belonging to the same structural component. The time histories of these stress tensors are then processed to deduce the peak and alternating stress intensities for each structural component. Finally for nodes shared across multiple components the maximum of the peak and alternating stresses is recorded as the 'nodal' stress. This approach prevents averaging of stresses across components and thus yields conservative estimates for nodal stresses at the weld locations where several components are joined together.

The peak stresses are compared against allowables values which depend upon the stress type (membrane, membrane+bending, alternating – Pm, Pm+Pb, S_{alt}) and location (at a weld or away from welds). These allowables are specified in the following section. For solid elements the most conservative allowable, Pm for membrane stress, is used, although bending stresses are nearly always present also. The structure is then assessed in terms of stress ratios formed by dividing allowables by the computed stresses at every node. Stress ratios less than unity imply that the associated peak and/or alternating stress intensities exceed the allowable levels. Post-processing tools calculate the stress ratios, identifying the nodes with low stress ratios and generating files formatted for input to the 3D graphics program, TecPlot, which provides more general and sophisticated plotting options than currently available in ANSYS.

The unsteady pressure loads applied to the dryer contain a strong 80Hz component (see Figure 5) which is not present in the plant. The erroneous signal is caused by the interaction between sensors used to record the unsteady pressures. The stress assessment was therefore performed with the 80Hz signal removed. Since the problem is linear, forcing the structure at a given frequency produces a steady state response at the same frequency. Therefore, attenuating the 80Hz signal is equivalent to attenuating the resulting stress response. Thus, rather than repeating the structural dynamics calculation, the 80Hz signal was simply filtered from the existing stress histories prior to calculating the peak and alternating stresses. For EPU cases with frequency shift 10% up and down, the components 88 Hz and 72 Hz respectively were removed.

4.4 Computation of Stress Ratios for Structural Assessment

The ASME B&PV Code, Section III, subsection NG provides different allowable stresses for different load combinations and plant conditions. The stress levels of interest in this analysis are

for the normal operating condition, which is the Level A service condition. The load combination for this condition is:

Normal Operating Load Combination = Weight + Pressure + Thermal

The weight and fluctuating pressure contributions have been calculated in this analysis and are included in the stress results. The static pressure differences and thermal expansion stresses are small, since the entire steam dryer is suspended inside the reactor vessel and all surfaces are exposed to the same conditions. Seismic loads only occur in Level B and C cases, and are not considered in this analysis.

Allowable Stress Intensities

The ASME B&PV Code, Section III, subsection NG shows the following (Table 4) for the maximum allowable stress intensity (Sm) and alternating stress intensity (Sa) for the Level A service condition. The allowable stress intensity values for type 304 stainless steel at operating temperature 550°F are taken from Table I-1.2 and Fig. I-9.2.2 of Appendix I of Section III, the ASME B&PV Code. The calculation for different stress categories is performed in accordance with Fig. NG-3221-1 of Division I, Section III, subsection NG.

Table 4. Maximum Allowable Stress Intensity and Alternating Stress Intensity for all areas other than welds. The notation Pm represents membrane stress; Pb represents stress due to bending; Q represents secondary stresses (from thermal effects and gross structural discontinuities, for example); and F represents peak stresses (due to local structural discontinuities, for example).

Type	Notation	Calculation	Allowable Value (psi)
Peak Stress Allowables:			
General Membrane	Pm	Sm	18,300
Membrane + Bending	Pm + Pb	1.5 Sm	27,450
Primary + Secondary	Pm + Pb + Q	3.0 Sm	54,900
Alternating Stress Allowable:			
Primary + Secondary + Peak	S_{alt}	Sa	13,600

When evaluating welds, either the calculated or allowable stress was adjusted, to account for a stress concentration factor. Specifically:

- For maximum allowable stress intensity, the allowable value is decreased by multiplying its value in Table 6.1 by 0.55.

- For alternating stress intensity, the calculated weld stress intensity is multiplied by a weld stress intensity (fatigue) factor of 1.8, before comparison to the Sa value given above.

The factors of 0.55 and 1.8 were selected based on the observable quality of the shop welds and NDE testing of all welds (excluding tack and intermittent welds) during fabrication. GE Purchase Specification for the HCGS Steam Dryer (21A9355 Section 9.2) called for liquid penetrant testing of all welds (excluding tack and intermittent welds) along the entire length or

circumference, using the guidance of ASME Boiler and Pressure Code, Paragraph N-6127.3. In addition, critical welds are subject to periodical visual inspections in accordance with the requirements of GE SIL 644. Therefore, for weld stress intensities, the allowable values are shown in Table 5.

Table 5. Weld Stress Intensities.

Type	Notation	Calculation	Allowable Value (psi)
Peak Stress Allowables:			
General Membrane	Pm	0.55 Sm	10,065
Membrane + Bending	Pm + Pb	0.825 Sm	15,098
Primary + Secondary	Pm + Pb + Q	1.65 Sm	30,195
Alternating Stress Allowables:			
Primary + Secondary + Peak	S_{alt}	Sa	13,600

Comparison of Calculated and Allowable Stress Intensities

The classification of stresses into general membrane or membrane + bending types was made according to the exact location, where the stress intensity was calculated; namely, general membrane, Pm, for middle surface of shell element, and membrane + bending, Pm + Pb, for other locations. For solid elements the most conservative, general membrane, Pm, allowable is used.

The structural assessment is carried out by computing stress ratios between the computed peak and alternating stress intensities, and the allowable levels. Locations where any of the stresses exceed allowable levels will have stress ratios less than unity. Since computation of stress ratios and related quantities within ANSYS is time-consuming and awkward, a separate FORTRAN code was developed to compute the necessary peak and alternating stress intensities, Pm, Pm+Pb, and S_{alt}, and then compare it to allowables. Specifically, the following quantities were computed at every node:

1. The peak membrane stress intensity, Pm (evaluated at the mid-thickness location for shells),
2. The peak stress intensity, Pm+Pb, (taken as the maximum of the peak stress intensity values at the bottom, top, and mid thickness locations, for shells),
3. The peak alternating stress, S_{alt}, (the maximum value over the three thickness locations is taken).
4. The minimum peak stress ratio assuming the node lies at a non-weld location:
   SR-P(nw) = min{ Sm/Pm, 1.5 * Sm/(Pm+Pb) }.
5. The alternating stress ratio assuming the node lies at a non-weld location,
   SR-a(nw) = Sa / (1.1 * S_{alt}),
6. The same as 4, but assuming the node lies on a weld,
   SR-P(w)=SR-P(nw)*0.55.
7. The same as 5, but assuming the node lies on a weld,
   SR-a(w)=SR-a(nw)/1.8.

Note that in steps 4 and 6, the minimum of the stress ratios based on Pm and Pm+Pb, is taken. The allowables listed in Table 4, Sm=18,300 psi and Sa=13,600 psi. The factors, 0.55 and 1.8, are the weld factors discussed above. The factor of 1.1 accounts for the differences in Young's moduli for the steel used in the steam dryer and the values assumed in alternating stress allowable. According to NG-3222.4 the effect of elastic modulus upon alternating stresses is taken into account by multiplying alternating stress S_{alt} at all locations by the ratio, $E/E_{model}=1.1$, where:

$E = 28.3\ 10^6$ psi, as shown on Fig. I-9.2.2. ASME BP&V Code
$E_{model} = 25.55\ 10^6$ psi (Table 2.1)

The nodes with stress ratios lower than 4 are plotted in TecPlot to establish whether they lie on a weld or not. The appropriate peak and alternating stress ratios, SR-P and SR-a, are thus determined and a final listing of nodes having minimum stress ratios is generated. Nodes identified as having the smallest stress ratios are listed below, in Table 7. The corresponding locations are depicted in Figure 19 to Figure 22.

5. Results

5.1 General Stress Distribution and Maximum Stress Locations

The maximum stress intensities obtained by post-processing the ANSYS stress histories for CLTP, EPU and EPU with frequency shift operating conditions are listed in Table 6. Contour plots of the peak and alternating stress intensities over the steam dryer structure are shown on Figure 15 (CLTP), Figure 16 (EPU), Figure 17 (EPU with -10% frequency shift), and Figure 18 (EPU with +10% frequency shift). The figures are oriented to emphasize the maximum stress regions. Note that these stress intensities *do not* account for weld factors. Further, it should be noted that since the allowable stresses vary with location, peak stress intensities do not necessarily correspond to regions of primary structural concern. Instead, structural evaluation is more accurately made in terms of the stress ratios which compare the computed stresses to allowable levels with due account made for stress type and weld factors. Comparisons on the basis of stress ratios are made in Section 5.2.

The tabulated stresses are obtained by computing the relevant stress intensities at every node and then sorting the nodes according to stress levels. The maximum stress node is noted and all neighboring nodes within 10 inches of the maximum stress node and its symmetric images (i.e., reflections across the x=0 and y=0 planes) are 'blanked' (i.e., excluded from the search for subsequent peak stress locations). Of the remaining nodes, the next highest stress node is identified and its neighbors (closer than 10 inches) blanked. The third highest stress node is similarly located and the search continued in this fashion until all nodes are either blanked or have stresses less than half the peak value on the structure or stress ratios lower than 4. The blanking of neighboring nodes is intended to prevent extracting peak stress nodes from essentially the same location on the structure.

Under both CLTP and EPU conditions the maximum stress intensities in most areas are low (less than 500 psi, or 5% of the most conservative critical stress). For the membrane stresses (Pm) the high stress regions come in three varieties. First, there are diffuse regions of high Pm over the curved hoods which directly result from the unsteady pressure loading. These stresses are generally well within allowables because they occur away from welds and do not have a significant static load component. While the outer hoods generally carry the brunt of the unsteady loading, the middle and inner hoods are also subjected to significant loads and, because they are thinner, they experience higher stresses. The second variety of high membrane stress occurs at the junctions of hood with adjoining structures – tie bars, closure plates and cover plates. These regions are more localized and are more critical from a structural assessment perspective because they contain welds and in some cases (tie bars and closure plates) also support significant static loads. The third variety is the localized stress in the vicinity of the dryer support mounts where the static load component tends to dominate.

The membrane + bending stress (Pm+Pb) distributions are quite different and show evidence of significant modal response in all cases. Modal excitations are most pronounced at EPU conditions with the +10% frequency shift (Figure 18b) where vibrations are most evident in the drain channels and the middle hoods outside of the thin closure plates. Again stress concentrations are also observed, particularly where the thin closure plates connect to the hoods

or vane banks, along the skirt/drain channel welds and where the curved hoods join to the vane end plates.

The alternating stress, S_{alt}, distributions are qualitatively similar to those for Pm+Pb. The modal excitations in the skirt region are now even more pronounced at the EPU conditions. For the case with +10% frequency shift, the modes are higher order (see Figure 18c) compared to the other EPU and CLTP cases where the alternating stress distribution over the curved hoods appears more diffuse indicating lower order modes. The skirt response occurs at approximately 120Hz and leads to high stresses in the submerged portion. Similar drain channel response modes and accompanying high stresses have appeared here in other calculations using alternate element types, mesh sizes, connection methods (bonded contacts) and hydrodynamic mass models. Since this region is not subjected to pressure loads it manifests a modal excitation which is not surprising since the drain channels and skirt are thin (and therefore easily excited) and of large dimension so that they support a significant number of response modes over the applied load frequency range. It appears therefore that the loading applied to the upper portion of the skirt above the waterline as well as to the structure above the upper support ring, incites one or more of the drain channel modes near resonance.

At EPU conditions, shifting the frequencies by ±10% has a more pronounced influence upon the bending stresses which is expected since most of the response modes involve bending. Shifting the frequencies up or down by 10% reduces the membrane stresses in both cases compared to the non-shifted results. Reducing frequencies by 10%, increases both the peak Pm+Pb stresses and alternating stresses, S_{alt}. Increasing frequencies by 10% produces a larger increase in S_{alt}, but actually reduces Pm+Pb. It is also interesting to note that for each of the load conditions, the alternating stresses can fall off in markedly different rates. Thus, at CLTP the top five stresses differ by less than 10%. At EPU conditions the difference is higher (38%) and at EPU with a 10% shift, the differences rise to 68%. This isolation of peak stress locations is further evidence of the excitation of only a small number of modes at the EPU conditions.

Table 6a. Locations with highest predicted stress intensities for 1/8th scale CLTP conditions.

Stress Category	Location		Location (in)				Stress Intensities (psi)		
		Weld	x	y	z	node	Pm	Pm+Pb	S_{alt}
Pm	1. Inner hood (top) near closure plate	No	109.0	-27.6	95.3	44886	7017	10033	1908
"	2. Upper ring / thick closure plate / vane end plate	Yes	-118.8	14.4	7.5	85994	4317	5915	465
"	3. Skirt / upper support ring	Yes	118.7	-5.9	-2.0	91960	4177	6002	707
"	4. Inner hood (bottom) / closure plate	Yes	-108.4	38.4	8.1	87035	4177	4354	956
"	5. Middle vane bank / closure plate (top)	Yes	-108.4	45.9	95.9	85891	4169	5237	1367
Pm+Pb	1. Inner hood (top) near closure plate	No	109.0	-27.6	95.3	44886	7017	10033	1908
"	2. Skirt / upper support ring	Yes	-118.8	-0.6	-2.0	79487	2556	9778	1276
"	3. Outer hood bottom / cover plate	Yes	59.1	101.4	7.5	93493	1793	7688	3431
"	4. Skirt / 45° drain pipe	Yes	88.2	79.6	-20.5	91083	2297	6663	1511
"	5. Upper ring / thick closure plate / vane end plate	Yes	-118.8	14.4	7.5	85994	4317	5915	465
S_{alt}	1. Lower inner hood	No	27.9	36.0	50.5	42098	1609	4015	3549
"	2. Drain channel (bottom) / skirt	Yes	118.2	-12.0	-94.3	93818	2219	3705	3496
"	3. Outer hood bottom / cover plate	Yes	59.1	101.4	7.5	93493	1793	7688	3431
"	4. Lower middle hood	No	25.6	69.3	29.9	37254	608	3838	3253
"	5. Middle hood (half-height)	No	-25.2	67.1	53.3	37915	817	3642	3230

Node numbers are retained for further reference.
Spatial coordinate are in the coordinate system, defined by the origin at the centerline of steam dryer 7.5" below bottom plates. The x-axis is parallel to the hoods, y-axis is normal to the hoods pointing from MSL AB to MSL CD, z-axis is vertical, positive up.
Thin closure plates - the 3/16 inch plates on the steam outlet side of the outer and middle vane banks. The straight vertical edge is welded to the vane bank end plate and on curved vertical edge is welded to the outside of the curved hood. These plates ensure that the steam exiting the vane banks is directed upward into the dome.
Thick closure plate - this 1/2 inch plate performs the same function as the thin closure plate, but it spans the steam outlet space between two inner hoods vane banks.
Supports - the vertical stiffeners on the inside of the hoods. The straight vertical edge is welded to the inlet of the vane bank assembly. The curved vertical edge is welded to the inside of the hood.

Table 6b. Locations with highest predicted stress intensities for 1/8th scale EPU conditions.

Stress Category	Location		Location (in)				Stress Intensities (psi)		
		Weld	x	y	z	node	Pm	Pm+Pb	S_{alt}
Pm	1. Inner hood (top) near closure plate	No	109.0	-27.6	95.3	44886	7860	11320	3138
"	2. Upper ring / thick closure plate / vane end plate	Yes	-118.8	14.4	7.5	85994	4613	6270	791
"	3. Middle vane bank / closure plate (top)	Yes	108.4	-45.9	95.9	91627	4562	5949	2216
"	4. Skirt / upper support ring	Yes	118.7	-5.9	-2.0	91960	4560	6634	1253
"	5. Middle hood / thin closure plate	Yes	-84.7	-59.3	95.0	85091	4411	6873	5064
Pm+Pb	1. Inner hood (top) near closure plate	No	109.0	-27.6	95.3	44886	7860	11320	3138
"	2. Skirt / upper support ring	Yes	-118.8	-0.6	-2.0	79487	2611	10733	2021
"	3. Outer hood bottom / cover plate	Yes	59.1	101.4	7.5	93493	1932	10689	6068
"	4. Drain channel (bottom) / skirt	Yes	118.2	12.0	-94.3	90843	2267	7586	5381
"	5. Skirt / 45° drain pipe	Yes	88.2	79.6	-20.5	91083	2575	7302	1913
S_{alt}	1. Drain channel (bottom) / skirt	Yes	118.2	-12.0	-94.3	93818	2982	6858	6282
"	2. Outer hood bottom / cover plate	Yes	59.1	101.4	7.5	93493	1932	10689	6068
"	3. Middle hood / thin closure plate	Yes	-84.7	-59.3	95.0	85091	4411	6873	5064
"	4. Trough thin section / perf. plate	Yes	73.4	-85.9	21.5	82164	711	4780	4700
"	5. Drain channel (bottom) / skirt	Yes	-73.8	93.1	-94.3	90834	2209	7049	4544

See Table 6a for locations nomenclature.

Table 6c. Locations with highest predicted stress intensities for 1/8th scale EPU conditions with -10% frequency shift.

Stress Category	Location		Location (in)				Stress Intensities (psi)		
		Weld	x	y	z	node	Pm	Pm+Pb	S_{alt}
Pm	1. Inner hood (top) near closure plate	No	109.0	-27.6	95.3	44886	7114	10027	1905
"	2. Trough thin section / trough bottom plate / outer hood support	Yes	-28.4	85.9	7.5	89554	5479	5755	4713
"	3. Middle hood (bottom) / cover plate	"	0.0	69.9	7.5	93321	5414	5417	4150
"	4. Upper ring / thick closure plate / vane end plate	"	-118.8	14.4	7.5	85994	5295	7179	1602
"	5. Outer hood (bottom) / hood support ./ cover plate	"	-28.4	-101.4	7.5	90374	5247	5341	5053
Pm+Pb	1. Thin closure plate, top/inner hood	Yes	-108.4	-27.9	94.9	88252	6921	12333	6617
"	2. Skirt / upper support ring	"	118.8	0.6	-2.0	88325	2663	10796	2084
"	3. Drain channel (bottom) / skirt	"	73.8	-93.1	-94.3	93833	2459	9004	6939
"	4. Thin closure plate, top/middle vane bank / outer end plate	"	-108.4	-45.9	95.9	90711	3837	8785	5617
"	5. Thin closure plate, top/middle hood	"	-84.7	-59.3	95.0	85091	5021	8217	6583
S_{alt}	1. Thin closure plate, top/middle hood	Yes	-84.7	59.8	94.3	87835	841	7093	6983
"	2. Drain channel (bottom) / skirt	"	73.8	-93.1	-94.3	93833	2459	9004	6939
"	3. Thin closure plate, top/inner hood	"	-108.4	-27.9	94.9	88252	6921	12333	6617
"	4. Thin closure plate, top/outer vane bank / outer end plate	"	-84.7	77.4	96.1	92445	1773	7228	6466
"	5. Thin closure plate, top/middle vane bank / outer end plate	"	-108.4	-45.9	95.9	90711	3837	8785	5617

See Table 6a for locations nomenclature.

Table 6d. Locations with highest predicted stress intensities for 1/8th scale EPU conditions with +10% frequency shift.

Stress Category	Location		Location (in)				Stress Intensities (psi)		
		Weld	x	y	z	node	Pm	Pm+Pb	S_{alt}
Pm	1. Inner hood (top) near closure plate	No	109.0	-27.6	95.3	44886	7122	10106	1939
"	2. Inner hood (bottom) / hood support	Yes	0.0	38.4	7.5	86960	4998	5266	3219
"	3. Thin closure plate, top/middle hood	"	-84.7	-59.3	95.0	85091	4905	7636	5824
"	4. Thin closure plate, bottom/inner hood	"	-108.4	38.4	8.1	87035	4716	4929	1413
"	5. Upper ring / thick closure plate / vane end plate	"	-118.8	14.4	7.5	85994	4409	6072	678
Pm+Pb	1. Skirt / upper support ring	Yes	-118.8	-0.6	-2.0	79487	2582	10382	1931
"	2. Thin closure plate, top/inner hood	"	108.4	27.9	94.9	85409	7042	10343	4470
"	3. Middle hood / end plate	"	-97.9	-69.4	27.5	84384	1254	8442	8252
"	4. Middle hood / thin closure plate (top)	"	-84.7	-59.3	95.0	85091	4905	7636	5824
"	5. Outer hood bottom / cover plate	"	59.1	101.4	7.5	93493	1870	7593	3197
S_{alt}	1. Middle hood / end plate	Yes	-97.9	-69.4	27.5	84384	1254	8442	8252
"	2. Middle hood / end plate	"	-98.3	-68.6	39.3	84398	1004	6948	6714
"	3. Thin closure plate, top/middle hood	"	-84.7	-59.3	95.0	85091	4905	7636	5824
"	4. Thin closure plate, top/outer vane bank / outer end plate	"	-84.7	-77.4	96.1	82694	1875	5591	5503
"	5. Middle hood / end plate	"	-99.0	67.4	51.1	84517	1198	5054	4907

See Table 6a for locations nomenclature.

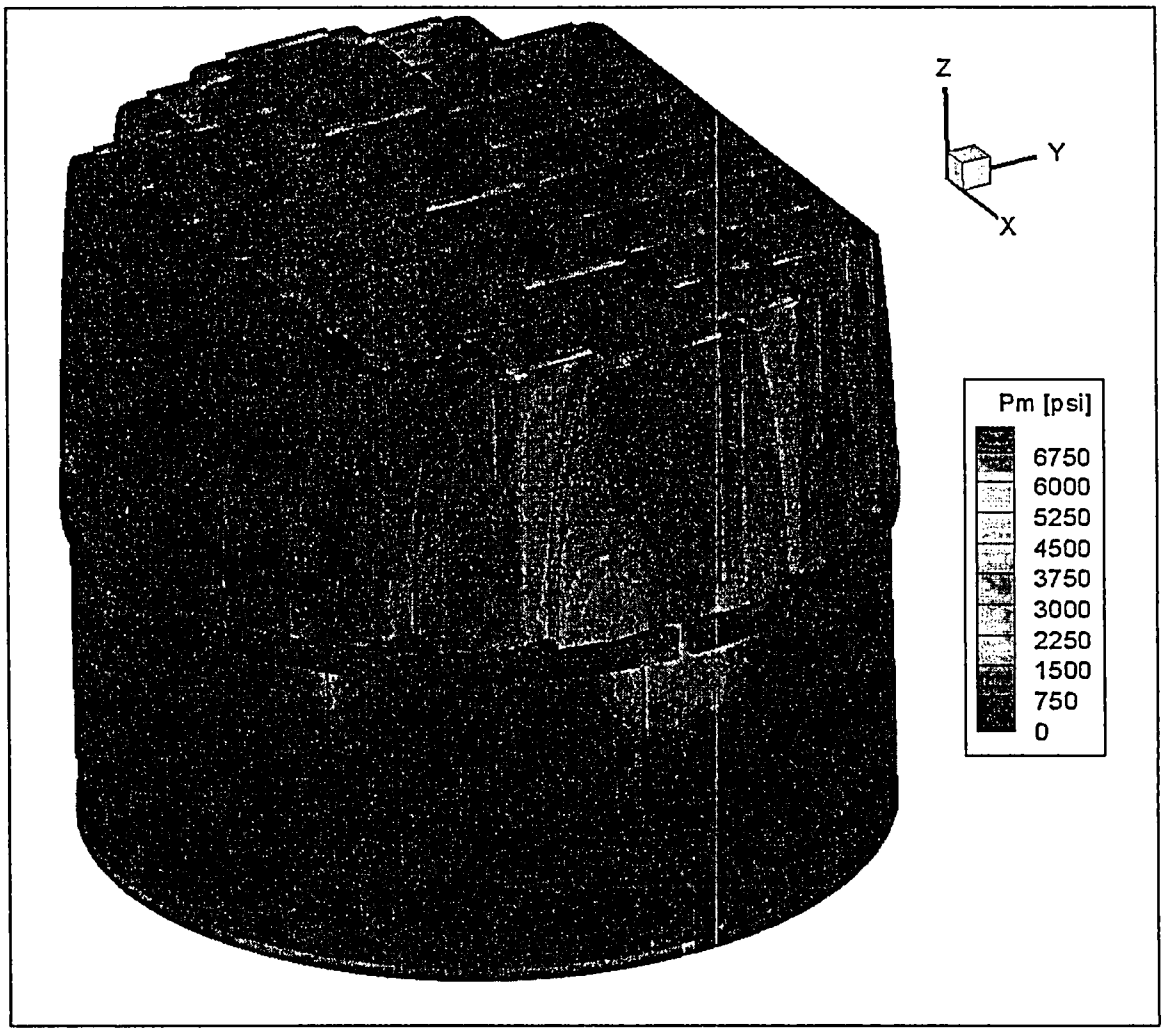

Figure 15a. Contour plot of peak membrane stress intensity, Pm, for 1/8th scale CLTP load. The maximum stress intensity is 7017 psi.

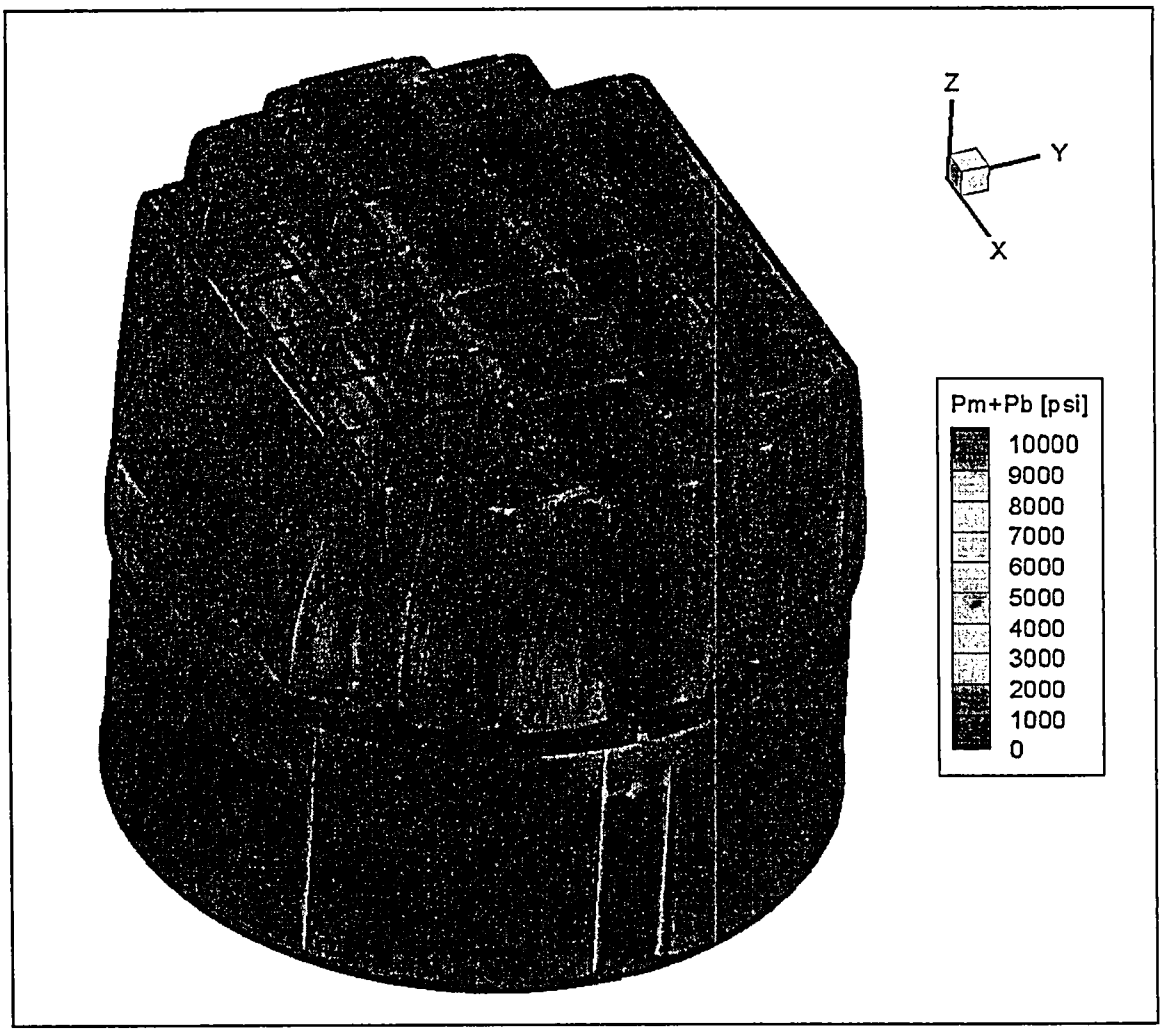

Figure 15b. Contour plot of peak membrane+bending stress intensity, Pm+Pb, for 1/8th scale CLTP load. The maximum stress intensity is 10033 psi.

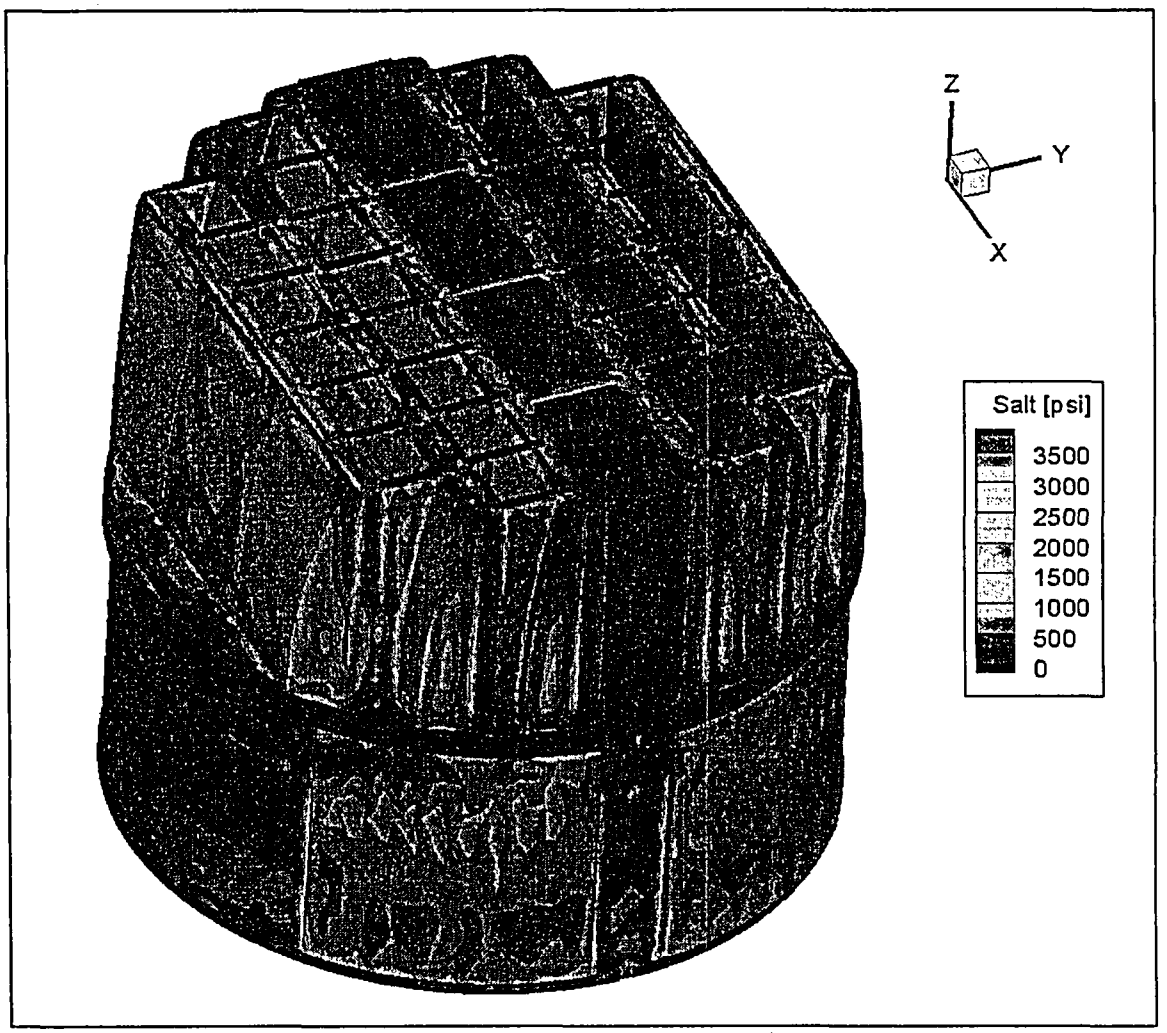

Figure 15c. Contour plot of alternating stress intensity, S_{alt}, for $1/8^{th}$ scale CLTP load. The maximum stress intensity is 3549 psi.

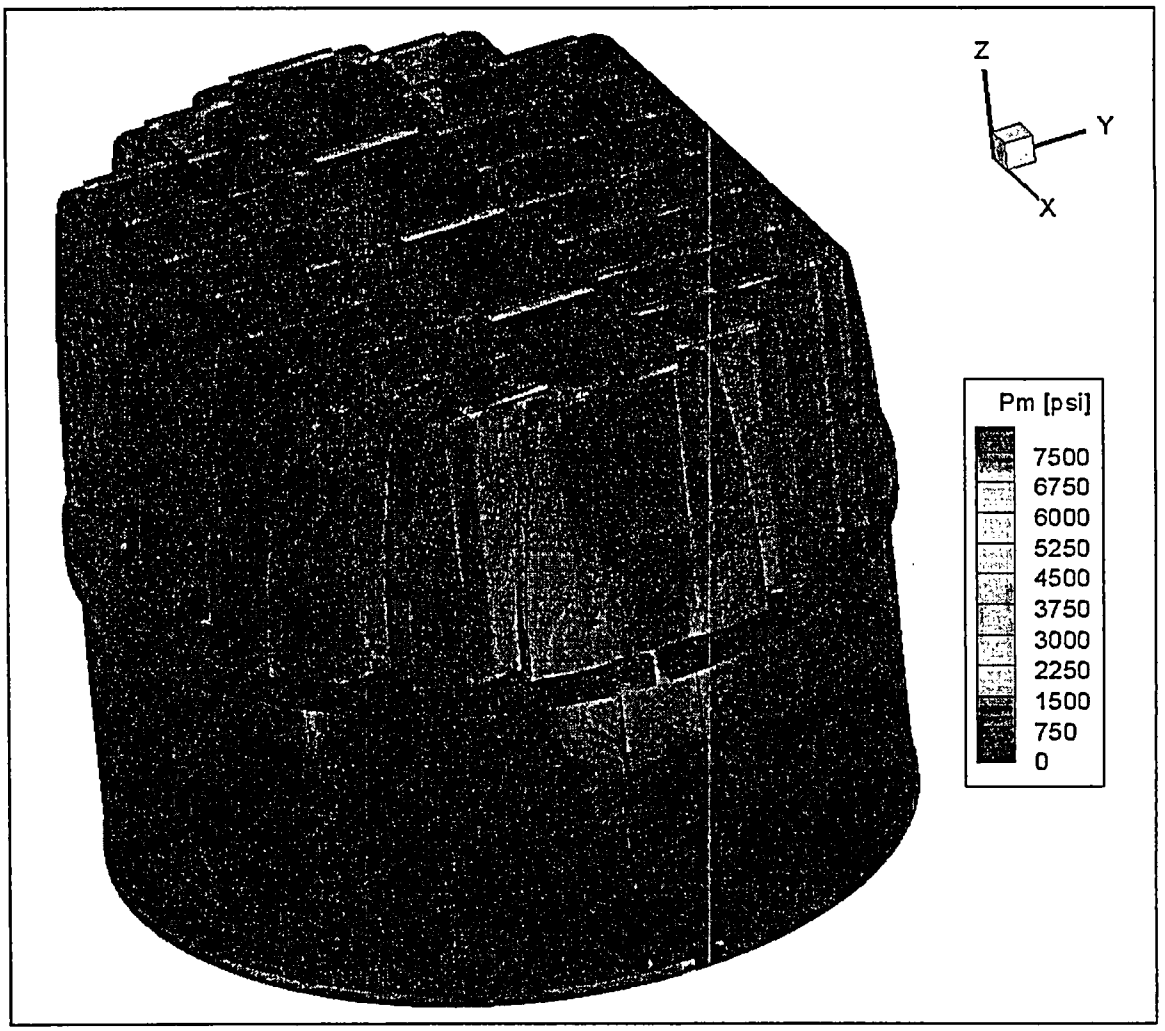

Figure 16a. Contour plot of peak membrane stress intensity, Pm, for 1/8th scale EPU load. The maximum stress intensity is 7860 psi.

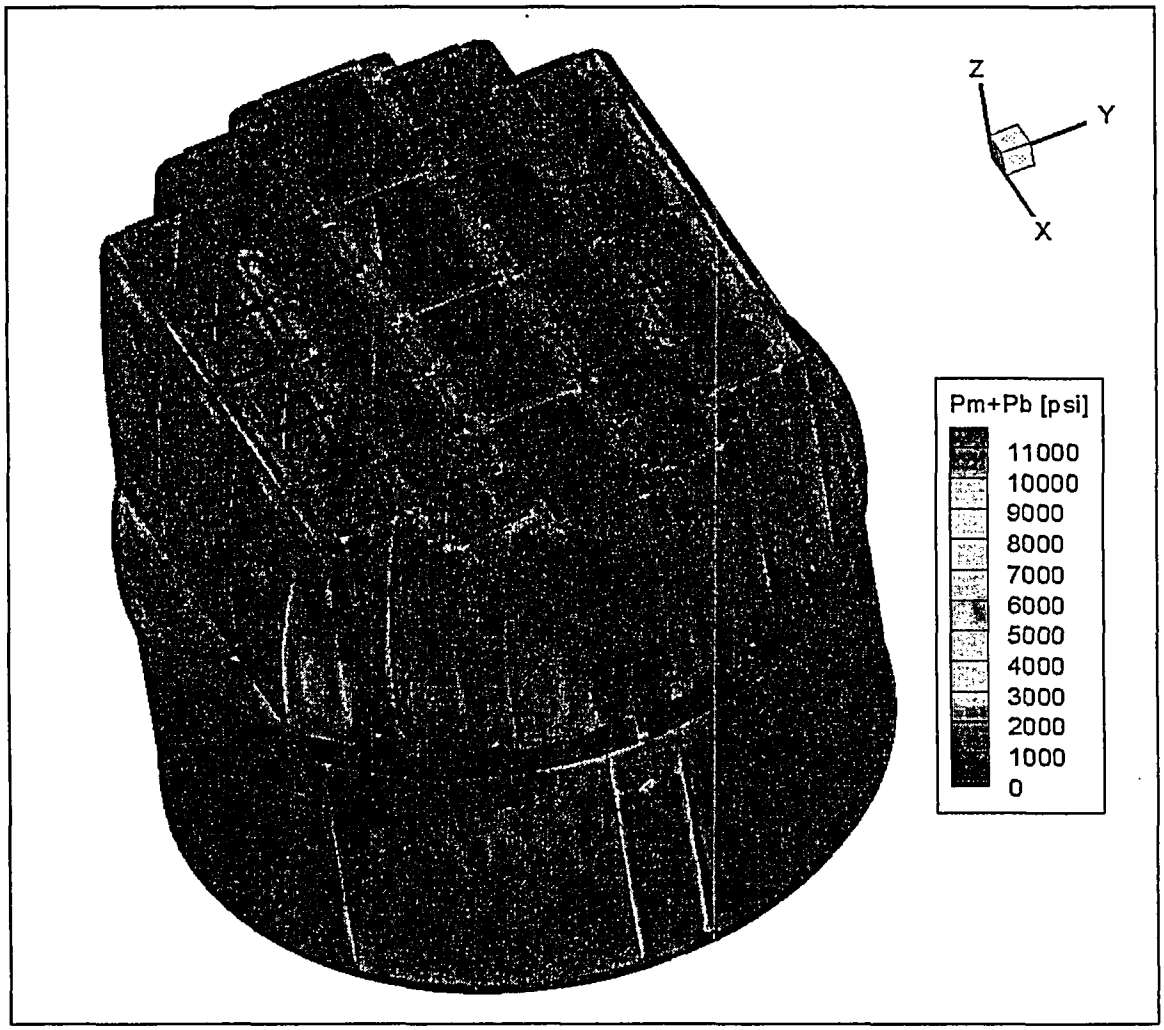

Figure 16b. Contour plot of peak membrane+bending stress intensity, Pm+Pb, for $1/8^{th}$ scale EPU load. The maximum stress intensity is 11320 psi.

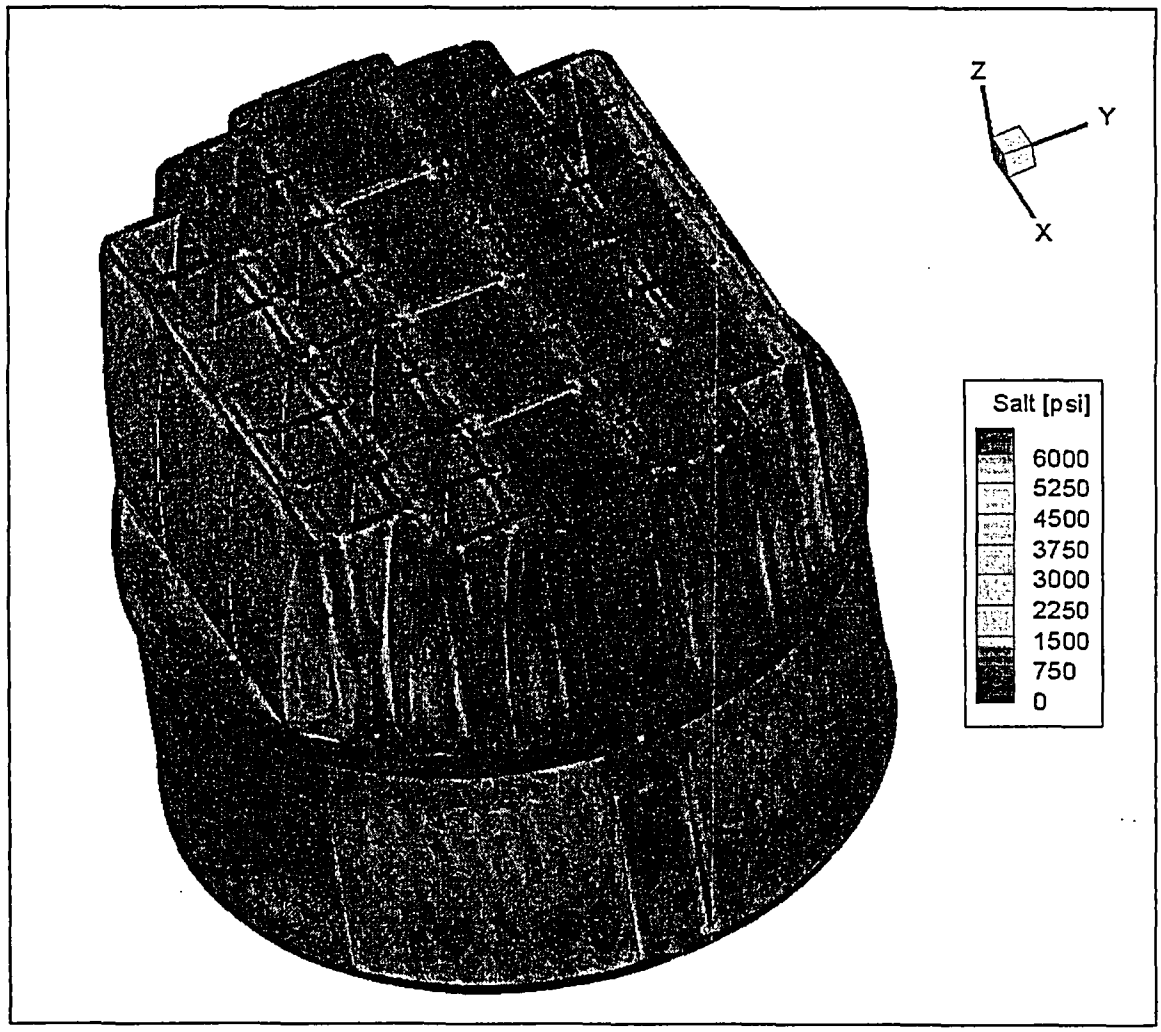

Figure 16c. Contour plot of alternating stress intensity, S_{alt}, for $1/8^{th}$ scale EPU load. The maximum stress intensity is 6282 psi.

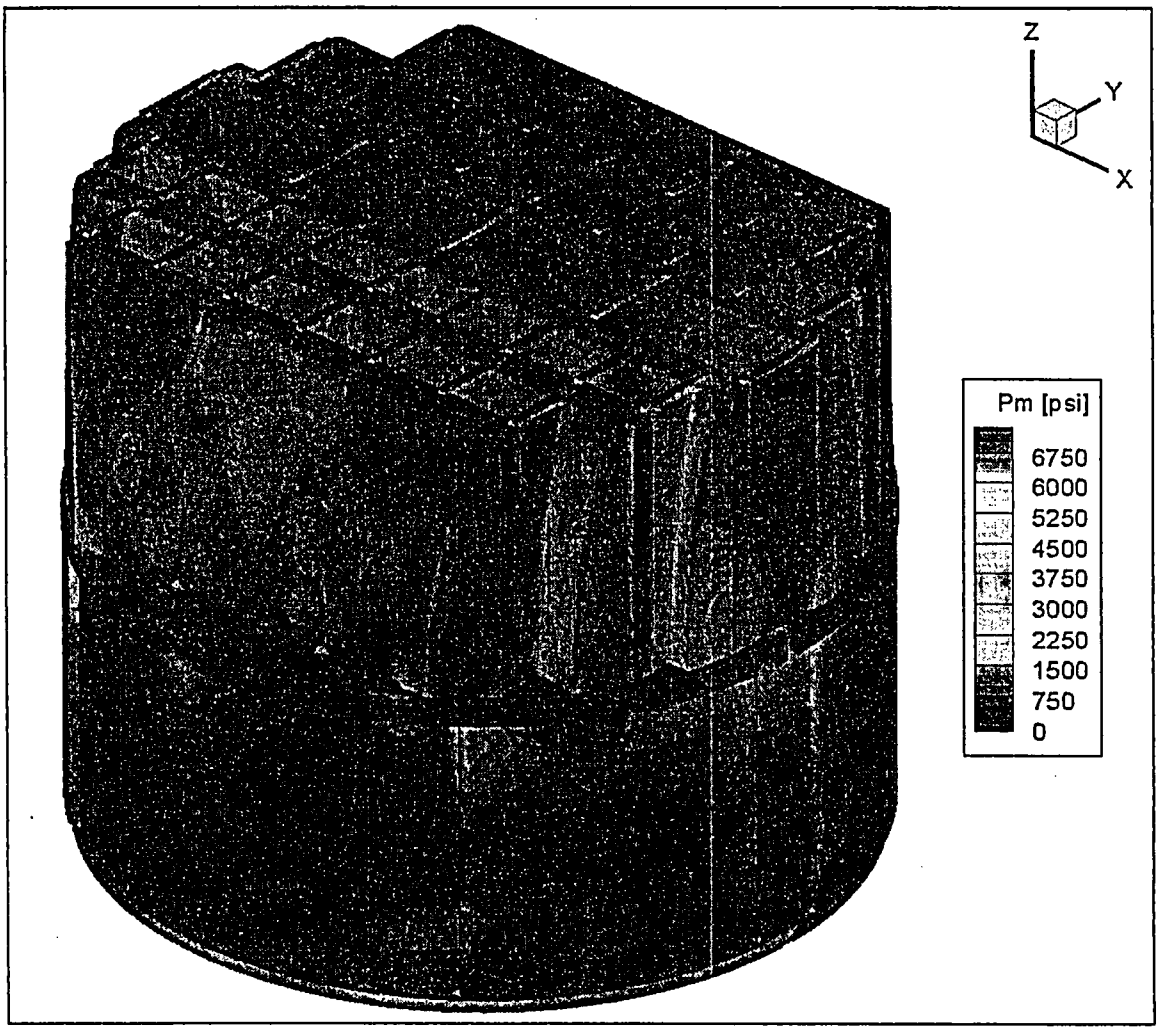

Figure 17a. Contour plot of peak membrane stress intensity, Pm, for 1/8th scale EPU load with -10% frequency shift. The maximum stress intensity is 7114 psi.

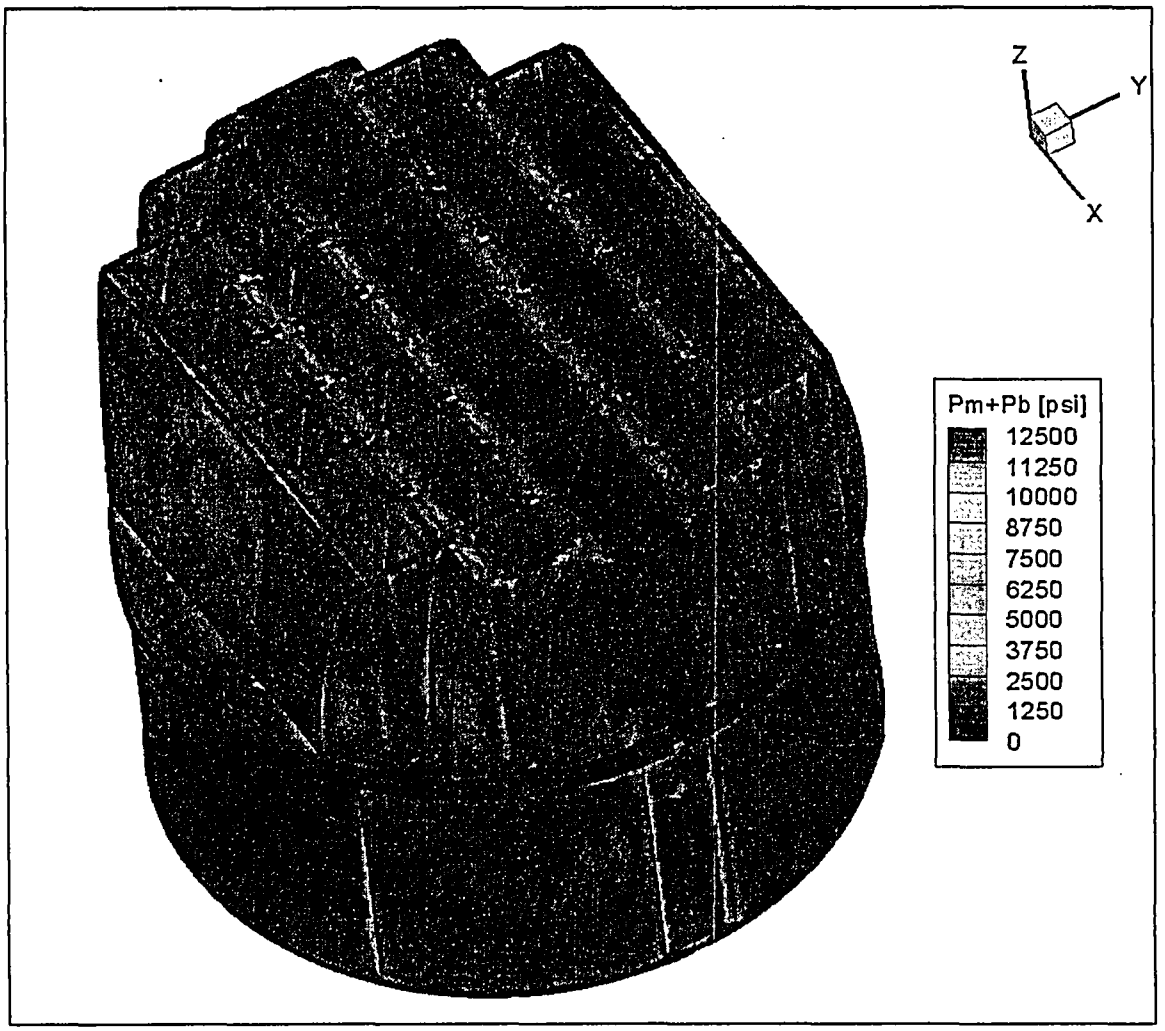

Figure 17b. Contour plot of peak membrane+bending stress intensity, Pm+Pb, for $1/8^{th}$ scale EPU load with -10% frequency shift. The maximum stress intensity is 12333 psi.

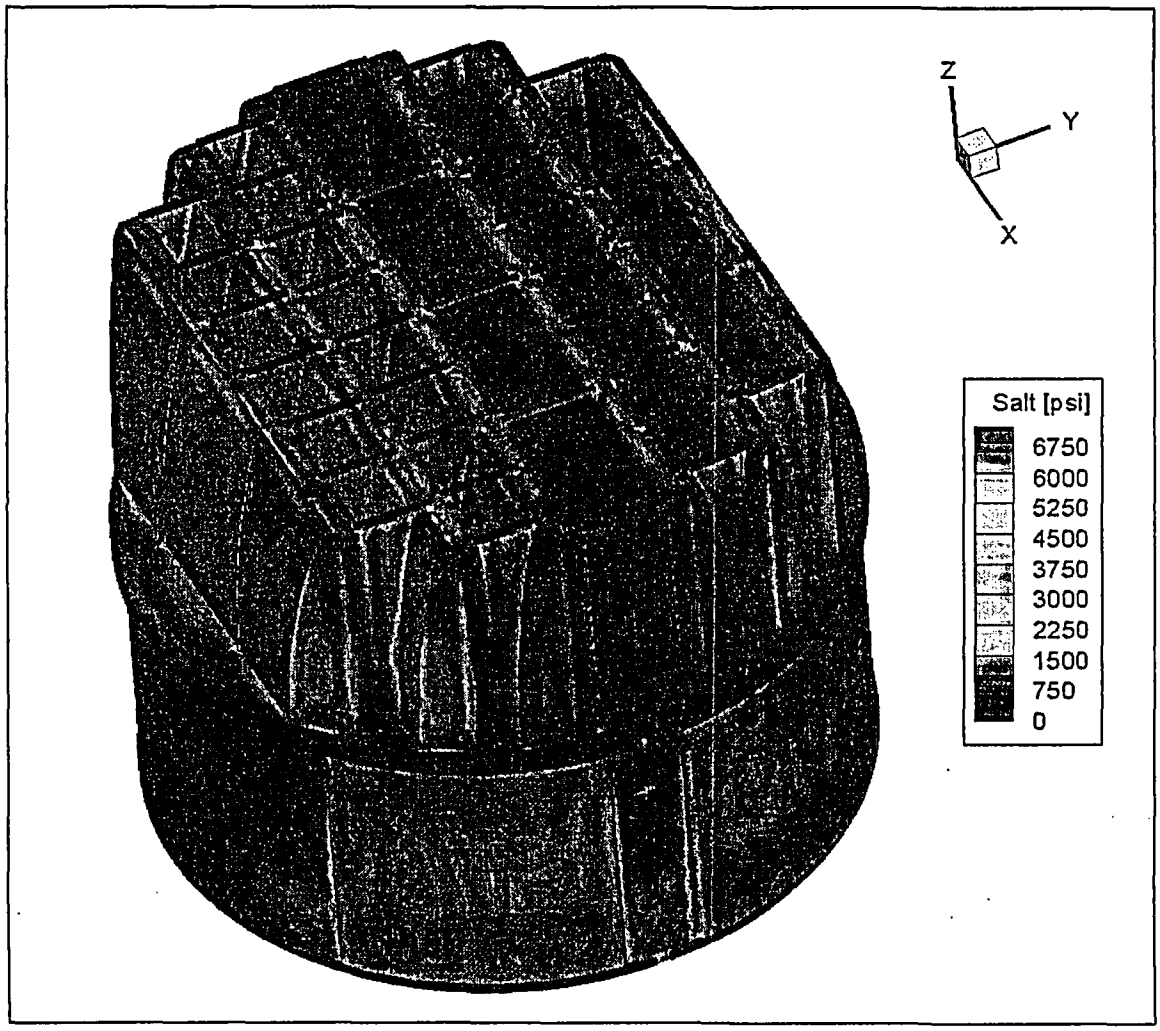

Figure 17c. Contour plot of alternating stress intensity, S_{alt}, for $1/8^{th}$ scale EPU load with -10% frequency shift. The maximum stress intensity is 6983 psi.

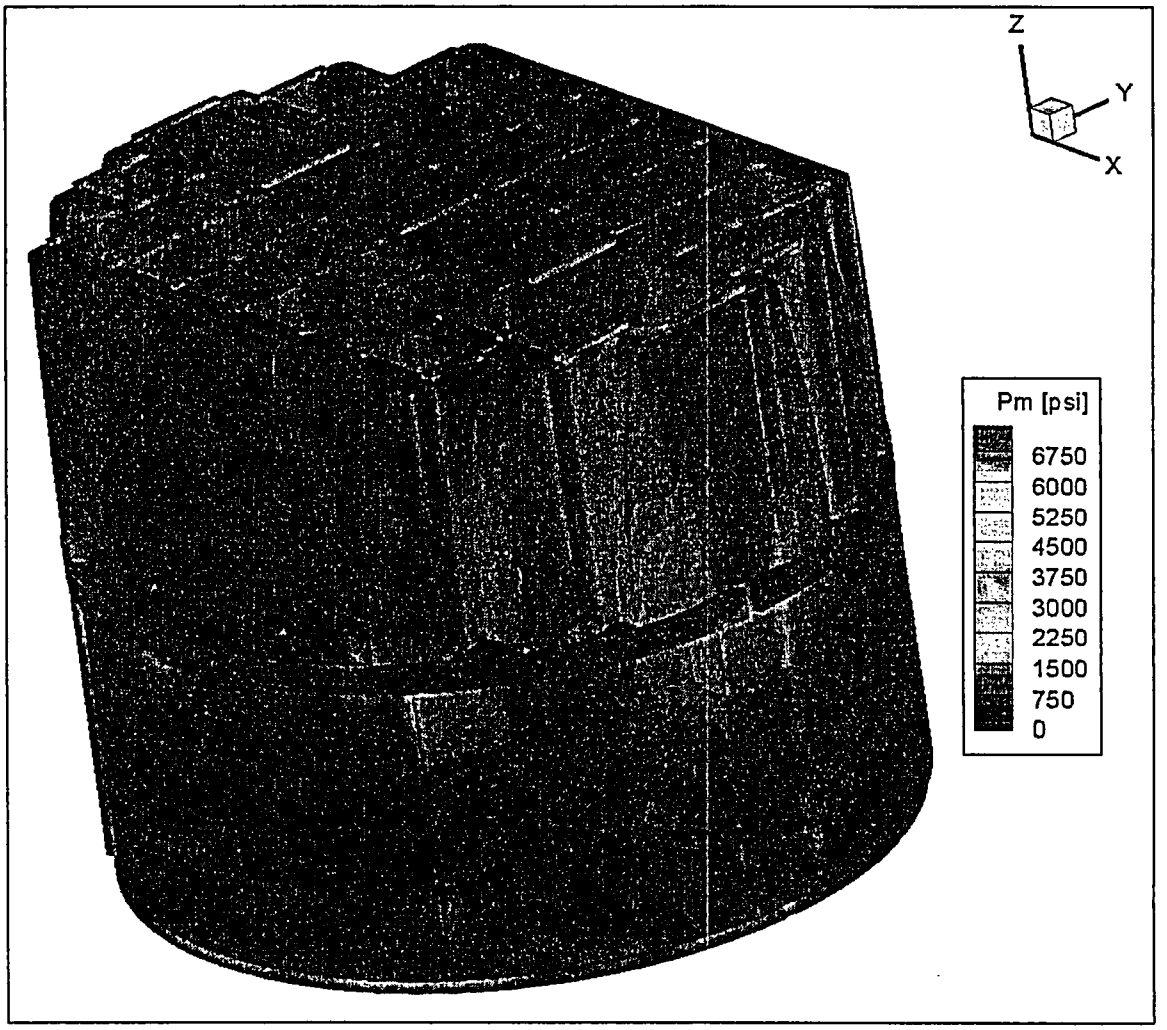

Figure 18a. Contour plot of peak membrane stress intensity, Pm, for 1/8th scale EPU load with +10% frequency shift. The maximum stress intensity is 7122 psi.

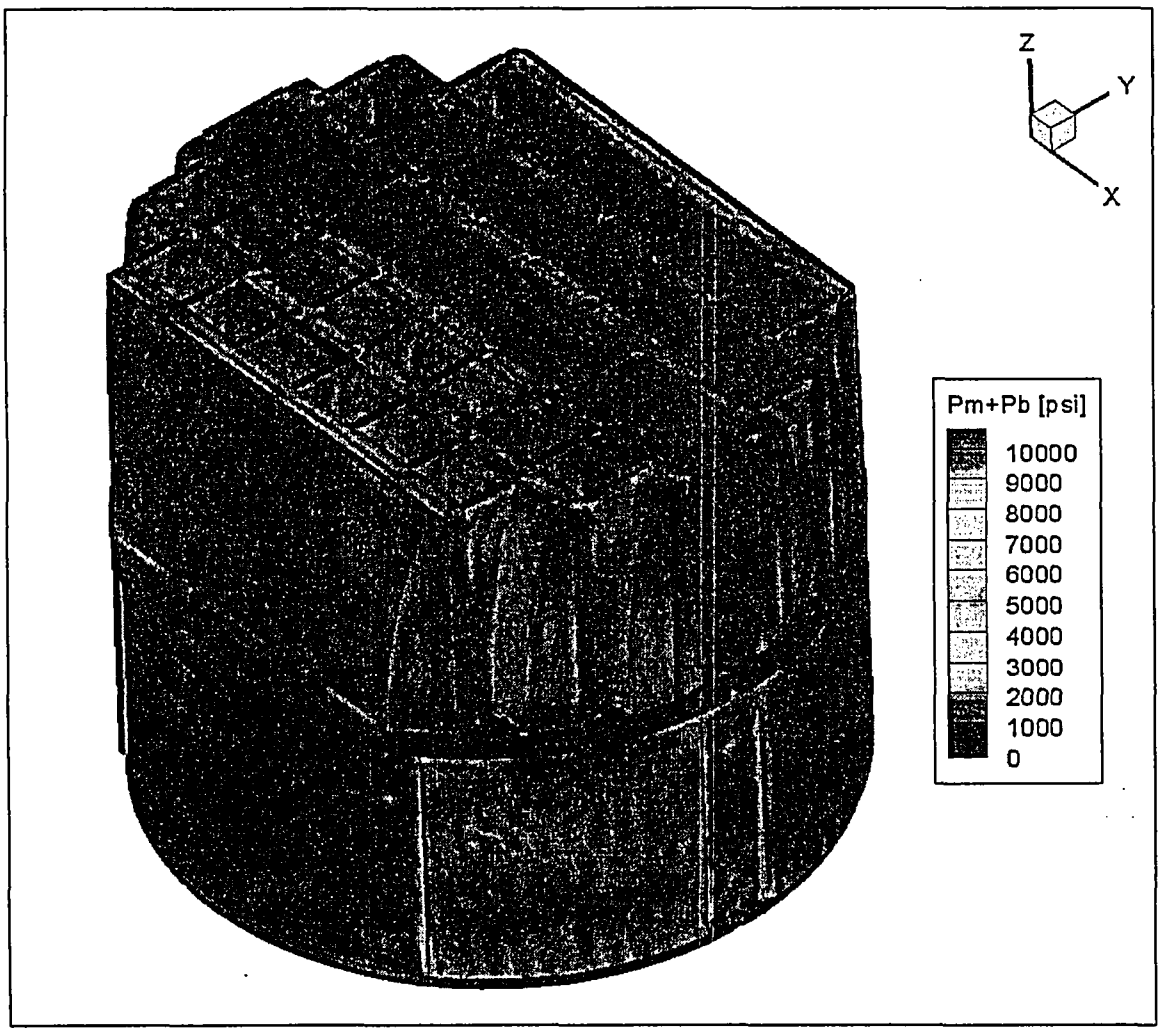

Figure 18b. Contour plot of peak membrane+bending stress intensity, Pm+Pb, for $1/8^{th}$ scale EPU load with +10% frequency shift. The maximum stress intensity is 10382 psi.

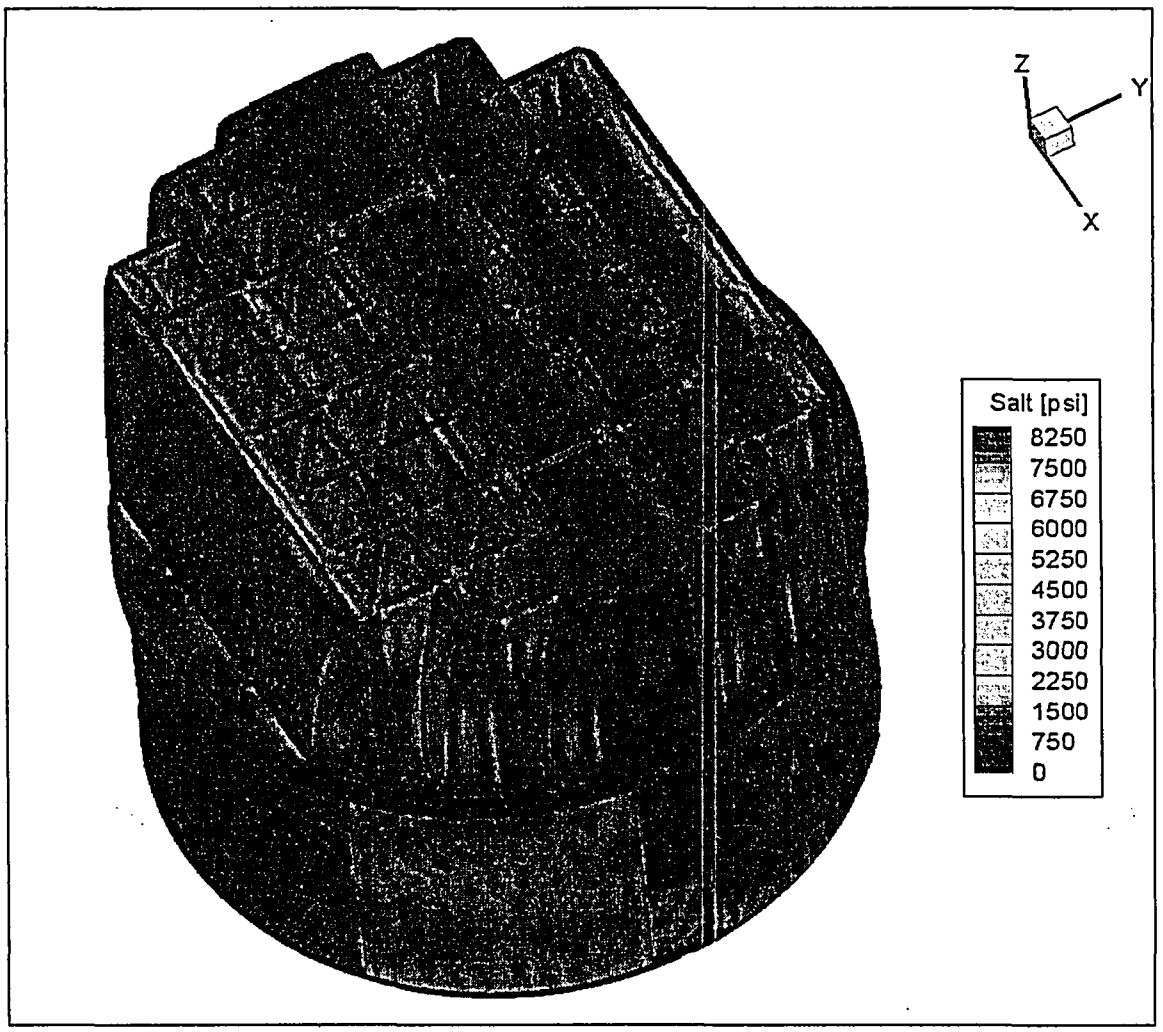

Figure 18c. Contour plot of alternating stress intensity, S_{alt}, for $1/8^{th}$ scale EPU load with +10% frequency shift. The maximum stress intensity is 8252 psi.

5.2 Load Combinations and Allowable Stress Intensities

The stress ratios computed for CLTP, EPU and EPU with frequency shift operating conditions are listed in Table 7. The stress ratios are grouped according to type (SR-P for peak membrane and membrane+bending stress, SR-a for alternating stress) and location (away from welds or on a weld).

In CLTP operation the minimum stress ratio 1.53 occurs at the junction of inner hood and thin closure plate. Other critical regions with low stress ratios are the base of the inner hood, the junction between the inner hood and its hood support and where the drain channel joins the skirt. All of these locations lie on welds as summarized in Table 7a and the accompanying Figure 19. The minimum stress ratio at a non-weld is SR-P=2.61 and occurs on the inner hood near the thin closure plate. In this case, the minimum stress ratio location is near, but not on, a weld. If the stress ratio for a weld were applied then the value would drop to 1.44 which is still well within the allowable level.

For the EPU loads, all stress ratios (reported in Table 7b and Figure 20) are reduced as expected from the generally higher stress intensities. The minimum stress ratios correspond to alternating stresses at welds with the minimum ratio, SR-a=1.09, occurring at the junction between the drain channel and skirt. The stress ratio where the outer hood meets the cover plate is only slightly larger (SR-a=1.13); all subsequent stress ratios are higher than 1.35. The minimum stress ratio locations are similar to the ones for CLTP and involve either the hoods or drain channels.

Shifting the frequencies in the EPU load condition reduces the stress ratios and produces different minimum stress ratio locations. For the -10% shift (Table 7c) the minimum stress ratio is now 0.984 which corresponds to a 10% reduction compared to the EPU condition without the shift. The minimum stress ratio location also changes from the drain channel/skirt junction to the weld connecting the thin closure plate to the middle hood. However, the stress ratio on the drain channel is also reduced to 0.990. All the stress ratios below 1.36 occur either on the thin closure plates or drain channels. For the +10% frequency shift (Table 7d), the minimum stress ratio becomes 0.832 (a 23% reduction compare to the EPU without frequency shift) and occurs on the weld joining the middle hood and end plate. The lowest stress ratios all occur on either the middle hood/end plate junctions or the thin closure plate welds. The drain channel welds which were the critical stress locations at EPU and EPU with -10% frequency shift, now have a relatively benign stress ratio of 1.56.

In summary, the general picture that emerges is that at EPU loads the frequencies shifts significantly affect the minimum stress ratios and reposition the peak stress locations to different parts of the structure. These indicate that the dryer has a rich modal structure so that shifting load frequencies results in the excitation of different modes.

Table 7a. Locations with minimum stress ratios for 1/8th scale at CLTP conditions. Stress ratios are grouped according to stress type (peak – SR-P; or alternating – SR-a) and location (away from a weld or at a weld). Bold text indicates minimum stress ratio of any type on the structure. Locations are depicted in Figure 19.

Stress Ratio	Location	Weld	Location (in.)				Stress Intensity (psi)			Stress Ratio	
			x	y	z	node	Pm	Pm+Pb	S_{alt}	SR-P	SR-a
SR-P	1. Inner hood near thin closure plate	No	109.0	-27.6	95.3	44886	7017	10033	1908	2.61	6.48
SR-P	**1. Inner hood / thin closure plate**	**Yes**	**-108.4**	**-27.9**	**94.9**	**88252**	**6595**	**9778**	**2907**	**1.53**	**2.36**
"	2. Skirt / upper support ring	"	-118.8	-0.6	-2.0	79487	2556	9778	1276	1.54	5.38
"	3. Outer hood bottom / cover plate	"	59.1	101.4	7.5	93493	1793	7688	3431	1.96	2.00
SR-a	1. Inner hood (half-height)	No	27.9	36.0	50.5	42098	1609	4015	3549	6.84	3.48
"	2. Lower middle hood	"	25.6	69.3	29.9	37254	608	3838	3253	7.15	3.80
"	3. Middle hood (half-height)	"	-25.2	67.1	53.3	37915	817	3642	3230	7.54	3.83
SR-a	1. Drain channel (bottom) / skirt	Yes	118.2	-12.0	-94.3	93818	2219	3705	3496	4.07	1.96
"	2. Outer hood bottom / cover plate	"	59.1	101.4	7.5	93493	1793	7688	3431	1.96	2.00
"	3. Middle hood / thin closure plate	"	-84.7	59.3	95.0	87837	3004	4328	3151	3.35	2.18

See Table 6a for locations nomenclature.

Table 7b. Locations with minimum stress ratios for 1/8th scale at EPU conditions. Stress ratios are grouped according to stress type (peak – SR-P; or alternating – SR-a) and location (away from a weld or at a weld). Bold text indicates minimum stress ratio of any type on the structure. Locations are depicted in Figure 20.

Stress Ratio	Location	Weld	Location (in.)				Stress Intensity (psi)			Stress Ratio	
			x	y	z	node	Pm	Pm+Pb	S_{alt}	SR-P	SR-a
SR-P	1. Inner hood near thin closure plate	No	109.0	-27.6	95.3	44886	7860	11320	3138	2.33	3.94
SR-P	1. Skirt / upper support ring	Yes	-118.8	-0.6	-2.0	79487	2611	10733	2021	1.41	3.40
"	2. Outer hood bottom / cover plate	"	59.1	101.4	7.5	93493	1932	10689	6068	1.41	1.13
"	3. Inner hood / thin closure plate	"	108.4	27.9	94.9	85409	7075	10369	3796	1.42	1.81
"	4. Drain channel (bottom) / skirt	"	118.2	12.0	-94.3	90843	2267	7586	5381	1.99	1.28
SR-a	1. Outer vane bank perforated plate	No	70.1	-85.9	42.1	62177	424	4379	4285	6.27	2.89
"	2. Outer vane bank perforated plate	"	75.0	-85.9	85.8	62265	973	4235	4176	6.48	2.96
"	3. Outer vane bank perforated plate	"	70.9	-85.9	30.5	62210	557	4231	4169	6.49	2.97
"	4. Outer vane bank perforated plate	"	73.5	-85.9	52.0	62322	457	4114	4107	6.67	3.01
SR-a	**1. Drain channel (bottom) / skirt**	**Yes**	**118.2**	**-12.0**	**-94.3**	**93818**	**2982**	**6858**	**6282**	**2.20**	**1.09**
"	2. Outer hood bottom / cover plate	"	59.1	101.4	7.5	93493	1932	10689	6068	1.41	1.13
"	3. Middle hood / thin closure plate	"	-84.7	-59.3	95.0	85091	4411	6873	5064	2.20	1.36
"	4. Trough thin section / perf. plate	"	73.4	-85.9	21.5	82164	711	4780	4700	3.16	1.46
"	5. Drain channel (bottom) / skirt	"	-73.8	93.1	-94.3	90834	2209	7049	4544	2.14	1.51

See Table 6a for locations nomenclature.

Table 7c. Locations with minimum stress ratios for 1/8th scale at EPU conditions with -10% frequency shift. Stress ratios are grouped according to stress type (peak – SR-P; or alternating – SR-a) and location (away from a weld or at a weld). Bold text indicates minimum stress ratio of any type on the structure. Locations are depicted in Figure 21.

Stress Ratio	Location	Weld	Location (in.)				Stress Intensity (psi)			Stress Ratio	
			x	y	z	node	Pm	Pm+Pb	S_{alt}	SR-P	SR-a
SR-P	1. Inner hood near thin closure plate	No	109.0	-27.6	95.3	44886	7114	10027	1905	2.57	6.49
SR-P	1. Inner hood / thin closure plate	Yes	-108.4	-27.9	94.9	88252	6921	12333	6617	1.22	1.04
"	2. Skirt / upper support ring	"	118.8	0.6	-2.0	88325	2663	10796	2084	1.40	3.30
"	3. Drain channel (bottom) / skirt	"	73.8	-93.1	-94.3	93833	2459	9004	6939	1.68	0.990
"	4. Thin closure plate, top/middle vane bank / outer end plate	"	-108.4	-45.9	95.9	90711	3837	8785	5617	1.72	1.22
"	5. Trough thin section / trough bottom plate / outer hood support	"	-28.4	85.9	7.5	89554	5479	5755	4713	1.84	1.46
SR-a	1. Thin closure plate (top)	No	-84.7	60.1	94.7	28598	1010	6142	5808	4.47	2.13
"	2. Middle hood, mid-height, outside of closure plate	"	-91.7	67.8	47.4	36713	1731	4858	4553	5.65	2.72
SR-a	**1. Thin closure plate, top/middle hood**	**Yes**	**-84.7**	**59.8**	**94.3**	**87835**	**841**	**7093**	**6983**	**2.13**	**0.984**
"	2. Drain channel (bottom) / skirt	"	73.8	-93.1	-94.3	93833	2459	9004	6939	1.68	0.990
"	3. Thin closure plate, top/inner hood	"	-108.4	-27.9	94.9	88252	6921	12333	6617	1.22	1.04
"	4. Thin closure plate, top/outer vane bank / outer end plate	"	-84.7	77.4	96.1	92445	1773	7228	6466	2.09	1.06
"	5. Thin closure plate, top/middle vane bank / outer end plate	"	-108.4	-45.9	95.9	90711	3837	8785	5617	1.72	1.22
"	6. Outer hood (bottom) / hood support ./ cover plate	"	-28.4	-101.4	7.5	90374	5247	5341	5053	1.92	1.36
"	7. Drain channel (bottom) / skirt	"	118.2	-12.0	-94.3	93818	2981	4904	4714	3.08	1.46
"	8. Trough thin section / trough bottom plate / outer hood support	"	-28.4	85.9	7.5	89554	5479	5755	4713	1.84	1.46
"	9. Middle hood (bottom) / backing bar	"	71.7	-69.9	8.5	89316	909	4756	4439	3.17	1.55
"	10. Middle hood (bottom) / hood support	"	0.0	69.9	7.5	93321	5414	5417	4150	1.86	1.66

See Table 6a for locations nomenclature.

Table 7d. Locations with minimum stress ratios for 1/8th scale at EPU conditions with +10% frequency shift. Stress ratios are grouped according to stress type (peak – SR-P; or alternating – SR-a) and location (away from a weld or at a weld). Bold text indicates minimum stress ratio of any type on the structure. Locations are depicted in Figure 22.

Stress Ratio	Location	Weld	Location (in.)				Stress Intensity (psi)			Stress Ratio	
			x	y	z	node	Pm	Pm+Pb	S_{alt}	SR-P	SR-a
SR-P	1. Inner hood (top) near closure plate	No	109.0	-27.6	95.3	44886	7122	10106	1939	2.57	6.38
SR-P	1. Inner hood / thin closure plate	Yes	108.4	27.9	94.9	85409	7042	10343	4470	1.43	1.54
"	2. Skirt / upper support ring	"	-118.8	-0.6	-2.0	79487	2582	10382	1931	1.45	3.56
"	3. Middle hood (mid-height) / end plate	"	-97.9	-69.4	27.5	84384	1254	8442	8252	1.79	0.832
"	4. Middle hood (top) / closure plate	"	-84.7	-59.3	95.0	85091	4905	7636	5824	1.98	1.18
SR-a	1. Middle hood, mid-height, outside of closure plate	No	-90.9	-69.3	29.7	48200	1850	6511	6232	4.22	1.98
"	2. Middle hood, mid-height, outside of closure plate	"	-91.6	-68.5	40.6	48082	1556	4686	4455	5.86	2.78
SR-a	**1. Middle hood / end plate**	**Yes**	**-97.9**	**-69.4**	**27.5**	**84384**	**1254**	**8442**	**8252**	**1.79**	**0.832**
"	2. Middle hood / end plate	"	-98.3	-68.6	39.3	84398	1004	6948	6714	2.17	1.02
"	3. Thin closure plate, top/middle hood	"	-84.7	-59.3	95.0	85091	4905	7636	5824	1.98	1.18
"	4. Thin closure plate, top/outer vane bank / outer end plate	"	-84.7	-77.4	96.1	82694	1875	5591	5503	2.70	1.25
"	5. Middle hood / end plate	"	-99.0	67.4	51.1	84517	1198	5054	4907	2.99	1.40
"	6. Thin closure plate, lower/middle hood	"	-84.7	-69.3	30.0	91692	1023	4703	4611	3.21	1.49
"	7. Thin closure plate, top/inner hood	"	108.4	27.9	94.9	85409	7042	10343	4470	1.43	1.54
"	8. Drain channel (bottom) / skirt	"	73.8	-93.1	-94.3	93833	1393	6637	4394	2.27	1.56
"	9. Outer hood / vane top cover / hood support	"	-28.4	-85.9	96.1	92306	1006	5956	4374	2.53	1.57
"	10. Drain channel (bottom) / skirt	"	118.2	12.0	-94.3	90843	1572	6558	4100	2.30	1.68

See Table 6a for locations nomenclature.

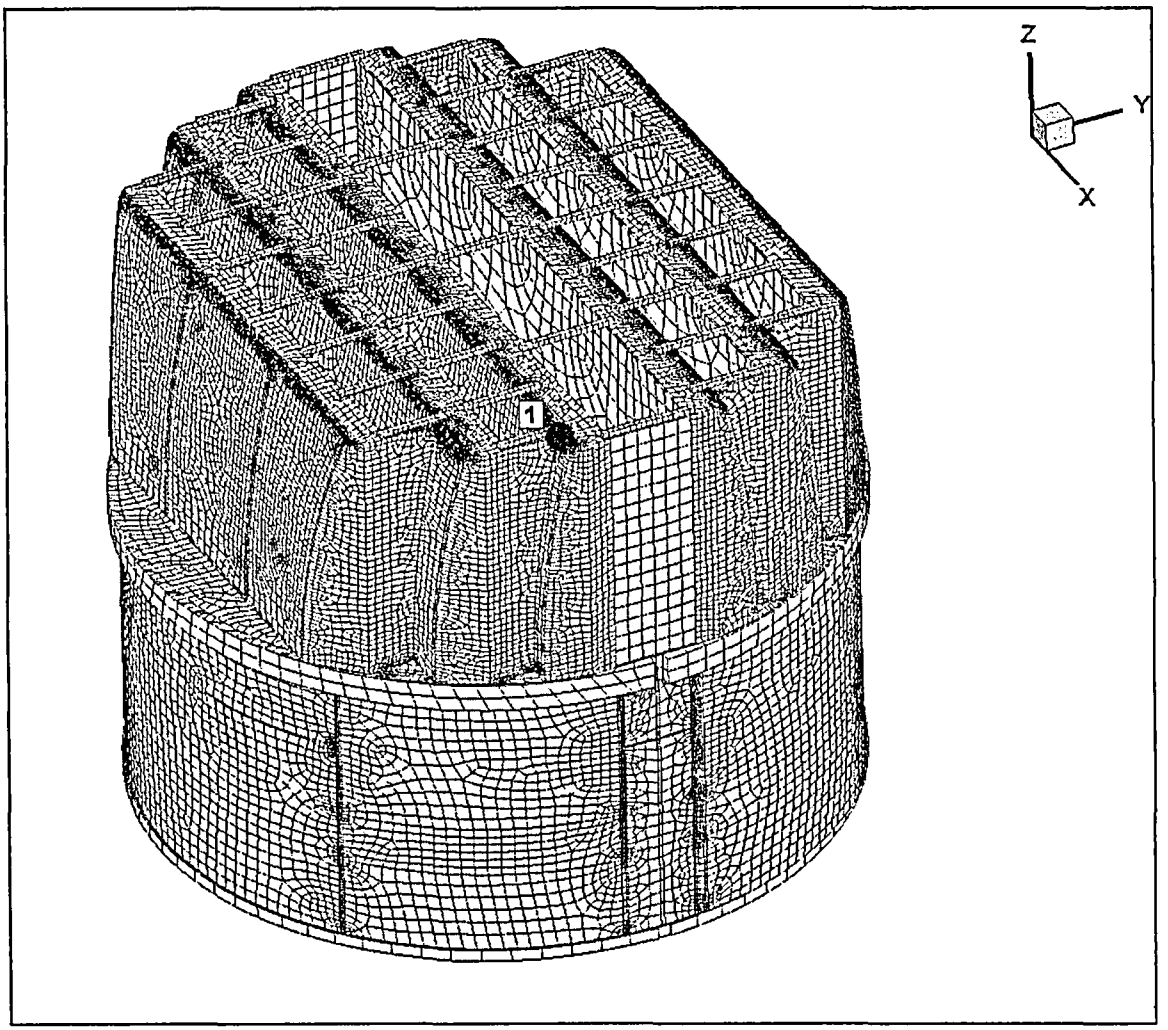

Figure 19a. Locations of minimum peak stress ratios, SR-P, at non-welds for CLTP operation. Numbers refer to the enumerated locations for SR-P values at welds in Table 7a.

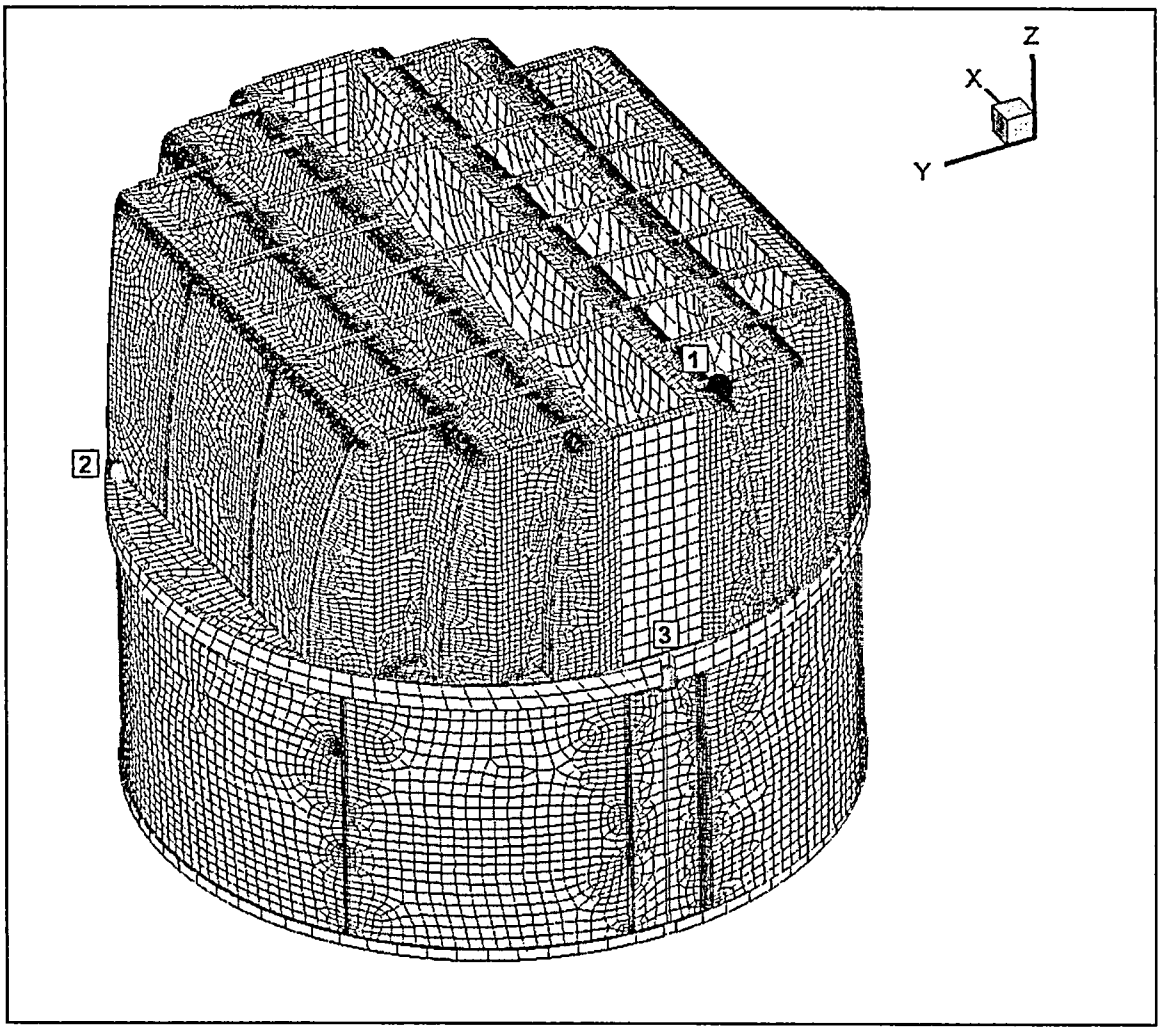

Figure 19b. Locations of minimum peak stress ratios, SR-P, at welds for CLTP operation. Numbers refer to the enumerated locations for SR-P values at welds in Table 7a.

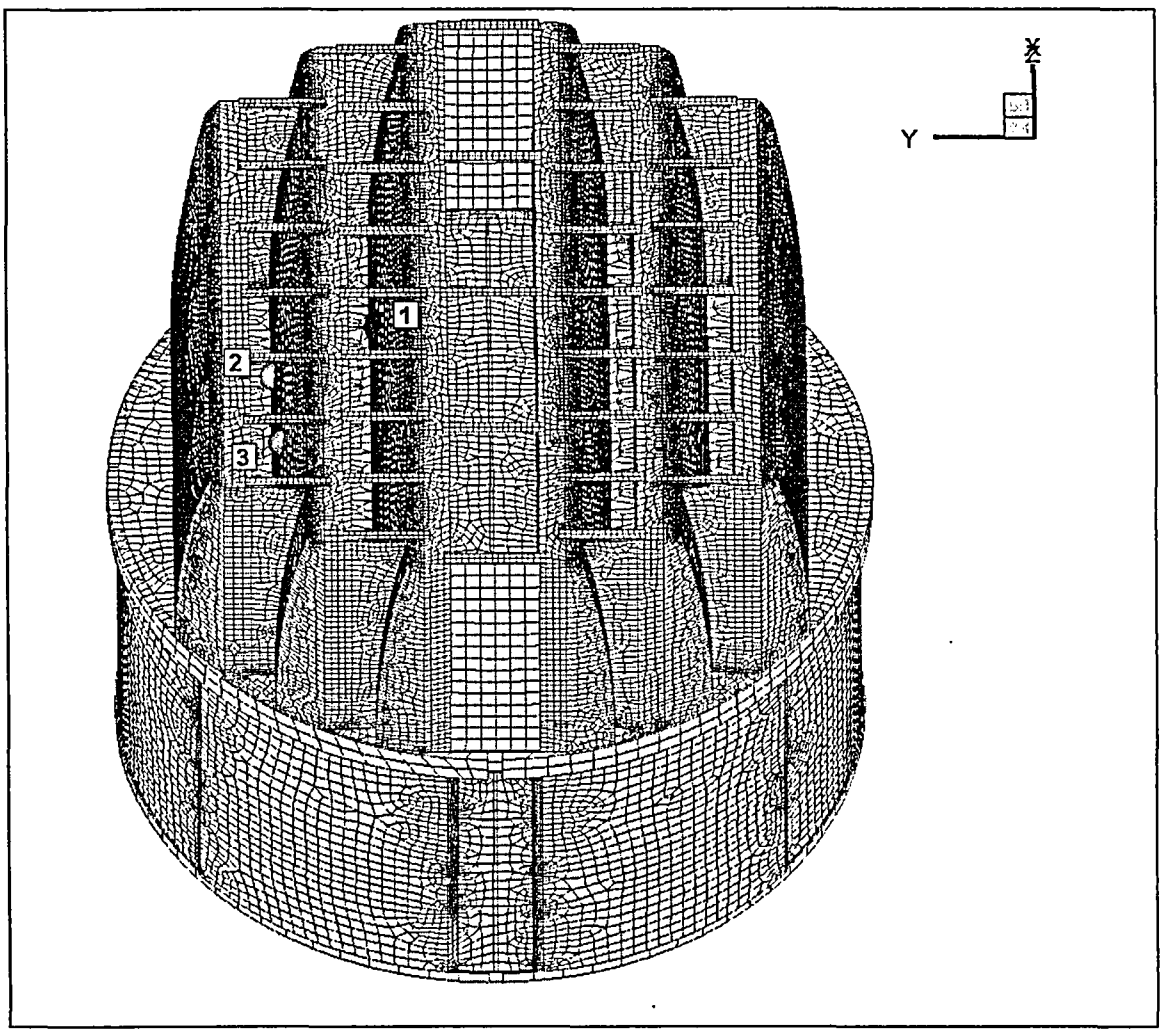

Figure 19c. Locations of minimum alternating stress ratios, SR-a, at non-welds for CLTP operation. Numbers refer to the enumerated locations for SR-a values at non-welds in Table 7a.

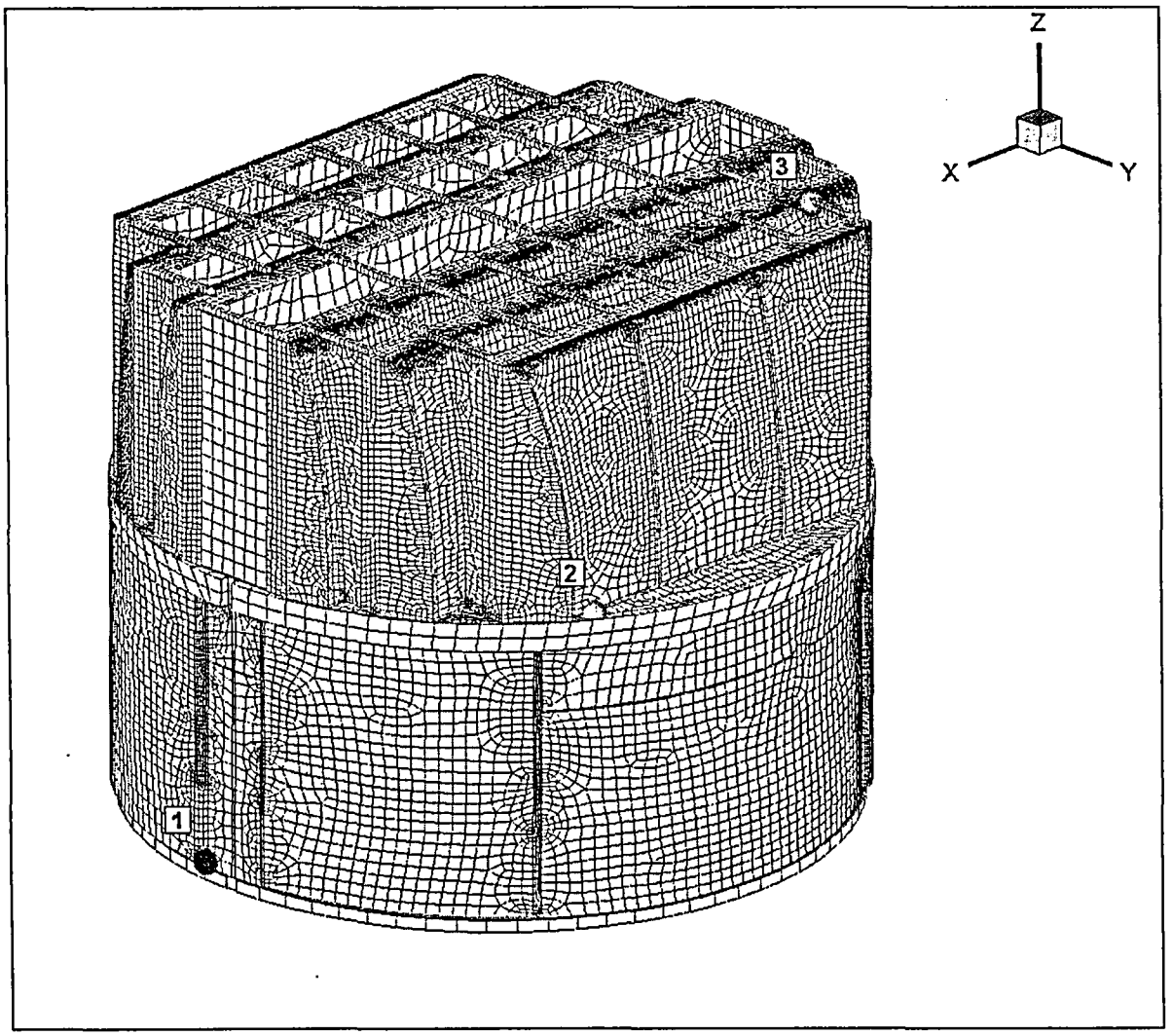

Figure 19d. Locations of minimum alternating stress ratios, SR-a, at welds for CLTP operation. Numbers refer to the enumerated locations for SR-a values at welds in Table 7a.

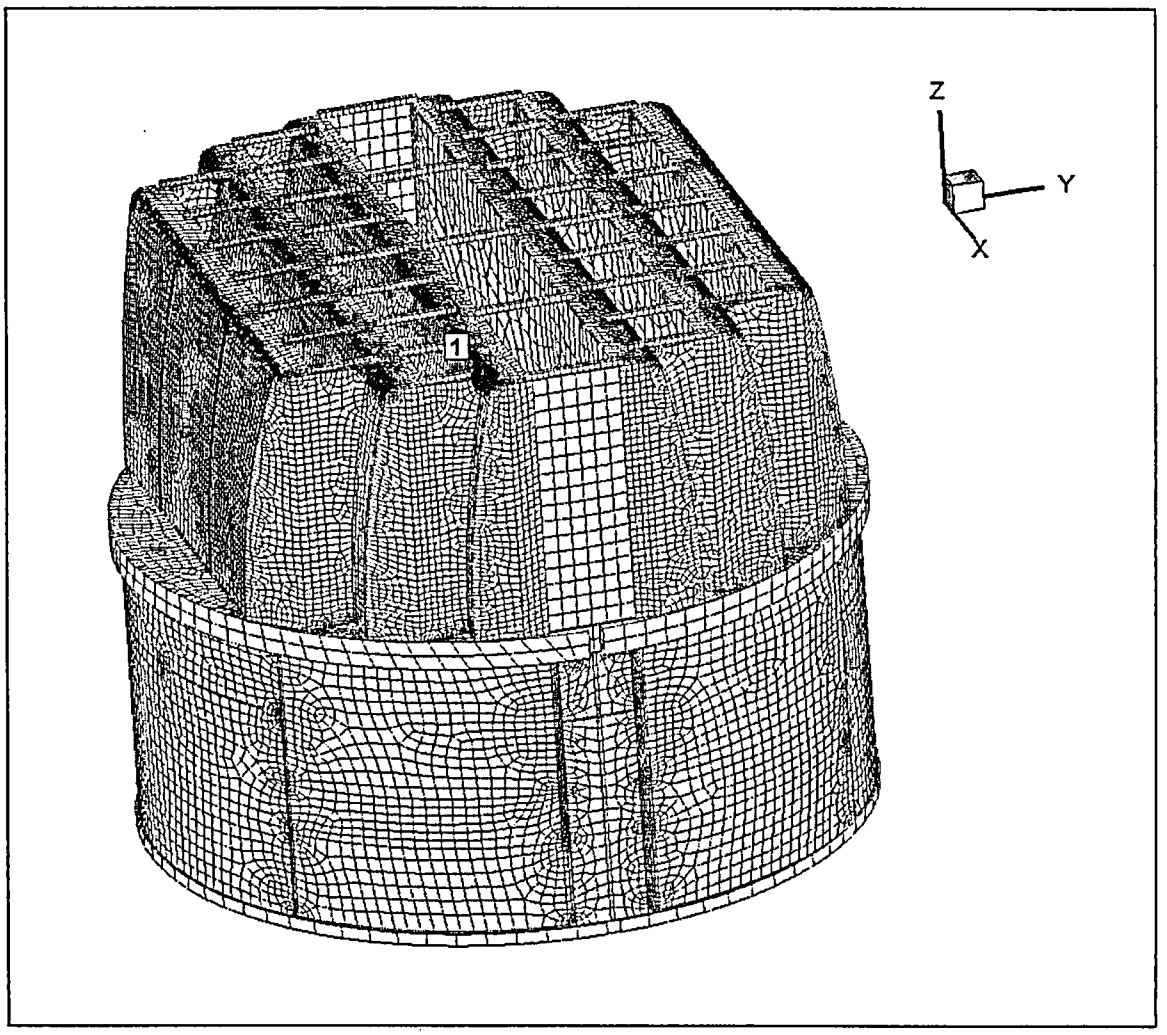

Figure 20a Locations of minimum peak stress ratios, SR-P, at non-welds for EPU operation. Numbers refer to the enumerated locations for SR-P values at welds in Table 7b.

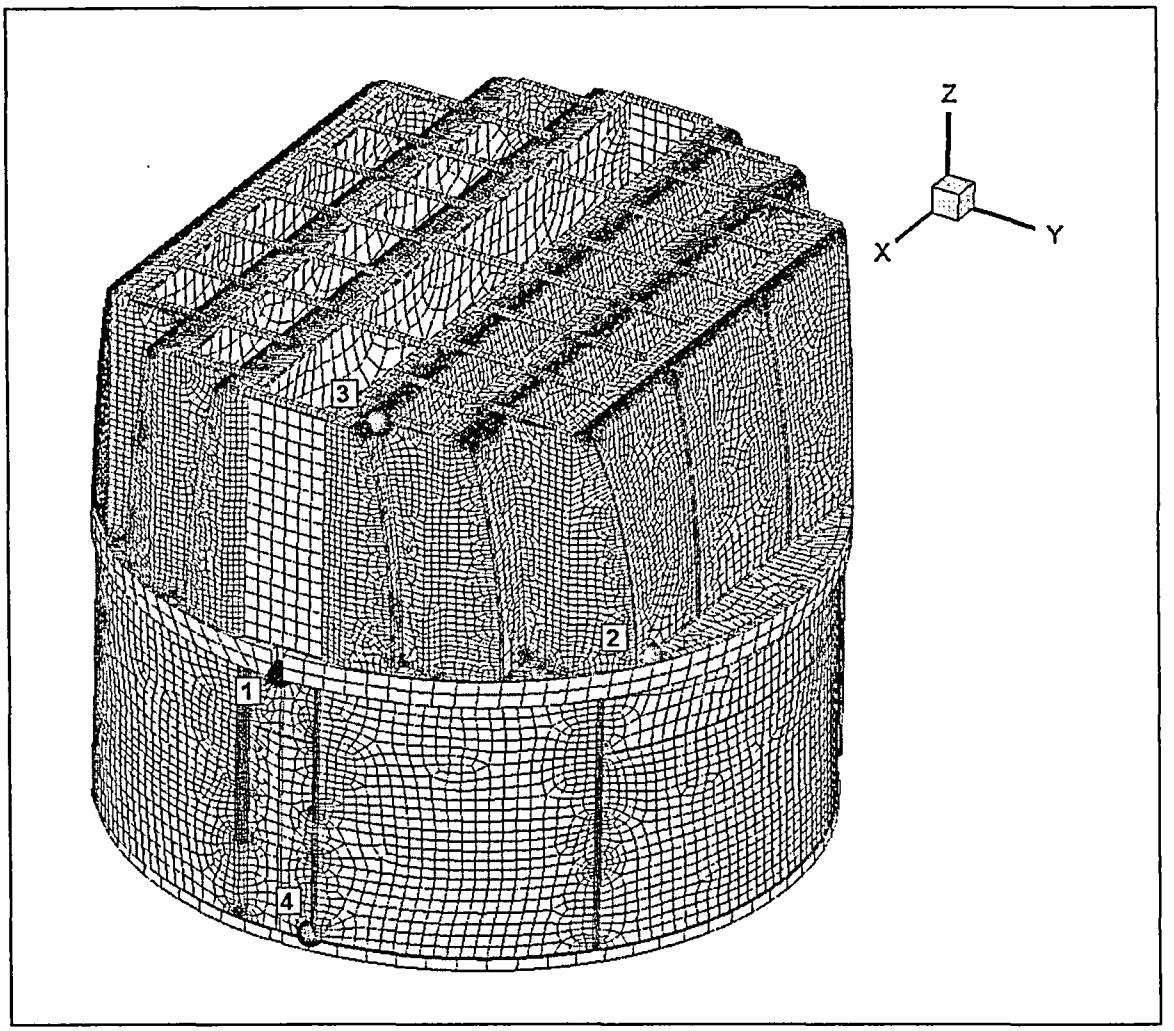

Figure 20b Locations of minimum peak stress ratios, SR-P, at welds for EPU operation. Numbers refer to the enumerated locations for SR-P values at welds in Table 7b.

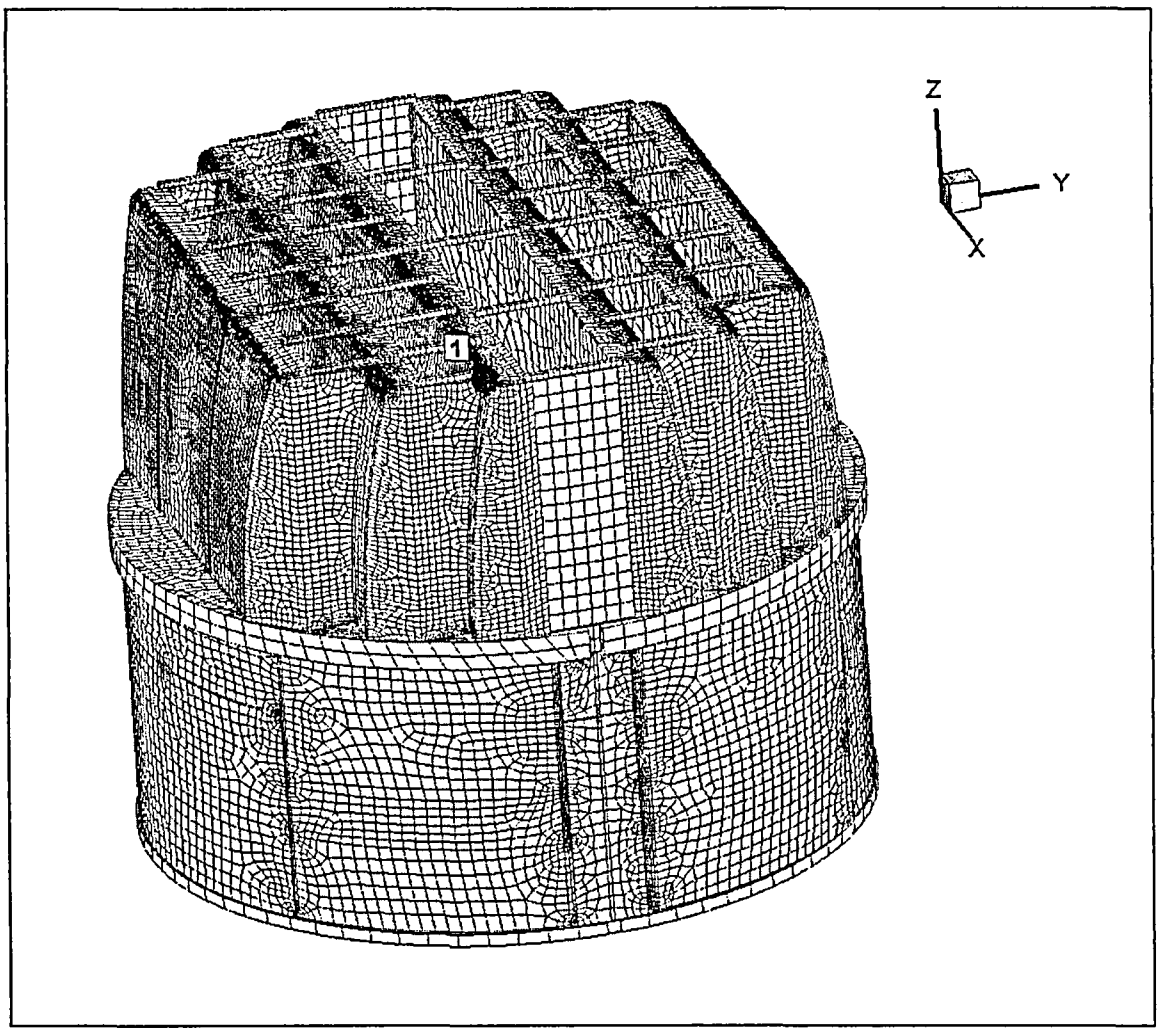

Figure 20c Locations of minimum alternating stress ratios, SR-a, at non-welds for EPU operation. Numbers refer to the enumerated locations for SR-a values at non-welds in Table 7b.

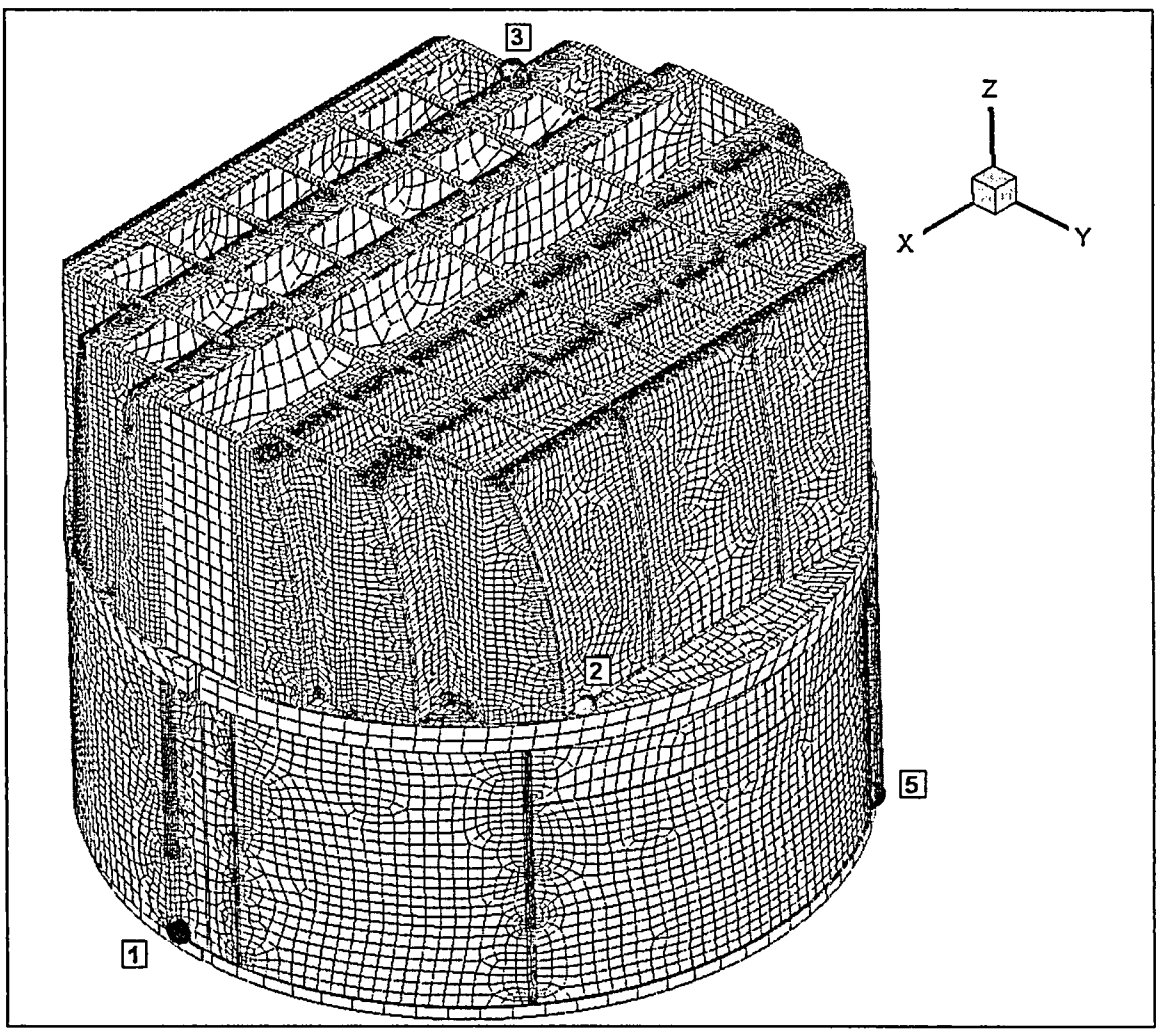

Figure 20d Locations of minimum alternating stress ratios, SR-a, at welds for EPU operation. Numbers refer to the enumerated locations for SR-a values at welds in Table 7b. First view showing enumerated locations 1-3 and 5.

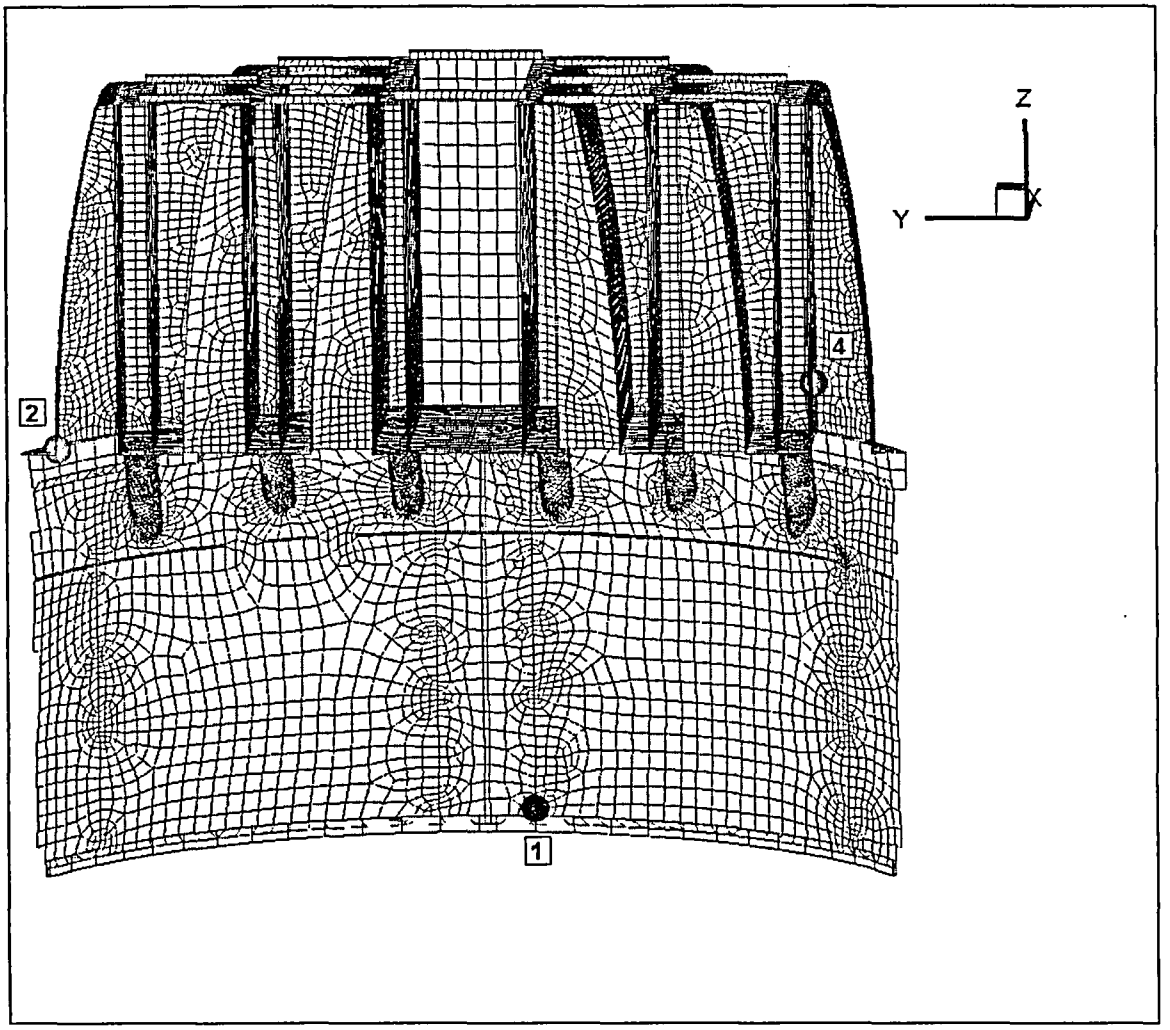

Figure 20e Locations of minimum alternating stress ratios, SR-a, at welds for EPU operation. Numbers refer to the enumerated locations for SR-a values at welds in Table 7b. Second cutaway view showing enumerated locations 1, 2 and 4.

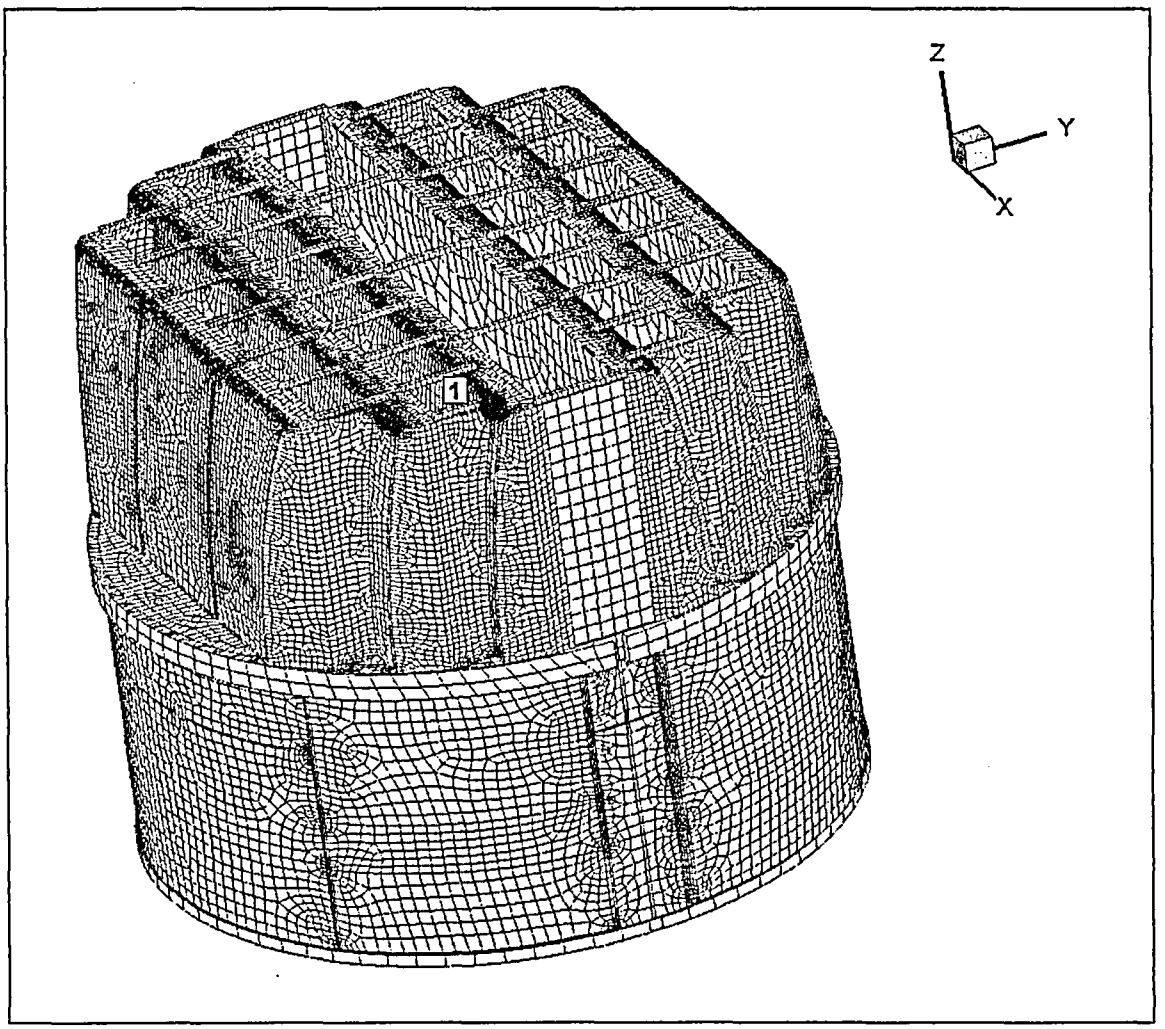

Figure 21a. Locations of minimum peak stress ratios, SR-P, at non-welds for EPU operation with -10% frequency shift. Numbers refer to the enumerated locations for SR-P values at welds in Table 7c.

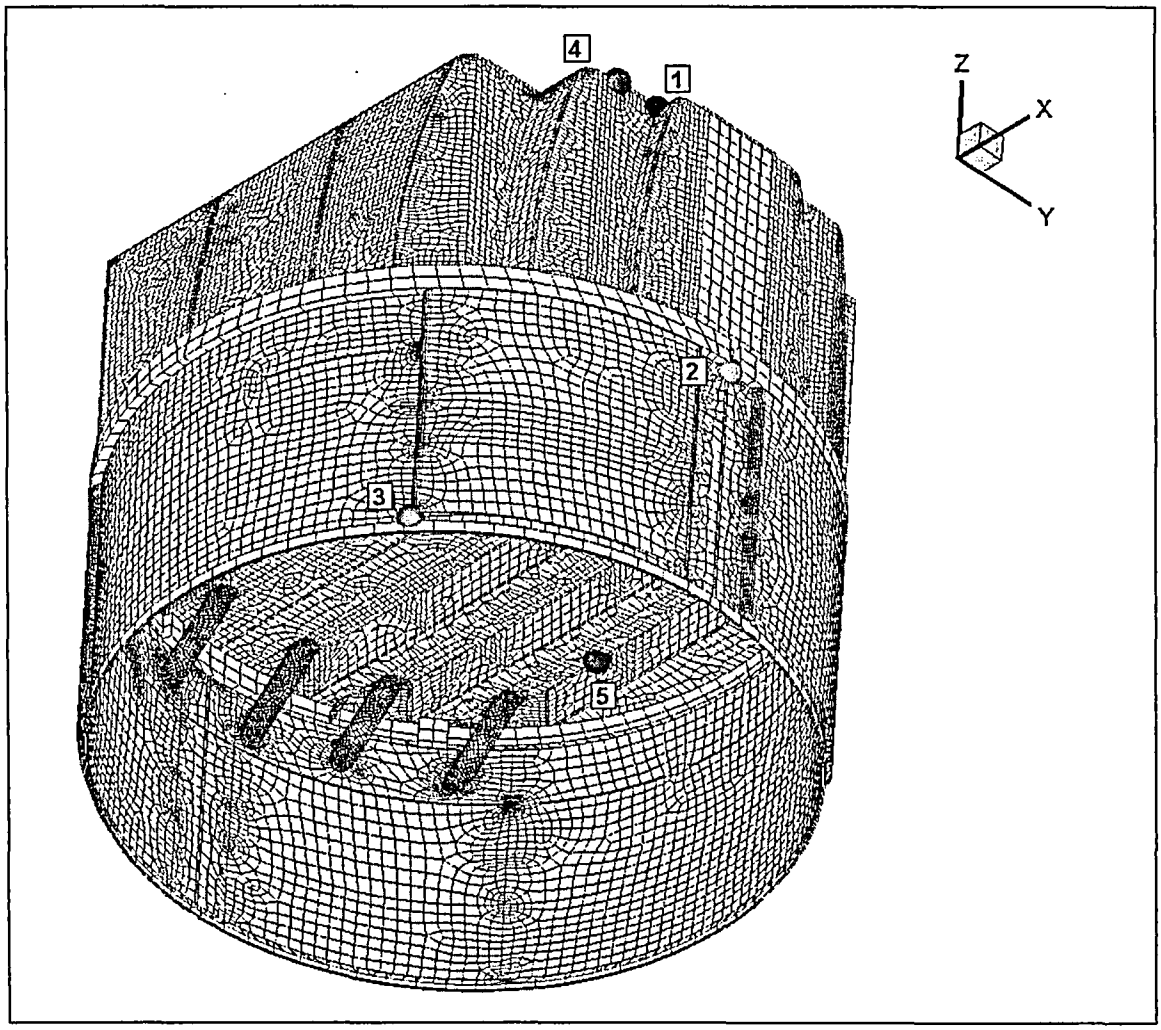

Figure 21b. Locations of minimum peak stress ratios, SR-P, at welds for EPU operation with -10% frequency shift. Numbers refer to the enumerated locations for SR-P values at welds in Table 7c.

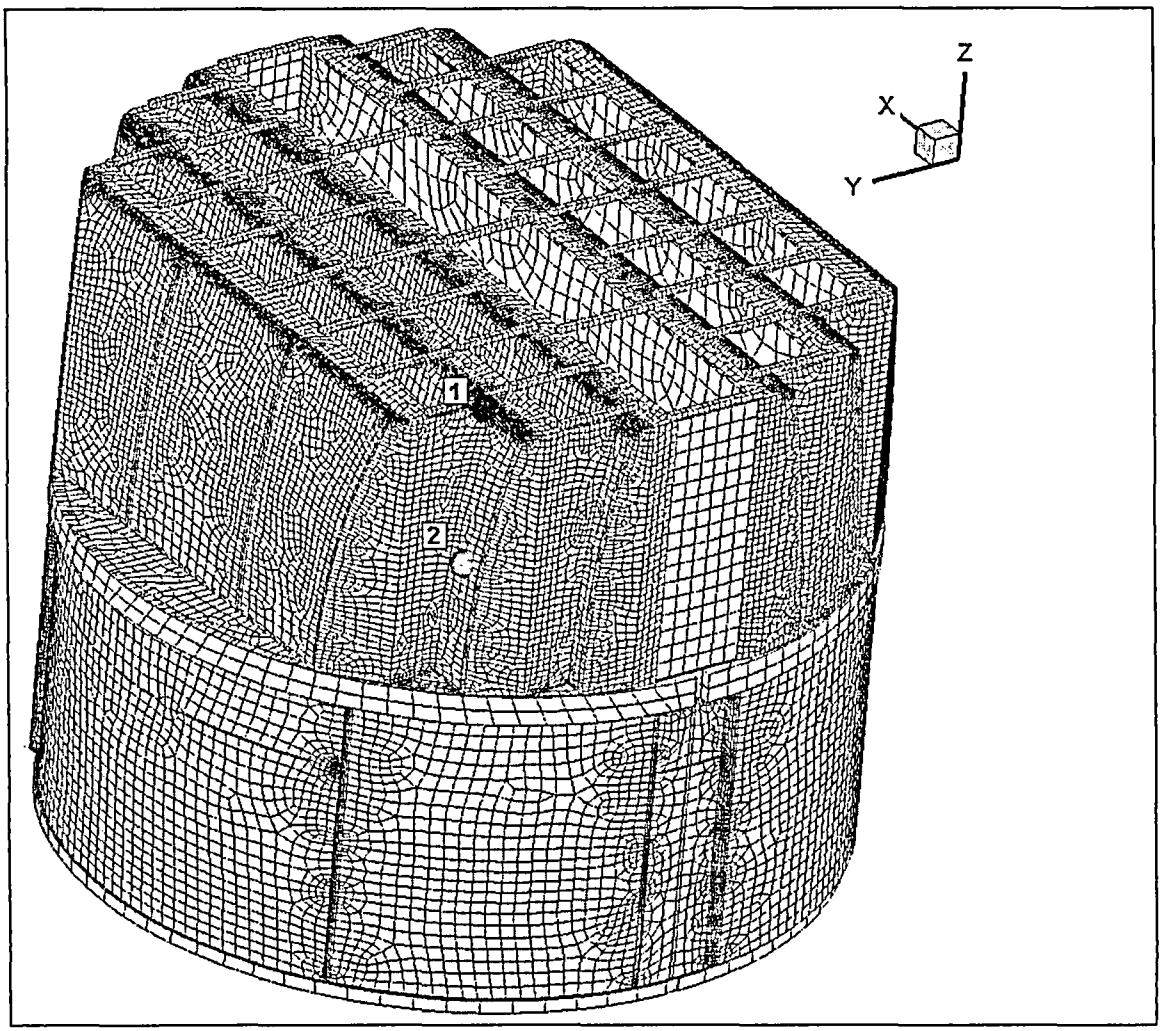

Figure 21c. Locations of minimum alternating stress ratios, SR-a, at non-welds for EPU operation with -10% frequency shift. Numbers refer to the enumerated locations for SR-a values at non-welds in Table 7c.

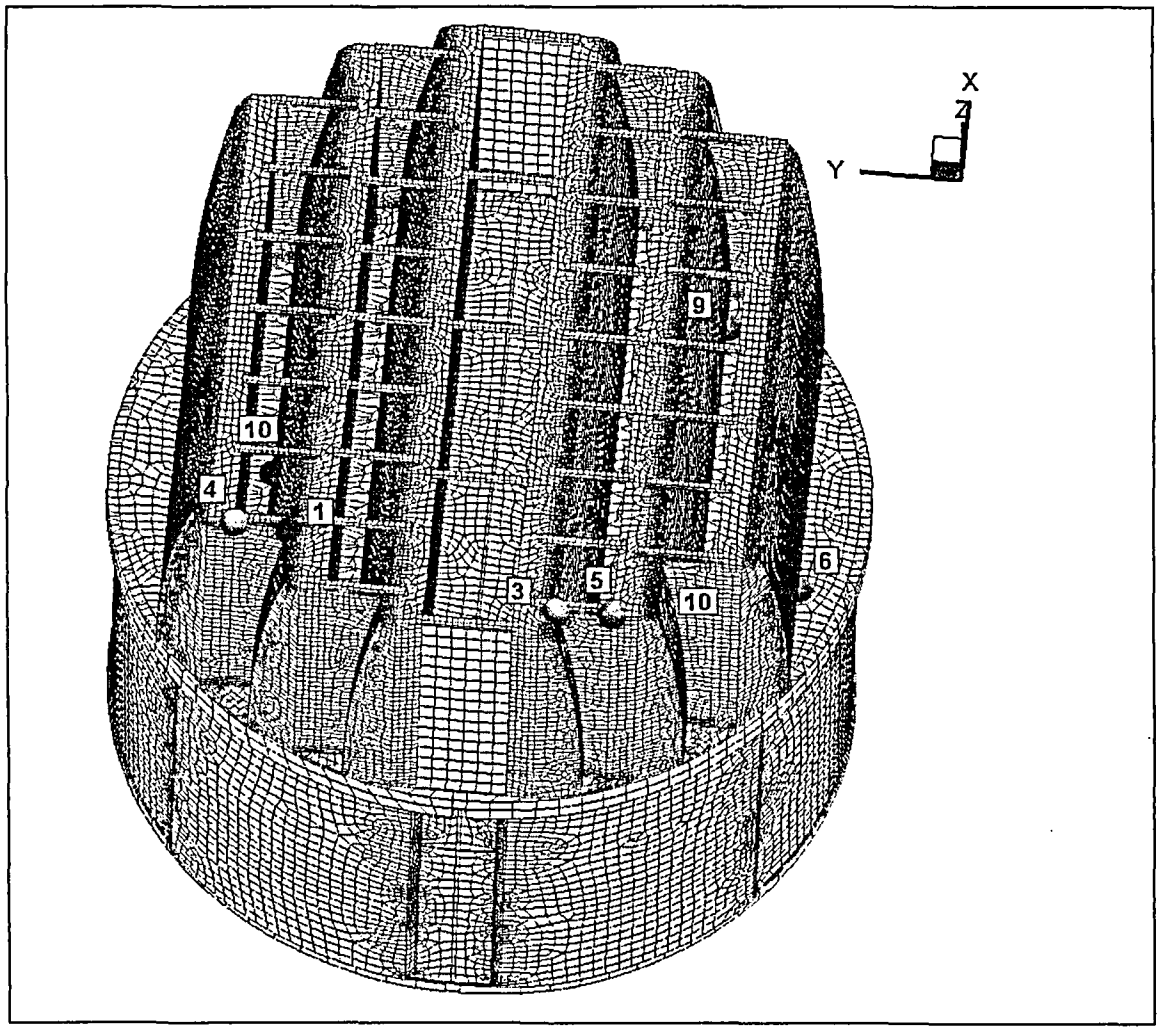

Figure 21d. Locations of minimum alternating stress ratios, SR-a, at welds for EPU operation with -10% frequency shift. Numbers refer to the enumerated locations for SR-a values at welds in Table 7c. First view showing enumerated locations 1, 3-6, 9 and 10.

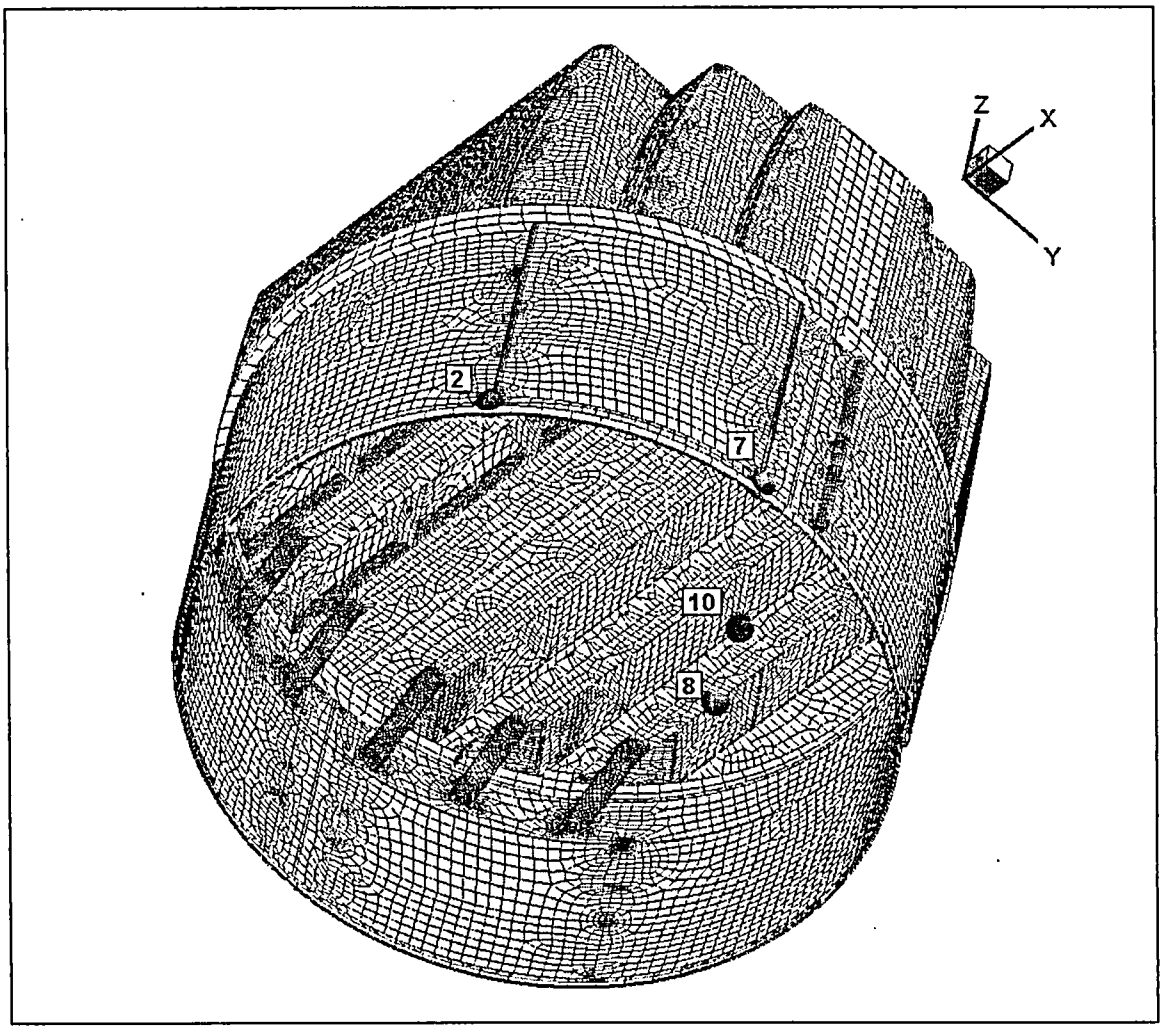

Figure 21e. Locations of minimum alternating stress ratios, SR-a, at welds for EPU operation with -10% frequency shift. Numbers refer to the enumerated locations for SR-a values at welds in Table 7c. Second view showing enumerated locations 2, 7, 8 and 10.

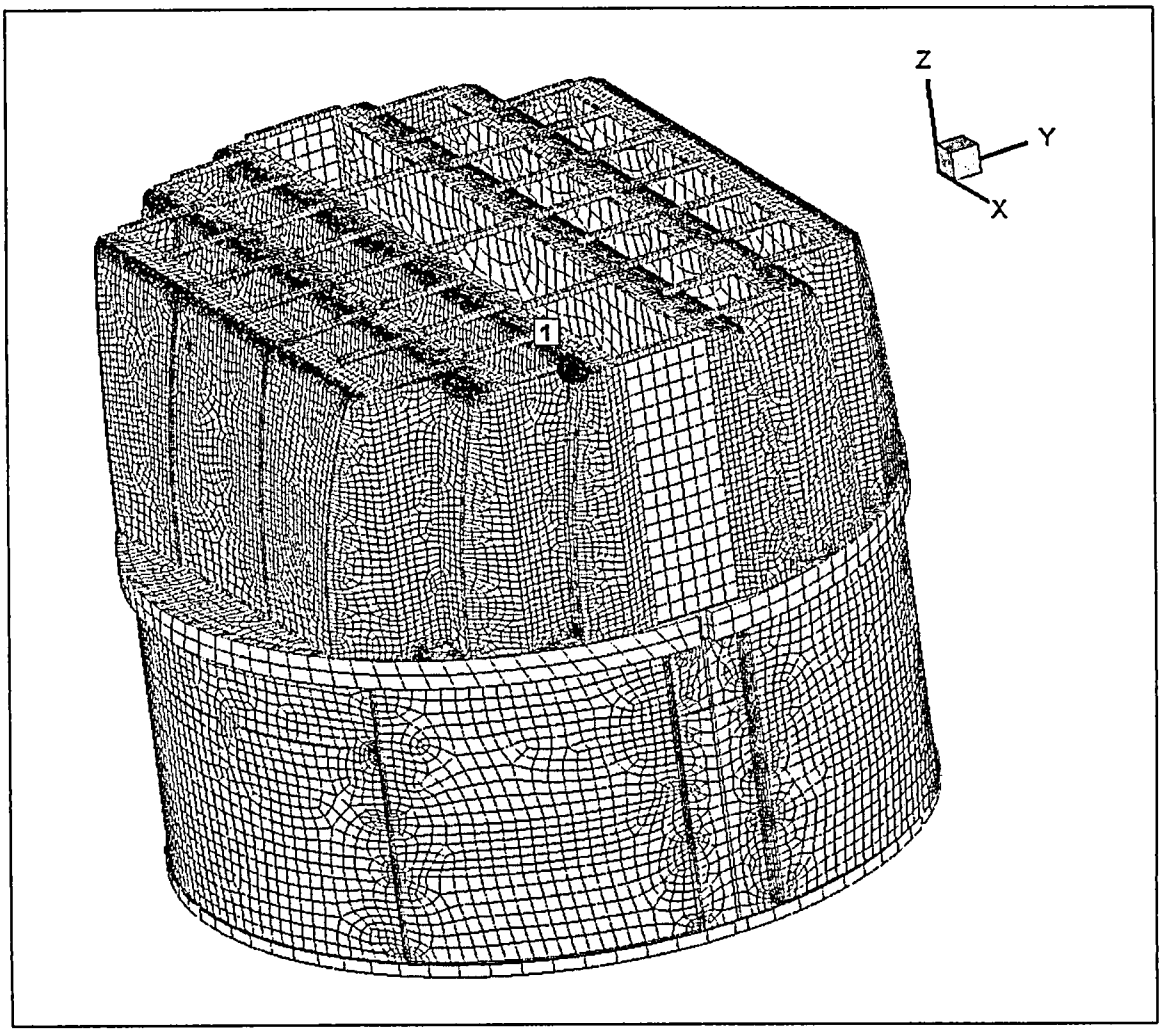

Figure 22a. Locations of minimum peak stress ratios, SR-P, at non-welds for EPU operation with +10% frequency shift. Numbers refer to the enumerated locations for SR-P values at welds in Table 7d.

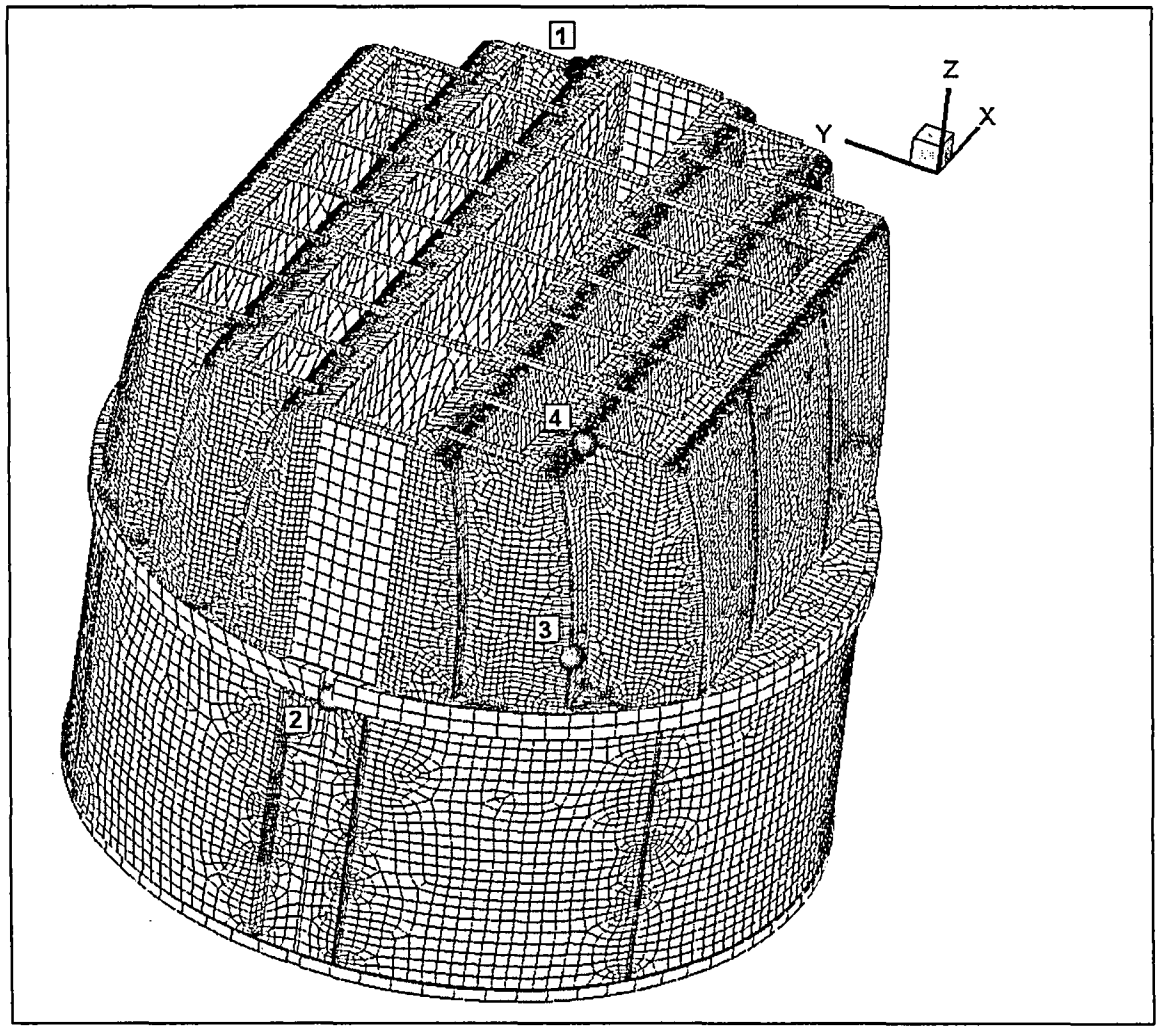

Figure 22b. Locations of minimum peak stress ratios, SR-P, at welds for EPU operation with +10% frequency shift. Numbers refer to the enumerated locations for SR-P values at welds in Table 7d.

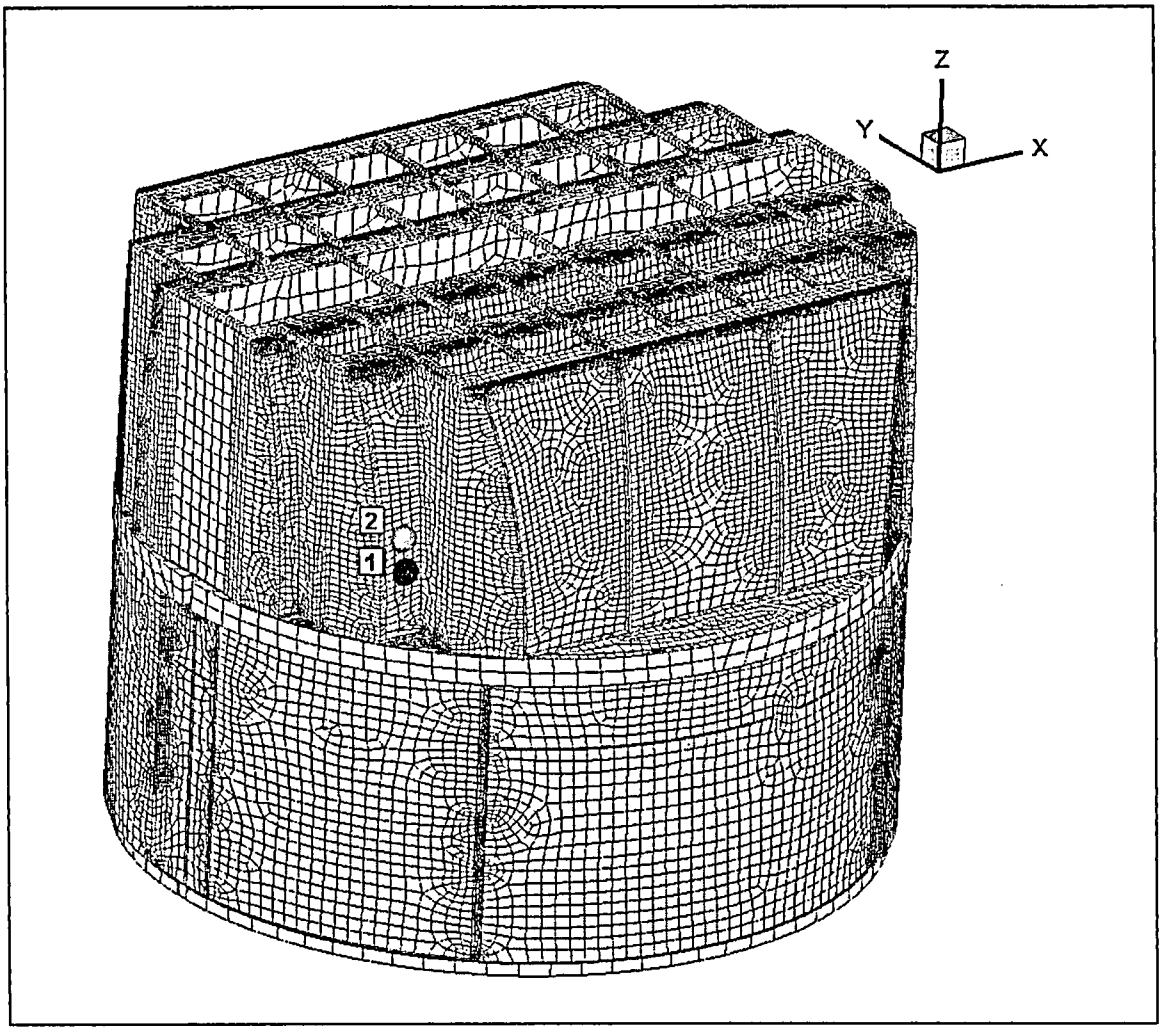

Figure 22c. Locations of minimum alternating stress ratios, SR-a, at non-welds for EPU operation with +10% frequency shift. Numbers refer to the enumerated locations for SR-a values at non-welds in Table 7d.

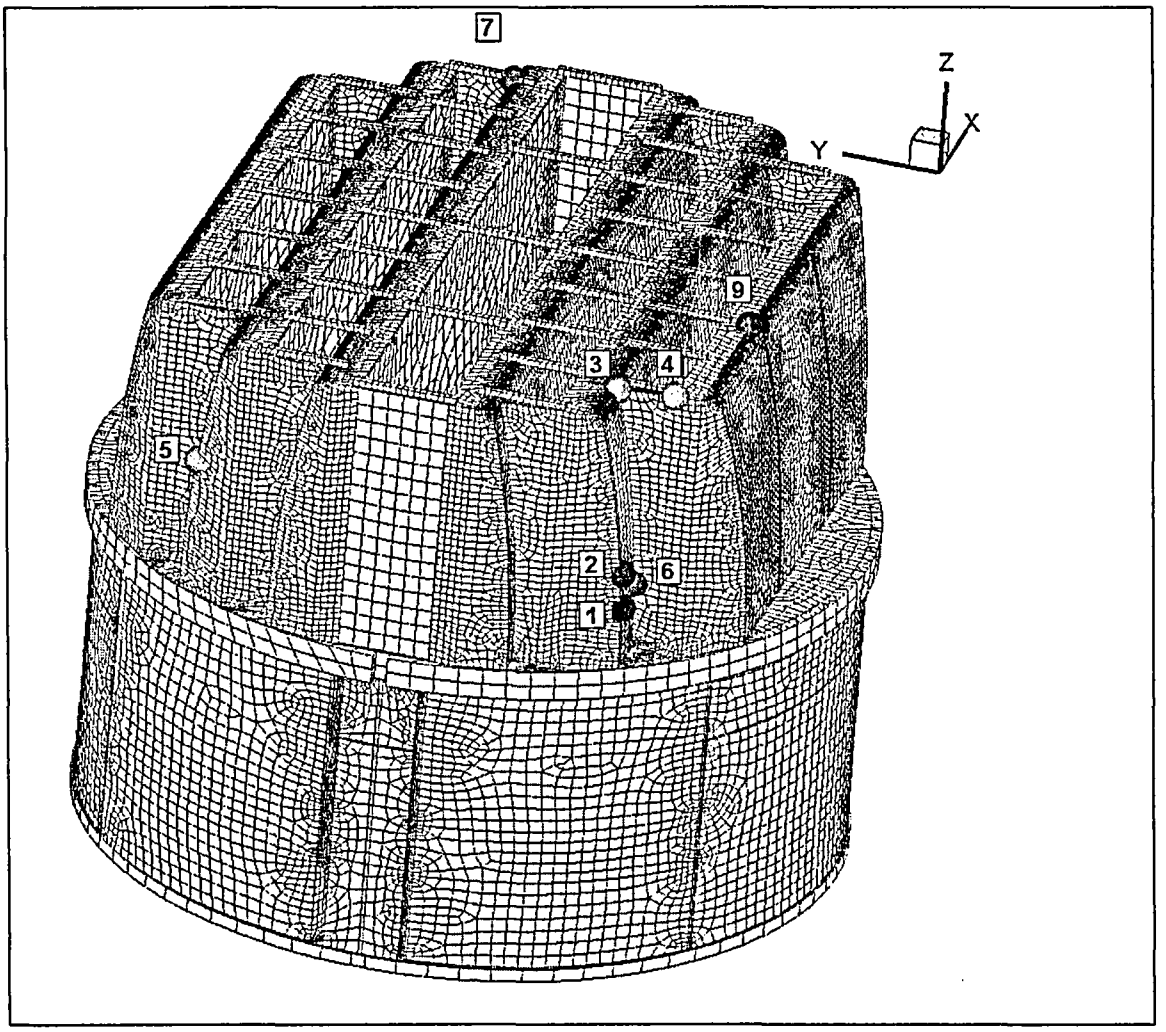

Figure 22d. Locations of minimum alternating stress ratios, SR-a, at welds for EPU operation with +10% frequency shift. Numbers refer to the enumerated locations for SR-a values at welds in Table 7d. First view showing enumerated locations 1-7 and 9.

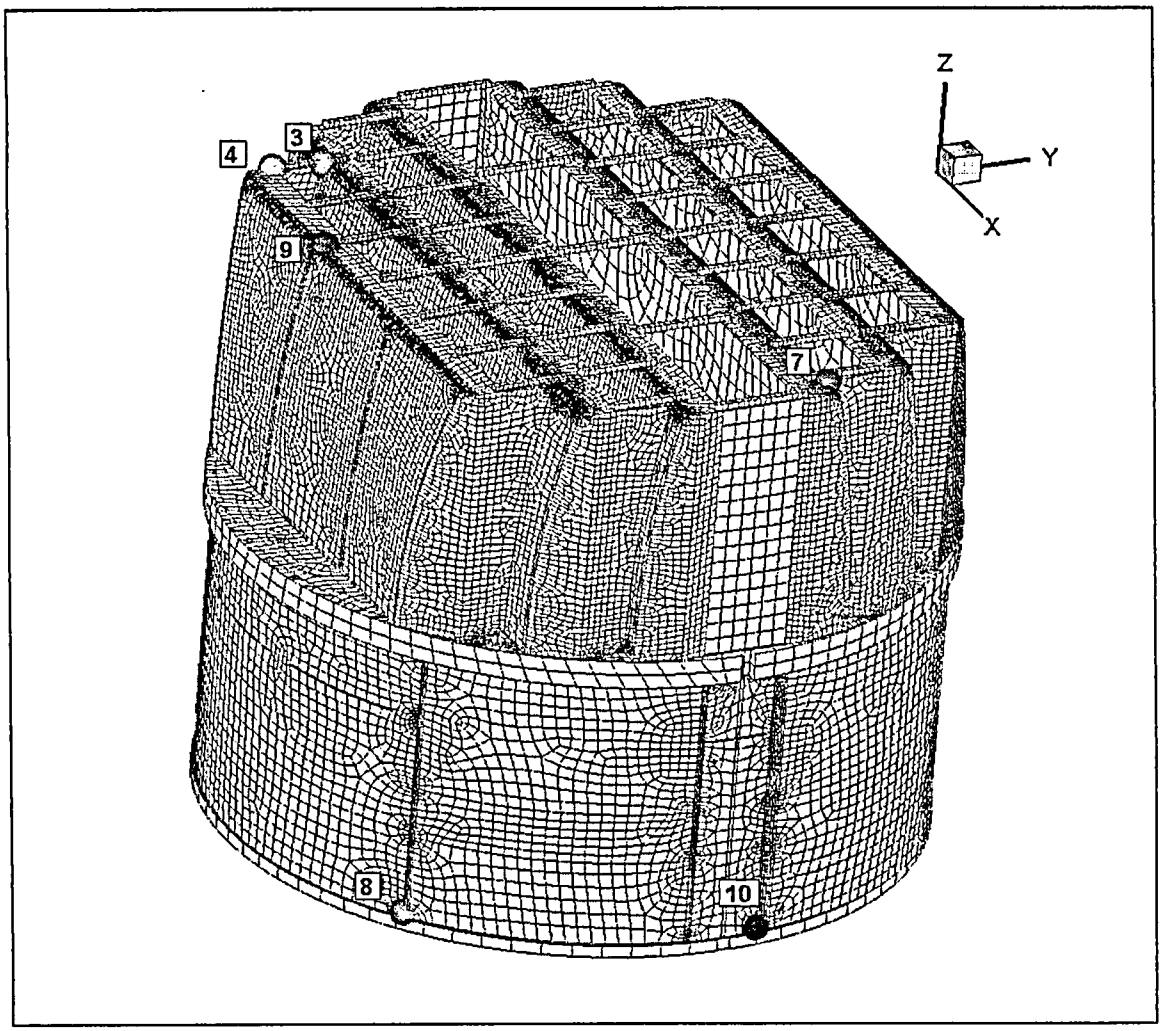

Figure 22e. Locations of minimum alternating stress ratios, SR-a, at welds for EPU operation with +10% frequency shift. Numbers refer to the enumerated locations for SR-a values at welds in Table 7d. Second view showing enumerated locations 3, 4 and 7-10.

5.3 PSD of Stress Time History

One way to assess the sensitivity of the analysis to uncertainty in frequency domain is to compare the stress responses obtained for the same load history with different time steps, corresponding to frequency shifting. In this section therefore, the PSDs are compared for nodes identified as having the lowest alternating stress ratios. The stress PSDs are estimated using 1405 time steps with approximately 0.7 Hz resolution. The selected nodes are:

93818 Located on the junction of drain channel and the skirt (minimum SR-a at CLTP and EPU). The associated PSDs are shown in Figure 23.

93493 Located on the junction of the outer hood and cover plate (second smallest SR-a at both CLTP and EPU). The PSDs at different loads are compared in Figure 24.

84384 Located at the junction of the middle hood and end plate (minimum SR-a at EPU with +10% frequency shift). The PSDs at different loads are compared in Figure 25.

87835 Located at junction of the closure plate and middle hood (minimum SR-a at EPU with -10% frequency shift). Figure 26 compares the PSDs for each load condition.

Several observations can be made. First, the EPU response at these locations has significant peaks approximately at the same frequencies as CLTP response, namely, approximately 120 Hz, 65 Hz and 50 Hz. The EPU response is generally higher, which is expected given the stronger pressure loading. When the frequencies are shifted the dominant peak for the EPU load occurring at 120 Hz is attenuated. However, new peaks occur about 132 Hz and 108 Hz corresponding to the shifted 120 Hz peaks. Hence the picture that emerges is that the main effect of frequency shifting is to excite the structural modes in the vicinity of the (suitably shifted) 120 Hz peak in the load.

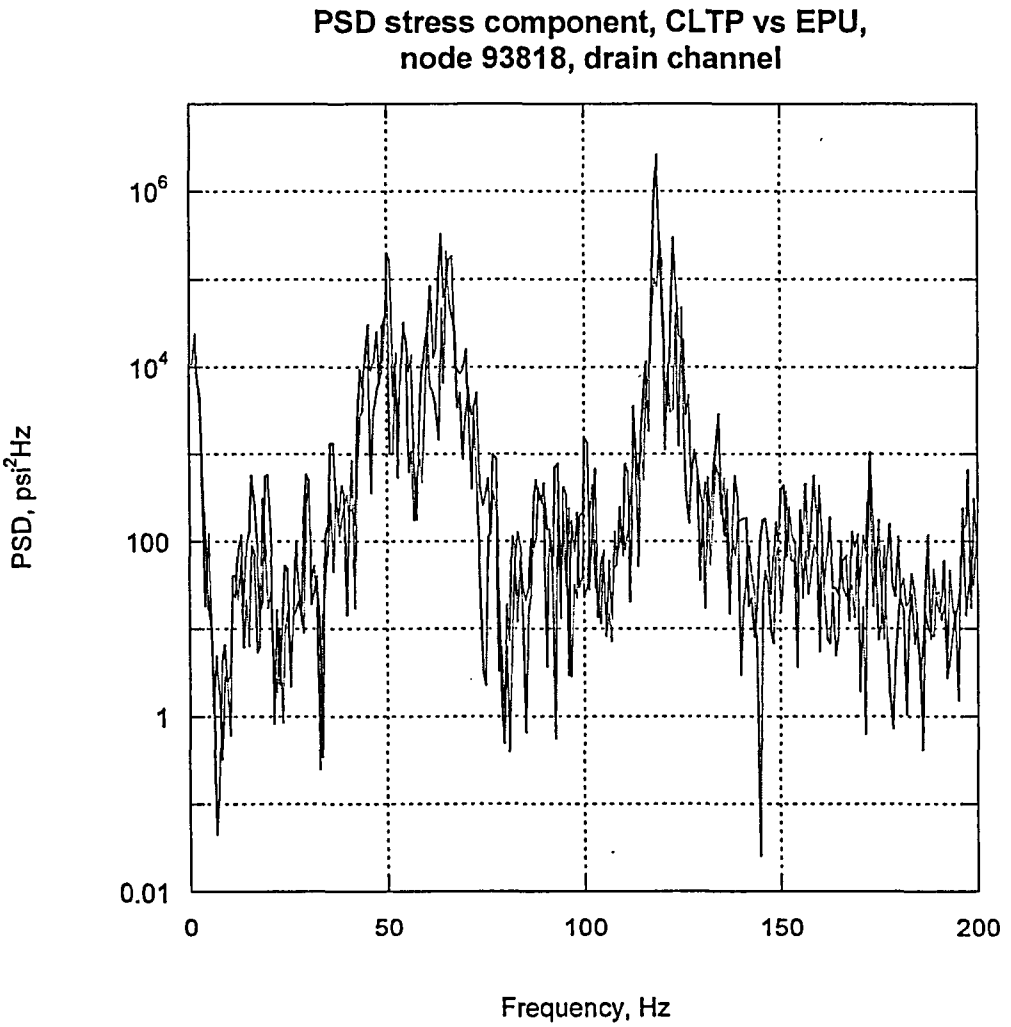

Figure 23a. PSD of the σ_{xx} stress response at node 93818 for CLTP and EPU operation. Red curve – CLTP; blue curve – EPU.

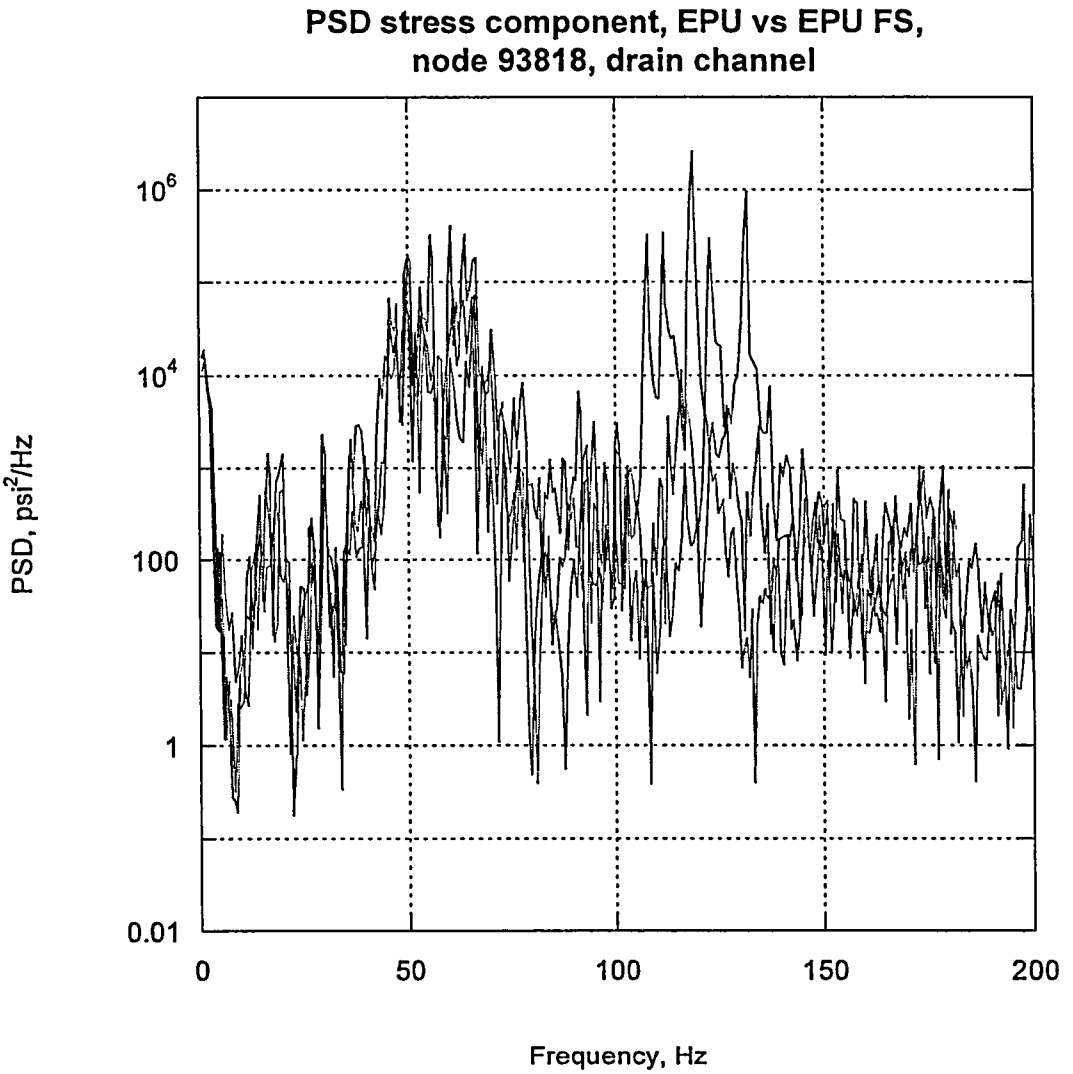

Figure 23b. PSD of the σ_{XX} stress response at node 93818 for EPU and EPU with frequency shift operation. Red curve – EPU, blue curve – EPU with +10% frequency shift, green curve – EPU with -10% frequency shift.

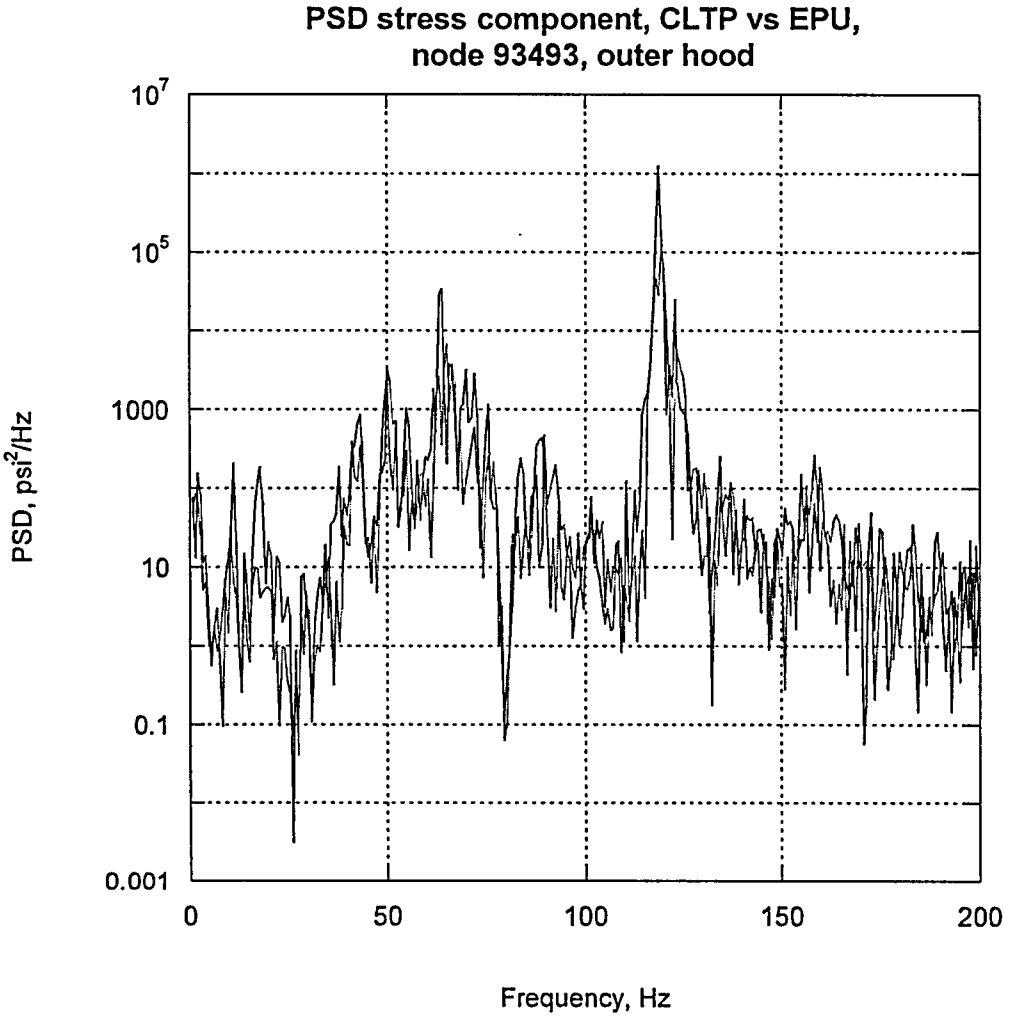

Figure 24a. PSD of the σ_{XX} stress response at node 93493 for CLTP and EPU operation. Red curve – CLTP; blue curve – EPU.

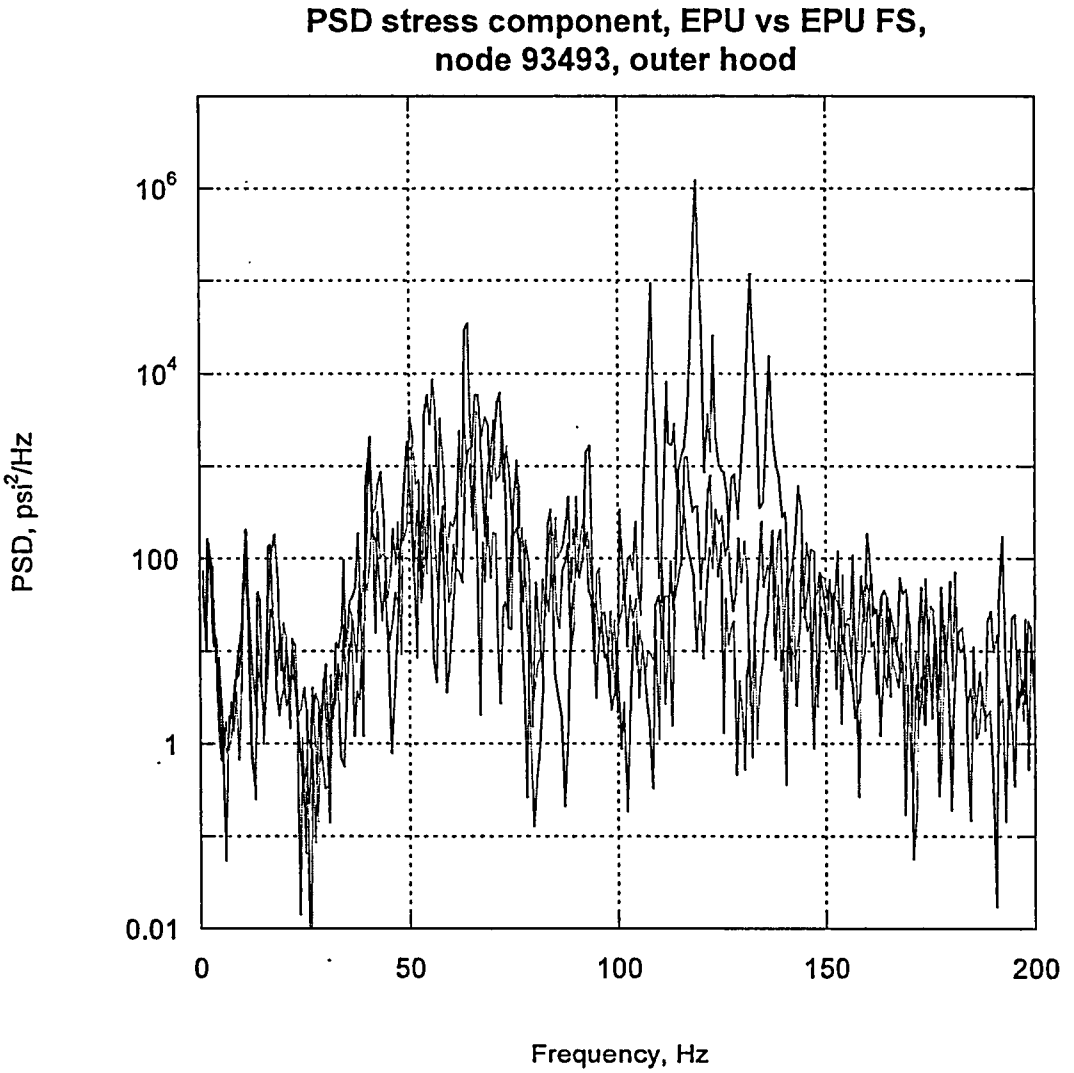

Figure 24b. PSD of the σ_{xx} stress response at node 93493 for EPU and EPU with frequency shift operation. Red curve – EPU, blue curve – EPU with +10% frequency shift, green curve – EPU with -10% frequency shift.

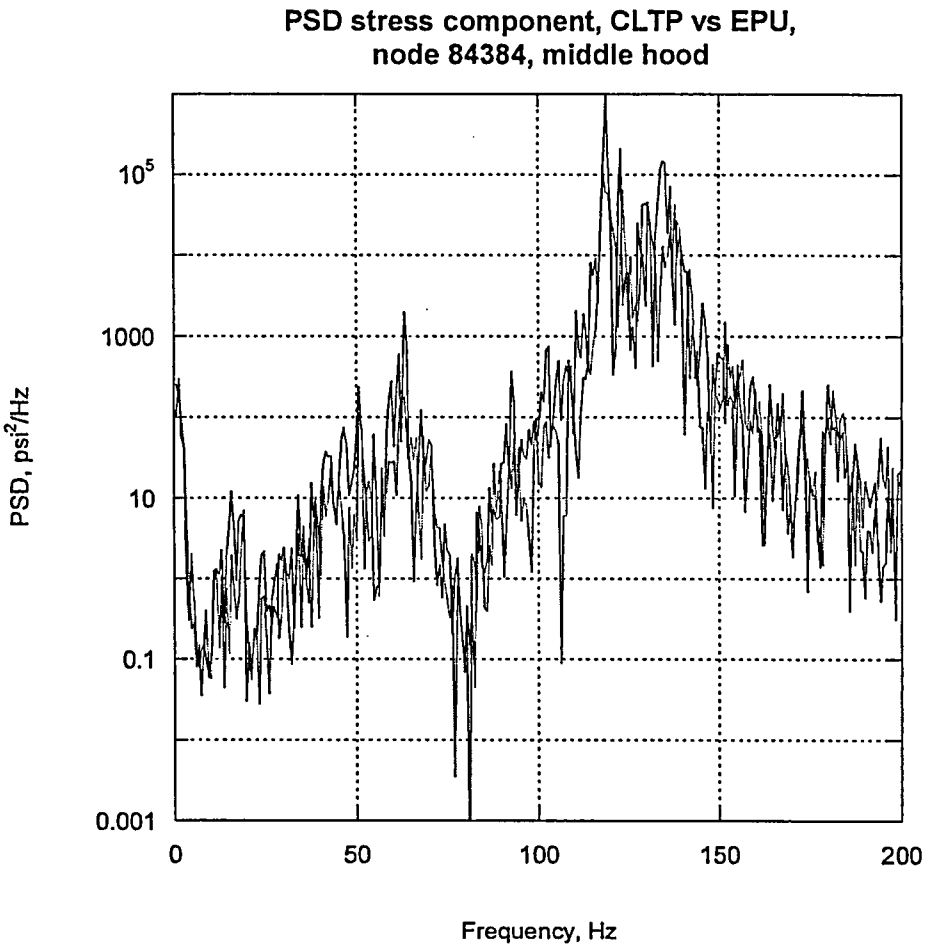

Figure 25a. PSD of the σ_{XX} stress response at node 84384 for CLTP and EPU operation. Red curve – CLTP; blue curve – EPU.

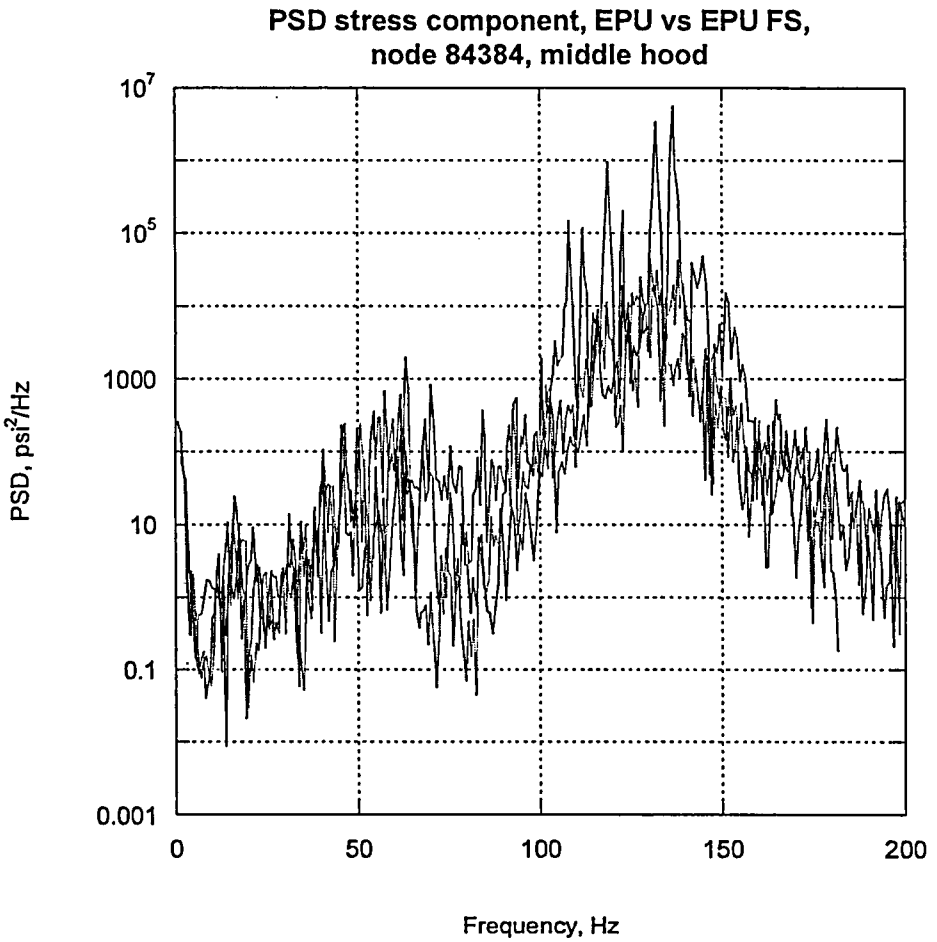

Figure 25b. PSD of the σ_{xx} stress response at node 84384 for EPU and EPU with frequency shift operation. Red curve – EPU, blue curve – EPU with +10% frequency shift, green curve – EPU with -10% frequency shift.

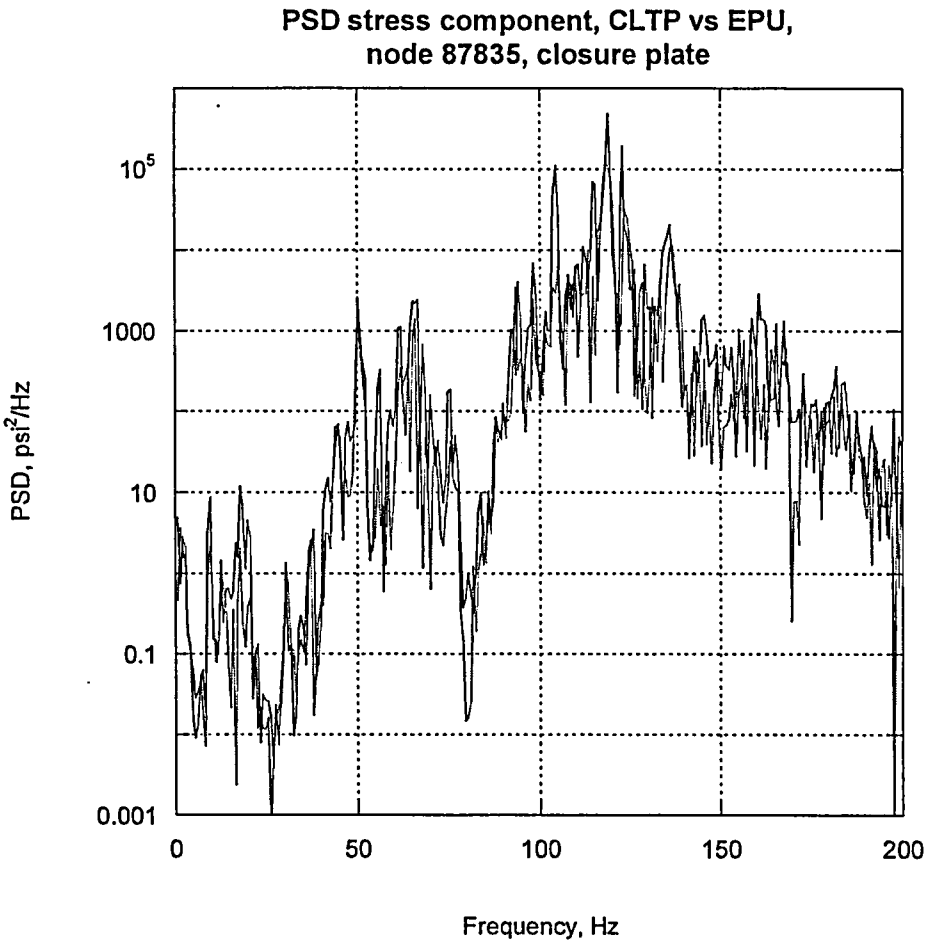

Figure 26a. PSD of the σ_{yy} stress response at node 87835 for CLTP and EPU operation. Red curve – CLTP; blue curve – EPU.

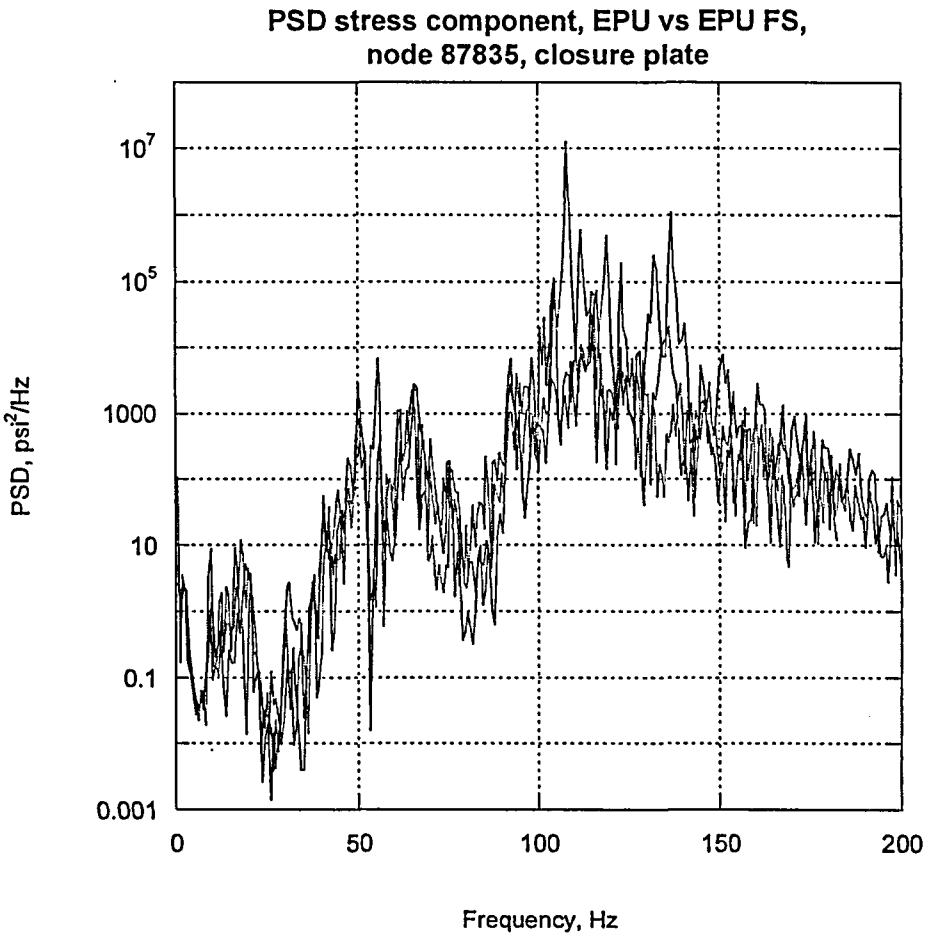

Figure 26b. PSD of the σ_{yy} stress response at node 87835 for EPU and EPU with frequency shift operation. Red curve – EPU, blue curve – EPU with +10% frequency shift, green curve – EPU with -10% frequency shift.

6. Conclusions

Maximum points of stress and calculated / allowable stress ratios have been obtained for the Hope Creek Unit 1 steam dryer at CLTP and EPU conditions using 1/8th scale measurement data. The CLTP and EPU loads obtained in a separate acoustic circuit model [1] were applied to a finite element model of the steam dryer consisting mainly of the ANSYS Shell 63 elements and brick continuum elements, for a duration of 2 seconds. The unsteady pressure loads contain a strong 80Hz component which is not present in the plant [4]. Therefore this frequency component was removed during post-processing. The resulting stress histories were analyzed to obtain peak and alternating stresses at all nodes for comparison against allowable levels. These results are tabulated in Table 7 of this report.

On the basis of these 1/8th scale loads, the dynamic analysis of the steam dryer shows that the steam flow and gravity loads produce the following minimum stress ratios:

CLTP	1.53
EPU	1.09
EPU with -10% frequency shift	0.984
EPU with +10% frequency shift	0.832

After removal of the 80 Hz signal, the dominant component in the load is approximately 120 Hz. Examination of the PSDs for the nodes exhibiting the minimum stress ratios, reveals that the main effect of frequency shifting is to excite the structural modes in the vicinity of the suitably shifted 120 Hz peak.

It is important to recognize that the results presented above do not account for any factors of conservatism and uncertainty in the applied loads. For example, the in-plant conservatism factor developed in [3] is 0.75 indicating that stress ratios should be multiplied by 1/0.75=1.33 to account for this factor. It is expected that when all factors are accounted for that the stress ratios will increase significantly (by approximately a factor of 2) so that all minimum stress ratios will be well within allowables during both CLTP and EPU operation.

7. References

1. Continuum Dynamics, Inc. June 2006. Estimating High Frequency Flow Induced Vibration in the Main Steam Lines at Hope Creek Unit 1: A Subscale Four Line Investigation of Standpipe Behavior. C.D.I. Report No. 06-16.

2. Meijers, P. 1985. Refined Theory for Bending and Torsion of Perforated Plates. *Journal of Pressure Vessel Technology* 108: 423-429.

3. Continuum Dynamics, Inc. July 2006. Hydrodynamic Loads on Hope Creek Unit 1 Steam Dryer to 200 Hz. C.D.I. Report No. 06-17.

4. Continuum Dynamics, Inc. August 2006. High and Low Frequency Steam Dryer Loads by Acoustic Circuit Methodology. C.D.I. Technical Memorandum No. 06-25P.

HOPE CREEK GENERATING STATION
FACILITY OPERATING LICENSE NPF-57
DOCKET NO. 50-354

REQUEST FOR LICENSE AMENDMENT
EXTENDED POWER UPRATE
EPU POWER ASCENSION TEST PLAN OVERVIEW

Introduction and Purpose

The Hope Creek Generating Station (HCGS) EPU Power Ascension Test Plan (PATP) "overview" describes the planned course of action for monitoring and evaluating the performance of the Steam Dryer as well as the Main Steam and Feedwater piping systems during power ascension testing and operation above 100% of the Current Licensed Thermal Power (CLTP). The PATP covers power ascension up to the full 115% Extended Power Uprate (EPU) condition to verify acceptable performance and steam dryer and piping system integrity. Through the establishment of operating limits, data collection and analysis, and any subsequent actions, the PATP will ensure that the integrity of the steam dryer and piping systems will be maintained in an acceptable state.

The detailed PATP and procedures will be developed after the completion of the Design Change Package for the extended power uprate (EPU). The plan will include specific hold points and durations during power ascension above CLTP; activities to be accomplished during hold points; plant parameters to be monitored; required inspections and walkdowns; data evaluation methods; acceptance criteria for monitoring and trending plant parameters; and actions to be taken, including interactions with NRC staff, if acceptance criteria are not satisfied.

PSEG will provide the detailed Power Ascension Test Plan to the NRC staff before increasing power above CLTP.

Scope

The PATP is primarily an initial power ascension test plan designed to assess steam dryer and selected piping system performance from 100% CLTP to 115% CLTP, and also to perform confirmatory inspections for a period of time following initial and continued operation at uprated power levels. Power ascension above 100% CLTP will be achieved in a series of 2.5% power step increases and holds at plateaus corresponding to 5% increments above CLTP. Elements of this plan will be implemented before EPU power ascension testing, and others may continue after power ascension testing.

There are three main elements of the PATP:

1. Slow and deliberate power ascension with defined hold points and durations, allowing time for monitoring and analysis.

2. A detailed power ascension monitoring and analysis program to trend steam dryer and critical piping system performance (through the monitoring of Main Steam Line strain gauges, piping accelerometers, and moisture carryover).

3. A long term inspection program to verify steam dryer and piping system performance at EPU conditions.

1. Power Ascension

Upon the completion of the final Design Change Package associated with the overall EPU effort, a detailed "Infrequently Performed Test Evolution" (IPTE) document will be developed for the implementation of the actual power ascension testing evolutions. The HCGS power ascension will occur over a period of time with gradual increases in power, hold periods, and engineering analysis of monitored data that must be approved by station management prior to subsequent power increases. Relevant data and evaluations will be transmitted to the NRC staff in accordance with the plan. The PATP includes (but is not limited to):

1. Power ascension rate of ~ 1% CLTP / hr
2. Hourly collection of steam line strain gauge and vibration data during power ascension
3. Data evaluated at every 2.5% CLTP power increase against acceptance criteria
4. Data evaluated against acceptance criteria and forwarded to the NRC at every 5% CLTP power increase

2. Monitoring and Analysis

The PATP is primarily an initial power ascension test plan designed to assess steam dryer and piping system performance and integrity from 100% CLTP to 115% CLTP. The assessment of the system / component performance and integrity will be completed through the analysis of both stress and moisture carryover data.

Power ascension above 100% CLTP will be achieved via the following "Power Ascension Test Plan" methodology:

- Maximum hourly power increase restriction – 1% CLTP per hour (~33.4 MWt)
- Obtain hourly steam line strain gauge and piping vibration data during power level increases
- Each 2.5% Power ascension (~84MWt) - Compare strain gauge / vibration data to acceptance criteria
- Each 2.5% Power ascension (~84MWt) - Obtain/ evaluate moisture carryover data

- Each 5% Power ascension "plateau" (In addition to 2.5% criteria)
  - o Perform plant walkdowns
  - o Review data evaluation and walkdown results with Station Management
  - o Provide data to NRC for review.

The duration of the individual "Hold Points" will be determined by the time required to obtain the specified data, complete the evaluation, and obtain the required level of approval to proceed.

As noted, system performance and integrity will be evaluated based on the review and analysis of both stress and moisture carryover values. For both the stress and moisture carryover elements, acceptance criteria will be established within the detailed IPTE for use in the subject analysis. Data evaluation / analyses will be performed by comparing actual obtained data against the acceptance criteria. Both the stress and moisture carryover criteria will provide two "threshold" action levels, which will be used in determining the acceptability of the continuance of power ascension increases. The following information further defines the "threshold" action levels for both the pipe stress and moisture carryover analyses:

Pipe Stress Evaluation
Data evaluation / analysis will be performed by comparing accelerometer data obtained at each 2.5% power ascension plateau over 100% CLTP against the acceptance criteria. The subject acceptance criteria as derived from Attachment No. 8, "Summary of FIV Investigation at EPU Conditions" will provide two "threshold" action levels, which will be (and the required "action"):

- Level 1: Allowable Stress Exceeded
  - o Action – Reduce power to previous acceptable level
- Level 2: Low Margin
  - o Action – Hold at current power level and re-evaluate

Main Steam Line Strain Gauge Monitoring / Evaluation
In addition to data collection through the use of accelerometers, data will be obtained for Main Steam line piping through the use of previously installed strain gauges. Evaluation of the strain gauge data will be by comparison against the limit curves developed from the steam dryer finite element analysis

Moisture Carryover Evaluation
Data evaluation / analysis will be performed by comparing moisture carryover data obtained at each 2.5% power ascension plateau over 100% CLTP against the predetermined acceptance criteria. The subject acceptance criteria will provide two "threshold" action levels, which will be specifically defined upon completion of the EPU Design Change Package (and the required "action"):

- Level 1: Moisture carryover criteria exceeded
  - o Action – Reduce power to previous acceptable level

- Level 2: Moisture carryover criteria exceeded
  - o Action – Hold at current power level and re-evaluate

Data Collection Methods and Locations

A. Pipe / Component Stress
   1. Piping Inside the Drywell
      Main Steam and Feedwater piping inside the drywell will be monitored using accelerometers with data recorded on a Data Acquisition System (DAS) located outside of the drywell. Monitoring locations were established based on detailed analysis of the HCGS piping which identified the optimal quantity and locations of the subject sensors.

   2. Components Inside the Drywell
      Individual components inside the drywell will be monitored using accelerometers with data recorded on a DAS located outside of the drywell. Locations will be chosen based upon recent industry experience with component failures during EPU conditions in conjunction with engineering judgment as to the susceptibility of the components. Currently, two (2) Main Steam Safety relief valves (SRVs) have been selected for monitoring.

   3. Piping Outside the Drywell
      Main Steam and Feedwater piping in the Main Steam Tunnel will be monitored using accelerometers and DAS equipment. Monitoring locations were established based on detailed analysis of the HCGS piping which identified the optimal quantity and locations of the subject sensors.

B. Steam Dryer
   1. Moisture Carryover
      Moisture Carryover data collection will be completed via the implementation of existing station operating procedures. Frequency of the data collection and required analysis (including any "hold" times) will be controlled via the IPTE.

   2. Steam Line Strain Gauges
      Strain Gauge locations as discussed in Attachment No.7 will be monitored. Data obtained from the strain gauges will be recorded on a DAS located outside of the drywell.

Inspections and Walkdowns
Piping classified in the OM-3 group 3 outside the drywell will be monitored visually, either by walkdown or cameras at each test plateau. If visual observation indicates significant vibration, the noted condition will be evaluated in more detail.

Other Monitoring
Plant data that may be indicative of off-normal steam dryer and or piping system performance will be monitored during power ascension (e.g. reactor water level, steam flow, feed flow, steam flow distribution between the individual steam lines). Plant data can provide an early indication of unacceptable steam dryer / system performance. The enhanced monitoring of selected plant parameters will be controlled by the IPTE and other plant procedures.

NRC Notifications
Per the provisions of the PATP methodology, obtained data / evaluations will be provided to the NRC staff at each 5% power ascension "plateau" over 100% CLTP.

Upon the completion of the IPTE, a written report on steam dryer / system performance during EPU power ascension testing will be forwarded to the NRC staff. The report will include evaluations or corrective actions that were required to obtain satisfactory steam dryer performance. Additionally, it will include relevant data collected at each power step, comparisons to performance criteria (design predictions), and evaluations performed in conjunction with steam dryer structural integrity monitoring.

3. **Post EPU Monitoring Program**
Monitoring of various plant parameters potentially indicative of steam dryer / system failure will be continue after completion of the IPTE. Monitoring results will be made available to the NRC Staff. The following inspections will be performed:

Moisture Carryover
Station operating procedures will be used to monitor operating moisture carryover conditions. Results will be reviewed / evaluated on a defined basis to monitor moisture carryover conditions.

Strain Gauge / Accelerometer Monitoring
As the previously installed strain gauges and accelerometers remain operable, future data collection may be performed as deemed appropriate during the remainder of the operating cycle following EPU implementation.

Steam Dryer Monitoring and Inspection
The steam dryer inspection and the monitoring of plant parameters potentially indicative of steam dryer failure will be conducted, as recommended by General Electric Service Information Letter 644, Rev. 1.

Attachment 24

LR-N06-0286
LCR H05-01, Rev. 1

HOPE CREEK GENERATING STATION
FACILITY OPERATING LICENSE NPF-57
DOCKET NO. 50-354

REQUEST FOR LICENSE AMENDMENT
EXTENDED POWER UPRATE

Continuum Dynamics, Inc.
Request for Withholding

Continuum Dynamics, Inc.

(609) 538-0444 (609) 538-0464 fax 34 Lexington Avenue Ewing, NJ 08618-2302

AFFIDAVIT

Re:: "Bounding Methodology to Predict Full Scale Steam Dryer Loads from In-Plant Measurements," C.D.I. Report 05-28P, Revision 1 prepared by Continuum Dynamics, Inc., dated May 2006 and C.D.I. Report 06-16, Revision 1 "Estimating High Frequency Flow Induced Vibration in the Main Steam Lines at Hope Creek Unit 1: A Subscale Four Line Investigation of Standpipe Behavior," prepared by Continuum Dynamics, Inc. dated September 2006

I, Alan J. Bilanin, being duly sworn, depose and state as follows:

1. I hold the position of President and Senior Associate of Continuum Dynamics, Inc. (hereinafter referred to as C.D.I.), and I am authorized to make the request for withholding from Public Record the Information contained in the documents described in Paragraph 2. This Affidavit is submitted to the Nuclear Regulatory Commission (NRC) pursuant to 10 CFR 2.390(a)(4) based on the fact that the attached information consists of trade secret(s) of C.D.I. and that the NRC will receive the information from C.D.I. under privilege and in confidence.

2. The Information sought to be withheld, as transmitted to PSEG Nuclear LLC as attachments to C.D.I. Letter No. 06199 dated 14 September 2006, C.D.I. Report 05-28P, Revision 1 entitled "Bounding Methodology to Predict Full Scale Steam Dryer Loads from In-Plant Measurements," prepared by Continuum Dynamics, Inc. dated May 2006 and C.D.I. Report 06-16, Revision 1 entitled "Estimating High Frequency Flow Induced Vibration in the Main Steam Lines at Hope Creek Unit 1: A Subscale Four Line Investigation of Standpipe Behavior" prepared by Continuum Dynamics, Inc. dated September 2006.

3. The Information summarizes:

   (a) a process or method, including supporting data and analysis, where prevention of its use by C.D.I.'s competitors without license from C.D.I. constitutes a competitive advantage over other companies;
   (b) Information which, if used by a competitor, would reduce his expenditure of resources or improve his competitive position in the design, manufacture, shipment, installation, assurance of quality, or licensing of a similar product;
   (c) Information which discloses patentable subject matter for which it may be desirable to obtain patent protection.

The information sought to be withheld is considered to be proprietary for the reasons set forth in paragraphs 3(a), 3(b) and 3(c) above.

4. The Information has been held in confidence by C.D.I., its owner. The Information has consistently been held in confidence by C.D.I. and no public disclosure has been made and it is not available to the public. All disclosures to third parties, which have been limited, have been made pursuant to the terms and conditions contained in C.D.I.'s Nondisclosure Secrecy Agreement which must be fully executed prior to disclosure.

5. The Information is a type customarily held in confidence by C.D.I. and there is a rational basis therefore. The Information is a type, which C.D.I. considers trade secret and is held in confidence by C.D.I. because it constitutes a source of competitive advantage in the competition and performance of such work in the industry. Public disclosure of the Information is likely to cause substantial harm to C.D.I.'s competitive position and foreclose or reduce the availability of profit-making opportunities.

I declare under penalty of perjury that the foregoing affidavit and the matters stated therein are true and correct to be the best of my knowledge, information and belief.

Executed on this 14 day of Sept 2006.

Alan J. Bilanin
Continuum Dynamics, Inc.

Subscribed and sworn before me this day: Sept. 14. 2006

Eileen P. Burmeister, Notary Public

EILEEN P. BURMEISTER
NOTARY PUBLIC OF NEW JERSEY
MY COMM. EXPIRES MAY 6, 2007